EZH2 AND FOXM1 CROSSTALK IN TRIPLE NEGATIVE BREAST CANCER

SYLVIA MAHARA

NATIONAL UNIVERSITY OF SINGAPORE

2015

EZH2 AND FOXM1 CROSSTALK IN TRIPLE NEGATIVE BREAST CANCER

SYLVIA MAHARA

B.Sc. (HONS) in Genetics
University of Melbourne, Australia

A THESIS SUBMITTED

FOR THE DEGREE OF DOCTOR OF PHILOSOPHY

CANCER SCIENCE INSTITUTE OF SINGAPORE

NATIONAL UNIVERSITY OF SINGAPORE

2015

Declaration

I hereby declare that the thesis is my original work and it has been written by me in its entirety. I have duly acknowledged all the sources of information which have been used in the thesis.

This thesis has also not been submitted for any degree in any university previously.

Sylvia Mahara

31st July 2015

Acknowledgment

I am very grateful for the helps offered by so many people that have led to the completion of this thesis. Firstly, I wish to thank my two supervisors; Prof. Yu Qiang for giving me an opportunity to conduct this exciting research, his attentive guidance and resourceful knowledge as well as his witty humors have made the project very enjoyable; Prof. Chng Wee Joo for providing me with the opportunity to work with him as a research assistant first and as his PhD student last. He has shown me firsthand the feel of fast-moving research and inevitably, it has nurtured my excitement and enthusiasm for the continuing voyage of research in science. Secondly, I wish to thank Puayleng for helping me with many experiments, as well as allowing me to 'steal' some of her reagents. I also wish to thank Yurike, Steven and Vania, the three amazing interns who have been relentlessly putting up with me and readily offering helps in my experiments.

I am extremely grateful to Cancer Science Institute of Singapore (CSI), NUS for sponsoring my PhD study. I would also like to express my appreciation to Genome Institute of Singapore (GIS), which has provided me with a great and conducive environment to pursue my project. It has been a great pleasure to work with my lab mates in both CSI and GIS.

Finally, I would like to express my deepest love and gratitude to my mother, father, brother and all of my family members. Thanks for providing me with mental supports, for tolerating my nonsense, for sharing my happiness as well as hardships throughout this difficult but enriching PhD journey.

Table of Contents

Abstract

Breast cancer development is a multistep progression that leads to an accumulation of genetic alterations. Other than genetic mutations, epigenetic changes also contribute to tumorigenesis and one of the key players is EZH2. EZH2 exerts its epigenetic repression activity over its target genes via histone modification, and its aberrant overexpression in breast cancer leads to repression of multiple tumor suppressor genes. At the same time, another key oncogenic driver, FOXM1, has also been consistently shown to be upregulated in breast cancer and is associated with aggressive type of breast cancer. In this study, we sought to dissect the crosstalk between EZH2 and FOXM1 in aggressive TNBC.

By combining our microarray data analysis in TNBC cell line with mRNA expression profiling using TCGA patient database, we observed an overlap between EZH2 and FOXM1 target genes in both proliferation and invasion pathways. Interestingly, we also observed an inverse correlation between EZH2 and its PRC2 complex target genes suggesting a non-canonical function of EZH2 in the context of aggressive TNBC subtype. Subsequent in-vitro cell-based assays showed that EZH2 positively modulated FOXM1-mediated invasion pathway. Through co-Immunoprecipitation, we demonstrated a physical interaction between EZH2 and FOXM1 and through ChIP qRT-PCR assay, we found co-occupancy of EZH2 and FOXM1 on the promoter of *MMP2* and *MMP7*.

Despite the inverse correlation between EZH2 and PRC2 complex target genes, this canonical function of EZH2 was not completely lost in TNBC subtype. In accordance to this, we also identified occupancy of PRC2 complex and its associated repressive

H3K27me3 mark on the same *MMP*s promoters. This observation revealed dual role of EZH2 acting in an antagonistic manner study, the crosstalk between EZH2 and FOXM1 activated the MMP-mediated invasion while the canonical EZH2/PRC2 complex mediated epigenetic repression. This epigenetic repression was reversed in response to nutrient stress and the equilibrium was tilted toward the *MMP*s promoters' transactivation by EZH2/FOXM1 complex, as evident from increased *MMP*s mRNA levels and heightened invasive capacity.

Taken together, this study proposed a model highlighting dual regulation of EZH2 in regulating MMP-mediated invasion in TNBC subtype. The balance between canonical and non-canonical roles of EZH2 could possibly be the determining factor in promoting a more aggressive breast cancer.

List of Tables

List of Figures

List of Abbreviations

AKT3	v-Akt Murine Thymoma Viral Oncogene Homolog 3
ALDH1A1	Aldehyde Dehydrogenase 1
AML	Acute Myeloid Leukemia
AR	Androgen Receptor
ATM	Ataxia-Telangiectasia Mutated
BL-1	Basal-Like 1
BL-2	Basal-Like 2
BMI-1	B Lymphoma Mo-MLV Insertion Region 1 Homolog
BRCA1	Breast Cancer 1, Early Onset
BSA	Bovine Serum albumin
CBP	CREB Binding Protein
CDH1	Cadherin Type 1
CDK1	Cyclin-Dependent Kinase 1
CDK2	Cyclin-Dependent Kinase 2
ChIP	Chromatin Immunoprecipitation
cDNA	Complementary DNA
DMEM	Dulbecco's Modified Eagle's Medium
DNMT	DNA Methyltransferase
DZNep	3-Deazaneplanocin A
EED	Embryonic Ectoderm Development
EGFR	Epidermal Growth Factor Receptor
EMT	Epithelial to Mesenchymal Transition

ER	Estrogen Receptor
ERBB2	V-Erb-B2 Avian Erythroblastic Leukemia Viral Oncogene Homolog 2
E(Z)	Enhancer of Zeste
EZH2	Enhancer of Zeste Homolog 2
FBS	Fetal Bovine Serum
FKH	Forkhead DNA Binding Domain
FOXC1	Forkhead Box Protein C1
FOXM1	Forkhead Box Protein M1
GATA4	GATA Binding Protein 4
GFP	Green Fluorescent Protein
HBV	Hepatitis B Virus
HCC	Hepatocellular Carcinoma
HDAC	Histone Deacytelase
HER2	Human Epidermal Growth Receptor 2
HIF	Hypoxia Inducible Factor
HRE	HIF Response Element
HSC	Hematopoietic Stem Cell
IDC	Invasive Ductal Carcinoma
ILC	Invasive Lobular Carcinoma
IM	Immunomodulatory
IP	Immunoprecipitation
IPA	Ingenuity Pathway Analysis
JAZF1	Juxtaposed With Another Zinc Finger Gene 1

JJAZF1	Joined to JAZF1
JMJD3	Jumonji Domain-containing protein3
JNK1	c-Jun N-terminal Protein Kinase 1
LAR	Luminal Androgen Receptor
M	Mesenchymal
MAPK	Mitogen-Activated Protein Kinase
MEGM	Mammary Epithelial Growth Medium
MMP	Matrix Metalloproteinase
MSL	Mesenchymal Stem-Like
MT-MMP	Membrane-Type Matrix Metalloproteinase
MYC	v-Myc Avian Myelocytomatosis Viral Oncogene Homolog
NOD/SCID	Non Obese Diabetic/Severe Combined Immunodeficient
NRD	N-terminal Autorepressor Domain
PAF	PCNA-Associated Factor
PARP	Poly-AD-Ribose Polymerase
PC	Polycomb
PcG	Polycomb Group proteins
PCNA	Proliferating Cell Nuclear Antigen
PDX	Patient-Derived Xenograft
PH	Polyhomeotic
PIK3CA	PhosphatidylInositol-4,5-bisphosphate 3-Kinase, Catalytic subunit Alpha
Plk-1	Polo-Like Kinase-1
PR	Progesterone Receptor

PRC2	Polycomb Repressive Complex 2
PTEN	Phosphatase and Tensin Homolog
RB1	Retinoblastoma 1
RING1	Ring Finger Protein 1
RIPA	Radioimmunoprecipitation Assay
RORα	Retinoic Acid-Related Orphan Nuclear Receptor α
ROS	Reactive Oxygen Species
RUNX3	Runt-Related Transcription Factor 3
siRNA	Small Interfering RNA
STAT3	Signal Transducer and Activator of Transcription 3
SUZ12	Suppressor of Zeste 12
TAD	Transactivation Domain
TGF-β	Transforming Growth Factor-Beta
TNBC	Triple Negative Breast Cancer
TP53	Tumor Protein 53
UTR	Untranslated Region
UTX	Ubiquitously Transcribed X Chromosome Tetratricopeptide Repeat Protein
VEGF	Vascular Endothelial Growth Factor
WT	Wild-Type
XRCC1	X-ray cross-complementing group 1

List of Publications

1. Zhou, J., C. Bi, L. L. Cheong, **S. Mahara**, S. C. Liu, K. G. Tay, T. L. Koh, Q. Yu, and W. J. Chng. "The Histone Methyltransferase Inhibitor, Dznep, up-Regulates Txnip, Increased Ros Production, and Targets Leukemia Cells in Aml." *Blood* 118, no. 10 (2011): 2830-9

2. Zhou, J., C. Bi, W. J. Chng, L. L. Cheong, S. C. Liu, **S. Mahara**, K. G. Tay, Q. Zeng, J. Li, K. Guo, C. P. Tan, H. Yu, D. H. Albert, and C. S. Chen. "Prl-3, a Metastasis Associated Tyrosine Phosphatase, Is Involved in Flt3-Itd Signaling and Implicated in Anti-Aml Therapy." *PLoS One* 6, no. 5 (2011): e19798

3. Zhou, J., L. L. Cheong, S. C. Liu, P. S. Chong, **S. Mahara**, C. Bi, K. O. Ong, Q. Zenf, and W. J. Chng. "The Pro-Metastasis Tyrosine Phosphotase, Prl-3 (Ptp4a3), Is a Novel Mediated of Oncogenic Function of Bcr-Abl in Human Chronic Myeloid Leukemia." *Mol Cancer* 11, (2012): 72.

CHAPTER 1: INTRODUCTION

1.1 Epidemiology of Breast Cancer

Breast cancer is one of the leading causes of cancer mortality in female malignancy, accounting to approximately half a million cancer related deaths worldwide (Ferlay et al. 2015). The disease accounts for 25.2% of all female cancer diagnoses globally and up to 29.3% in Singapore, where the lifetime risk is one in sixteen (2013).

Based on Singapore cancer registry, there has been a 65.9% increment in the age-standardized mortality rate over the past three decades, which is the highest among all of the reported cancer deaths in female population (2012b). However, the 5-year age-standardized observed survival rate has seen an improvement of 72.3% for the same period of time. This improvement is largely attributed to the early detection through screening and advances in cancer therapy in recent years.

1.1.1 Anatomical Structure of Breast Tissue

The subcutaneous anatomical structure of female breast tissue consists of breast parenchyma supported by a complex network of stroma, adipose, vascular and lymphatic systems (Figure 1.1.) (Jesinger 2014). The breast parenchyma is made up of lobules and ducts, the milk-producing glands and the milk-carrying tiny tubes/tracts respectively and it is at either of these sites that a breast cancer is first initiated and confined. In the absence of medical intervention, the tumor cells have a potential to become invasive by infiltrating adjacent tissues.

The invasive breast cancers that first arise from the lobules are known as invasive lobular carcinomas (ILC), while those arise from the ducts are known as invasive ductal

carcinomas (IDC). Approximately 80% of breast cancer occurrences belong to the IDC group (Sandhu et al. 2010) hence, it warrants both medical and research attentions.

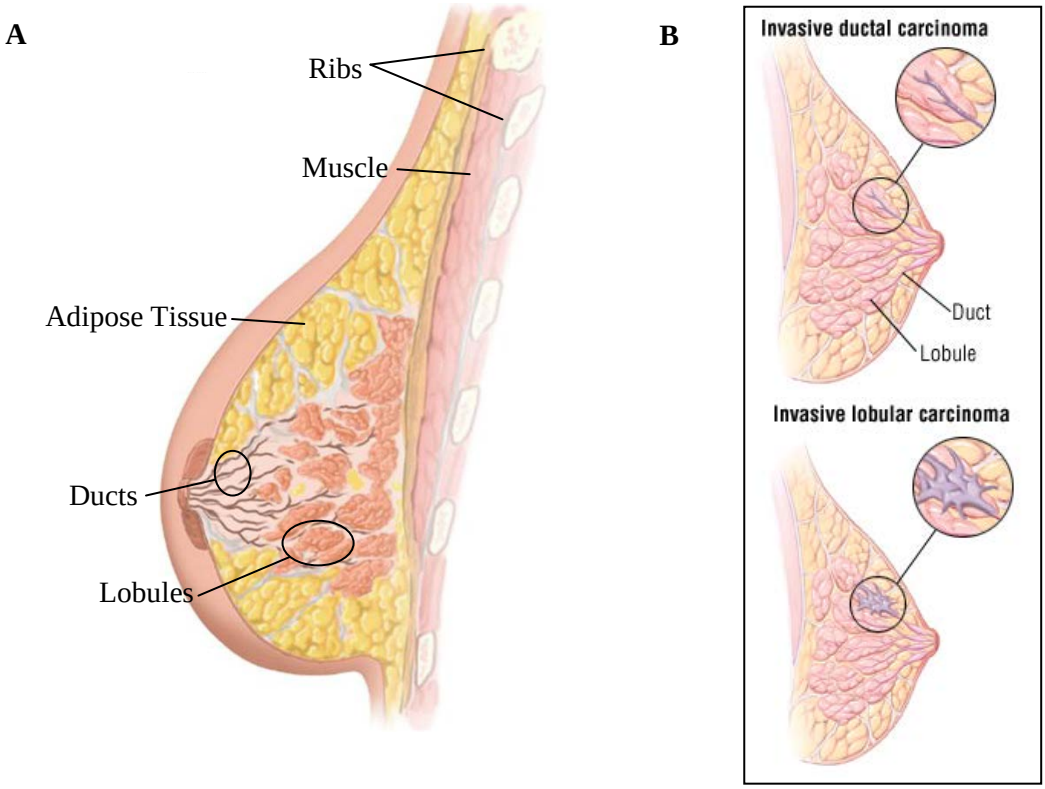

Figure 1.1. Anatomical structure of female breast tissue and origin of site for different types of invasive breast carcinomas.

A. Anatomical structure of female breast tissue at a subcutaneous level showing an intricate subcutaneous network lobules and ducts supported by adipose tissue. (Figure extracted and modified from (Jesinger 2014).)
B. Origin of site for incidence of IDC and ILC. Blue color-code denotes cancerous tissues. (Figure extracted and modified from http://www.drugs.com/health-guide/breast-cancer.html, assessed on 4th June 2015.)

1.1.2 Molecular Subtypes of Invasive Ductal Carcinoma

One of the characteristics of a solid tumor is intra-tumor heterogeneity. This is especially evident within patients diagnosed with IDC displaying different clinical presentations; diverse morphological feature, molecular signaling, metastasis pattern and

clinical outcome. Early attempts to deconstruct the biological heterogeneity by comparing global gene expression analysis in normal and IDC have identified four distinct intrinsic subtypes of breast cancer (Perou et al. 2000; Sorlie et al. 2001; Sorlie et al. 2003): Luminal A, Luminal B, HER2-enriched and Basal-like subtypes (Figure 1.2.).

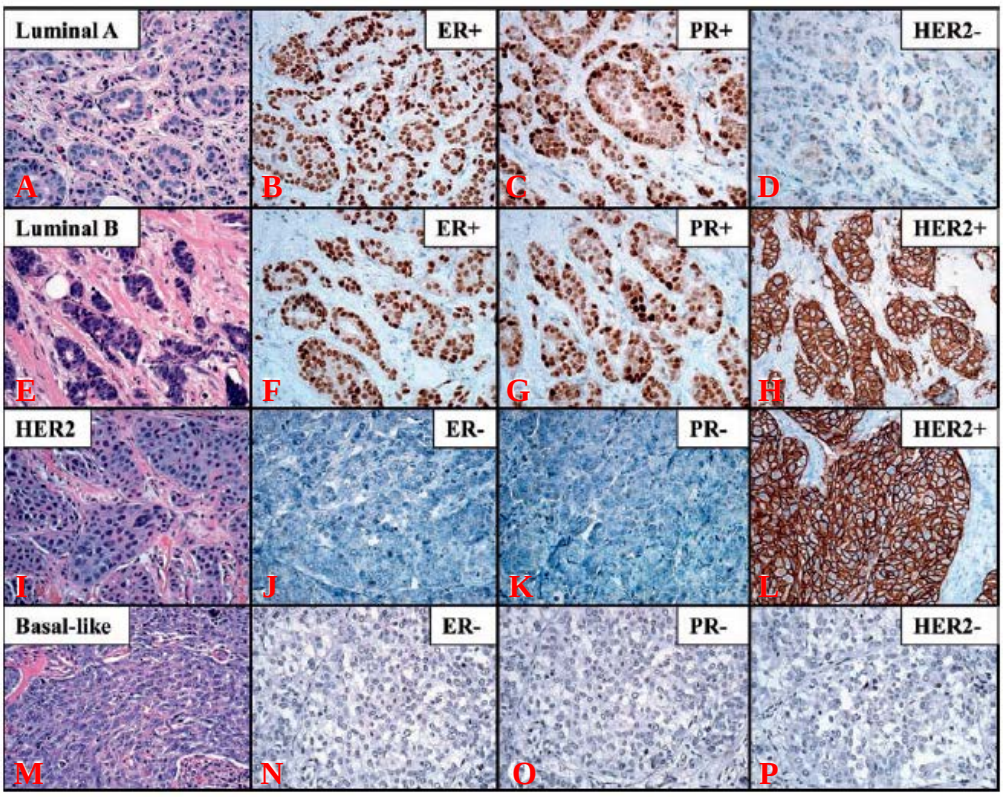

Figure 1.2. Four molecular intrinsic subtypes of invasive ductal carcinoma.
Differential immunohistochemical staining for estrogen receptor (ER), progesterone receptor (PR) and human epidermal growth receptor (HER2) on multiple breast tumor tissues identified four subtypes of breast cancer. Panels A-D: Luminal A subtype immunostains positive for ER and PR. Panels E-H: Luminal B subtype immunostains positive for ER, PR and HER2. Panels I-L: HER2-enriched subtype immunostains positive for HER2. Panels M-P: Basal-like subtype immunostains negative for all receptors. (+) denotes positive immunostaining and (–) denotes negative immunostaining. (Figure was extracted and modified from (Sandhu et al. 2010).)

1.1.2.1 Luminal Subtype

Approximately 70-75% of IDC express hormone receptors i.e. ER+ and PR+ breast cancers and they are classified as a luminal breast cancer subtype (Sandhu et al. 2010). Based on the differential HER2 expression and proliferation rate, this particular subtype can be further subclassified into luminal A (ER+, PR+ and HER2-) and luminal B subtypes (ER+, PR+ and HER2+) (Figure 1.2.) (Perou et al. 2000; Sorlie et al. 2001; Sorlie et al. 2003; Sandhu et al. 2010).

Due to the presence of hormone receptors, patients diagnosed with luminal subtype generally response well toward endocrine therapy targeted against ER and PR receptors, and are associated with good prognosis (Figure 1.3.). However, within the luminal subtype, luminal B is associated with a worse prognosis compared with luminal A. The difference in the clinical outcome is due to differential responses toward endocrine therapy (Brenton et al. 2005).

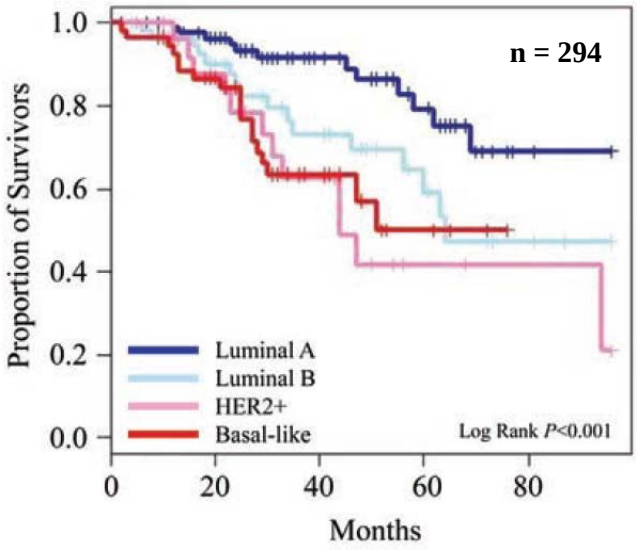

Figure 1.3. A Kaplan-Meier survival plot in IDC patients.
A survival plot for 294 IDC patients stratified according to their molecular intrinsic subtypes. Dark and light blue lines denote patients subclassified under luminal A and luminal B subtypes respectively. Pink line denotes patients subclassified under HER2-enriched subtype and red line denotes patients subclassified under Basal-like subtype. *P*-value was calculated using the Log-rank test. (Figure was extracted and modified from (Sandhu et al. 2010).)

1.1.2.2 HER2-enriched Subtype

HER2-enriched subtype is accounted for approximately 20% of IDC patients. This particular subtype does not express any hormone receptors however, it is characterised by a gene amplification of v-erb-b2 avian erythroblastic leukemia viral oncogene homolog 2 (ERBB2), resulting in an overexpression of HER2 receptor.

Patients with HER2-enriched subtype was known to be associated with the worst prognosis among IDC patients (Figure 1.3.). However, with the development of targeted therapy against HER2 receptor, this subtype of patients have experienced significant improvement in the clinical outcome (Baselga et al. 2006).

1.1.2.3 Basal-like or Triple Negative Breast Cancer (TNBC) Subtype

Of these 4 molecular intrinsic subtypes, basal-like subtype is of particular interest due to its highly aggressive clinical behavior and is associated with poor prognosis (Figure 1.3.). Basal-like subtype is characterized by the lack of all three receptors (ER-, PR-, HER2-) and is often called triple negative breast cancer (TNBC) subtype. This particular subtype accounts for approximately 15% of IDC patients (Foulkes et al. 2003).

The terms basal-like and TNBC subtypes are used interchangeably however, basal-like subtype is distinct from TNBC subtype by the differential expression of cytokeratin 5/6 and epidermal growth factor receptor (EGFR) (Sandhu et al. 2010). On the other hand, the term basal-like is not commonly used in a clinical setting hence, basal-like subtype is often classified as TNBC subtype. For the interest of this thesis, the term TNBC will be used instead.

Even within the TNBC breast cancer, a high degree of heterogeneity has been observed and reported. By comparing gene expression profiles from 21 breast cancer data sets for TNBC gene signature, Lehman and colleagues have further identified 6 subclassifications of TNBC subtype; basal-like 1 (BL-1), basal-like 2 (BL-2), immunomodulatory (IM), mesenchymal (M), mesenchymal stem-like (MSL) and luminal androgen receptor subtypes (LAR) (Figure 1.4) (Lehmann et al. 2011b).

The highly proliferative nature of TNBC breast cancer is reflected by the identification of both BL-1 and BL-2 TNBC subtypes. Both subtypes are characterized by their high expression for genes involved in cell cycle and proliferation. Particularly in BSL-2, an additional high gene expression associated with metabolism has also been observed (Lehmann et al. 2011b).

As the name suggested, IM subtype is highly associated with activated immune processes. Although there was an initial concern of the enrichment for the immune signaling pathway could be the reflection of the tumor microenvironment rather than the intrinsic expression. However, with the identification of a similar proportion of microdissected tumor samples expressing activated immune signaling genes found across different patient cohorts, this concern has been eliminated (Lehmann et al. 2011b).

Since TNBC is highly associated with aggressive clinical behavior, Lehman and colleagues have also identified a mesenchymal subclassification of TNBC subtype; M and MSL subtype, which are both associated with cell motility and differentiation processes. However, unique to MSL subtype is the association with cytokine signaling, angiogenesis and drug resistance-associated signaling pathways (Lehmann et al. 2011b).

The last subclassification of TNBC subtype is known as LAR due to its high expression for hormonally regulated pathway. This particular subtype is the most unique among all of the TNBC subclassification because intrinsically, LAR breast cancer is negative for hormone receptor expression i.e. ER- and PR-. Instead, LAR subtype is driven by androgen signaling pathway and it shares a small degree of overlapping with MSL subtype (Lehmann et al. 2011b).

Despite the advancement in the molecular stratification of TNBC breast cancers, the treatment is still limited to a conventional chemotherapy. This further reflects the complexity nature of TNBC associated with its clinically aggressive behavior.

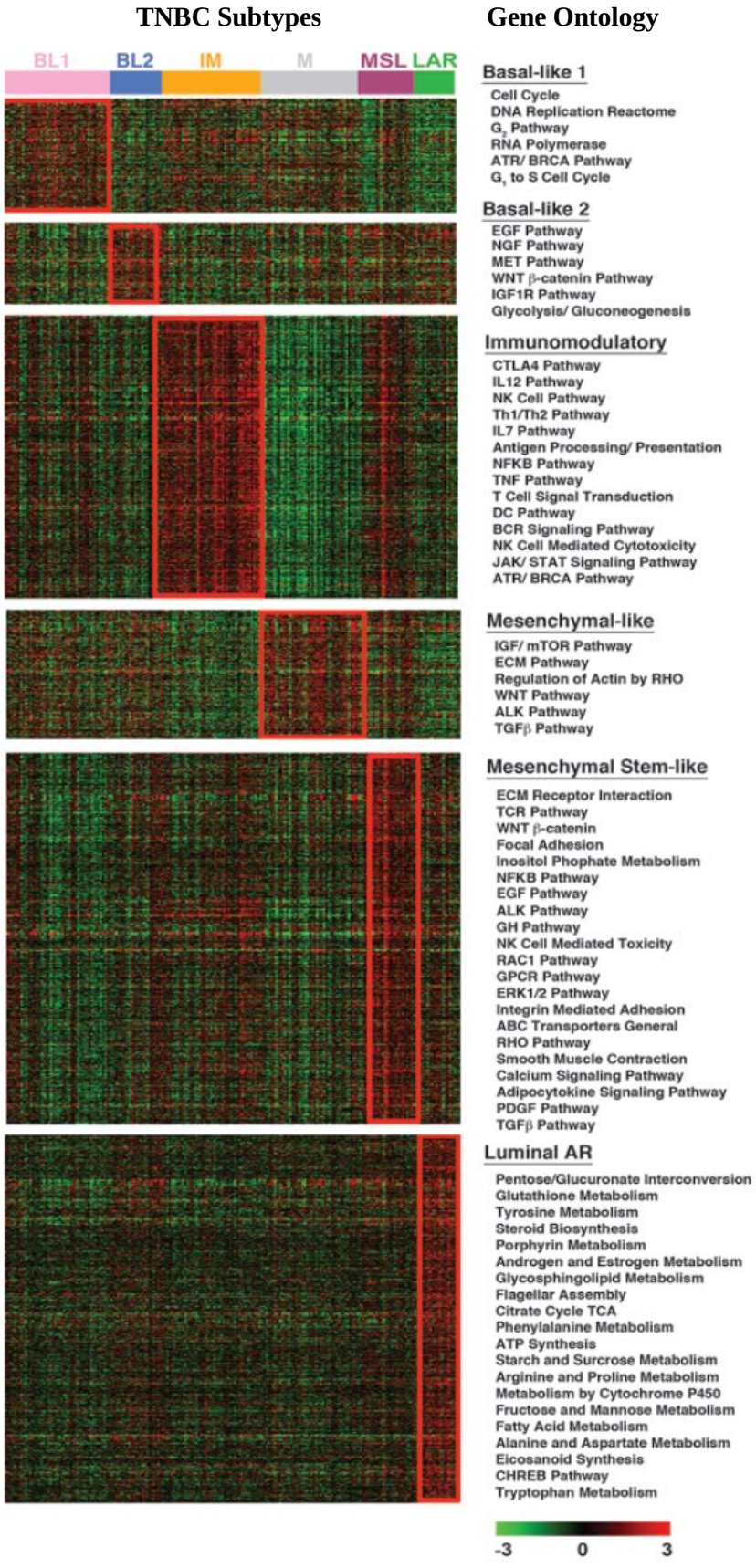

Figure 1.4. Six subclassification of TNBC breast cancer subtype. Hierarchical gene clustering showing differently expressed genes used to subclassify TNBC subtype into BL-1, BL-2, IM, M, MSL and LAR. Gene ontology terms for top canonical pathways associated with each subtypes is shown. *P*-value was calculated using the Log-rank test. (Figure was extracted and modified from (Lehmann et al. 2011b).)

1.1.3 Aggressive Nature of TNBC

Pathologically, TNBC breast cancers are characterised by higher proliferative rate, higher propensity to metastasize, greater risk of early relapses and higher rates of mortality compared with other IDC subtypes (Perou et al. 2000; Sorlie et al. 2001; Sorlie et al. 2003; Brenton et al. 2005; Carey et al. 2007; Sandhu et al. 2010; Lehmann et al. 2011a; Isakoff et al. 2015; Telli et al. 2015).

The higher propensity to metastasize, which is one of the characteristics of TNBC breast cancers, further underscores its highly aggressive clinical behavior (Perou et al. 2000; Sorlie et al. 2001; Sorlie et al. 2003; Brenton et al. 2005; Carey et al. 2007; Sandhu et al. 2010; Lehmann et al. 2011a; Isakoff et al. 2015; Telli et al. 2015). This particular subtype has a tendency to disseminate to brain and lung, but less likely to metastasize to lymph nodes, liver or bone (Tsuda et al. 2000). This factor eventually contributes to a high degree of mortality rate often observed in TNBC patients.

Furthermore, Sorlie and colleagues have reported that 100% of TNBC patients succumb to their disease within 4 years of diagnosis (Sorlie et al. 2001). Some of the TNBC patients do respond to treatment however, a higher likelihood of relapse observed and it eventually contributes to a poor survival outcome (Carey et al. 2007).

There are two properties of TNBC breast cancer that directly contribute to its aggressive nature associated with highly metastatic potential; stem cell maintenance (Wicha et al. 2006) and epithelial-mesenchymal transition (EMT) (Mani et al. 2008).

1.1.3.1 Contribution of Stem Cell to Aggressive Breast Cancer

A high proportion of TNBC cancer cells express both surface makers of CD44 high and CD23 low and aldehyde dehydrogenase 1 (ALDH1A1), which are characteristics of breast cancer stem cell (Wicha et al. 2006). Wicha and colleagues proposed that these breast cancer cells with a stem cell-like phenotype directly attribute to high metastatic potential by maintaining a subset of TNBC cells with tumorigenic potential.

However, not all TNBC cells expressing the stem-cell like profiles are stem cell per se. Furthermore, Visvader and colleagues argued that breast cancer stem cell could be originated from a differentiated cell that has acquired an ability for self-renewal (Visvader and Lindeman 2008).

1.1.3.2 Contribution of EMT to Aggressive Breast Cancer

Another property that confers metastatic potential to TNBC breast cancer is an EMT process. EMT is a transitional process in which epithelial cells lose their cell polarity to assume a more spindle-like phenotype, which is often associated with a more aggressive and invasive behavior in cancer cells (Hanahan and Weinberg 2011).

Mani and colleagues showed that induction of transcription factors associated with EMT i.e. Snail or Twist is not only capable of transforming a normal mammary epithelial cell into a migratory mesenchymal-like phenotype, but also an acquisition of stem cell-like phenotype (Mani et al. 2008). Since EMT phenotype is often overlapped with cancer stem cell phenotype, it remains unclear to which degree these two pathways contribute toward aggressive TNBC phenotype (Visvader and Lindeman 2008).

Despite the conundrum between cancer stem cell and EMT, they both have a strong association with propensity to metastasize in breast cancer. The event leading to metastasis is first initiated by the degradation of basement membrane, following differentiation to a more motile mesenchymal phenotype facilitated by EMT process, before disseminating into distant organs (Shook and Keller 2003). One of the key components that aids in the disruption of basement membrane is matrix metalloproteinases (MMPs).

1.1.3.3 Contribution of MMP to Aggressive Breast Cancer

MMPs are a group of enzymes with the ability to disrupt extracellular matrix lining the basement membrane and it has been directly implicated in breast cancer progression (Boire et al. 2005). MMPs can be further classified into six subgroups based on their structural domains: collagenases, gelatinases, stromelysins, matrilysins, membrane-type (MT)-MMPs and other MMPs (Visse and Nagase 2003).

Several reports have identified genetics polymorphisms found within the promoters of several *MMP*s, with majority resulting in their increased transcriptional activities, are associated with increased risk of breast cancer (Wieczorek et al. 2012). They include; *MMP1*, *MMP2*, *MMP3*, *MMP7*, *MMP8*, *MMP9*, *MMP12*, *MMP13* and *MMP21*.

The combined poor pathological features associated with TNBC breast cancers highlighted above together with its restricted option for any targeted therapy account for its higher rate of mortality among other IDC stubypes. These observations highlight the requirement to further examine the molecular aberrations associated with TNBC, in order

to uncover any potential molecular targets for the development of a better therapeutic treatment for this group of patients.

1.1.4 Oncogenic Pathway Associated with TNBC

The development of cancer in general is a multistep progression involving the activation of oncogenes and gradual loss of function of tumor suppressor genes. An intensive utilization of five hightroughput sequencing platforms involving DNA copy number array, DNA methylation array, exom sequencing, messenger RNA arrays, microRNA sequencing and reverse-phase protein arrays have identifed several dysregulated signaling pathway associated with TNBC cancer progression, which will be outlined here (2012a).

1.1.4.1 The Role of Tumor Suppressor Loss in TNBC progression

Tumor suppresor genes are known for their protective roles in normal cells against tumorigenesis. In their efforts to prevent tumorigenesis, they either repress the cell cycle progression of mutated cell in a bid to allow DNA repair machinery to fix the mutational error or potentiate the mutated cell to undergo cell death. Inadvertently, loss or inactivation of tumor suppressor genes does occur and those implicated in TNBC cancer progression are *TP53*, *RB1*, *BRCA1* and *PTEN* (2012a).

Tumor protein p53 (*TP53*) is a tumor suppressor gene encoding for p53 protein. Aptly named as guardian of the genome, p53 induces cell-cycle arrest and activates DNA

repair machinery in the event of cells exposed to various DNA-damaging induced stresses or mutagens (Yin et al. 2002). When the repair is not possible, p53 redirects the mutated cells to undergo apoptosis instead. Hence, loss of p53 contributes to tumor progression since the mutated cells are unable to undergo apoptosis and ultimately lead to their proliferation. Inactivation of *TP53* has also been implicated in breast cancer and particularly in TNBC breast cancers, where approximately 84% of TNBC breast cancers exhibit loss of p53 function (2012a).

In addition to loss of p53 function, loss of retinoblastoma 1 (*RB1*) tumor suppressor gene is also another feature only seen in TNBC breast cancers (Herschkowitz et al. 2008). It encodes for a nuclear phosphoprotein that regulates the cell cycle progression from G1 to S phase and inactivation of both of its alleles resulting in a rare chilhood malignancy, retinoblastoma (Weinberg 1995). Approximately 20% of TNBC breast cancers show loss or mutated pRb, which is not observed in other IDC subtypes (2012a).

BRCA1 (Breast cancer 1, early onset) tumor suppressor gene encodes for BRCA1 protein has several roles in cellular processes, which involved maintenance of chromosomal stability, DNA repair, cell cycle and apoptosis (Yoshida and Miki 2004). Collectively, those roles help to protect cells in response to DNA damage and germline mutation of BRCA1 has been associated with TNBC breast cancers (Bhattacharyya et al. 2000; Foulkes et al. 2003; 2012a).

1.1.4.2 The Role of Oncogenic Activation in TNBC Progression

Other than loss of tumor suppressor genes, several activations of oncogenes have also been reported in TNBC breast cancers and they are *PIK3CA*, *AKT3*, *MYC*, *HIF1A* and *FOXM1* (2012a). Both phosphatidylinositol-4,5-bisphosphate 3-kinase, catalytic subunit alpha (*PIK3CA*) and v-akt murine thymoma viral oncogene homolog 3 (*AKT3*) form a signal transduction pathway, PI(3)K/AKT pathway, commonly abberated in breast cancer and its activity is the highest in TNBC (2012a). It has been suggested that high activity of PI(3)K/AKT pathway in TNBC is in part due to loss of a tumor suppressor phosphatase and tensin homolog (PTEN) and/or gene amplification of *PIK3CA* (2012a).

The *MYC* (v-myc avian myelocytomatosis viral oncogene homolog) proto-oncogene encodes for a transcription factor with diverse cellular processes in proliferation, transformation, apoptosis and glycolysis (Dang 1999). Amplification of MYC has been implicated in breast cancer progression (Mariani-Costantini et al. 1988; Munzel et al. 1991) and particularly in TNBC subtype with 40% of TNBC breast cancer samples exhibit *MYC* focal gain (Chandriani et al. 2009; 2012a).

As breast cancer cells grow in 3-dimensional structure in-vivo, some of the tumors contain hypoxic regions due to their distant location from accessible blood vessels. Cancer cell has adopted several mechanisms to survive the decrease in oxygen availability and one of them is an activation of hypoxia inducible factor (HIF) transcription factors; HIF-1 and HIF-2 (Semenza 2012). HIF-1 and HIF-2 have different physiological roles with HIF-2 main role in adult red blood cell production (Haase 2010). HIF-1 forms a heterodimer between HIF-1α subunit and HIF-1β subunit. HIF-1α is degraded under normoxic condition via von Hippel–Lindau E3-ubiquitin ligase complex,

while HIF-1β is contitutively expressed (Wang et al. 1995). Abberant activation of HIF-1α has been observed in breast cancer progression especially in mediating invasion and metastasis pathway (2012a; Gilkes and Semenza 2013).

In addition, using PARADIGM, a method that allow simulataneous analysis of mutiple genome-wide sequencing platforms to predicts the degree of which a pathway's activities are more altered in one group of biological samples than another (Vaske et al. 2010), has also identified a comparably high activity of the HIF-1α, MYC and FOXM1 (forkhead box protein M1) regulatory pathways exclusively in TNBC breast cancers than other IDC subtypes (Figure 1.5.) (2012a). This observation suggests that the above pathways could potentially be the driving events in TNBC progression and interestingly, those pathways also overlap with serous ovarian cancer network, suggesting a possible convergence in term of oncogenic pathway between these two solid tumors.

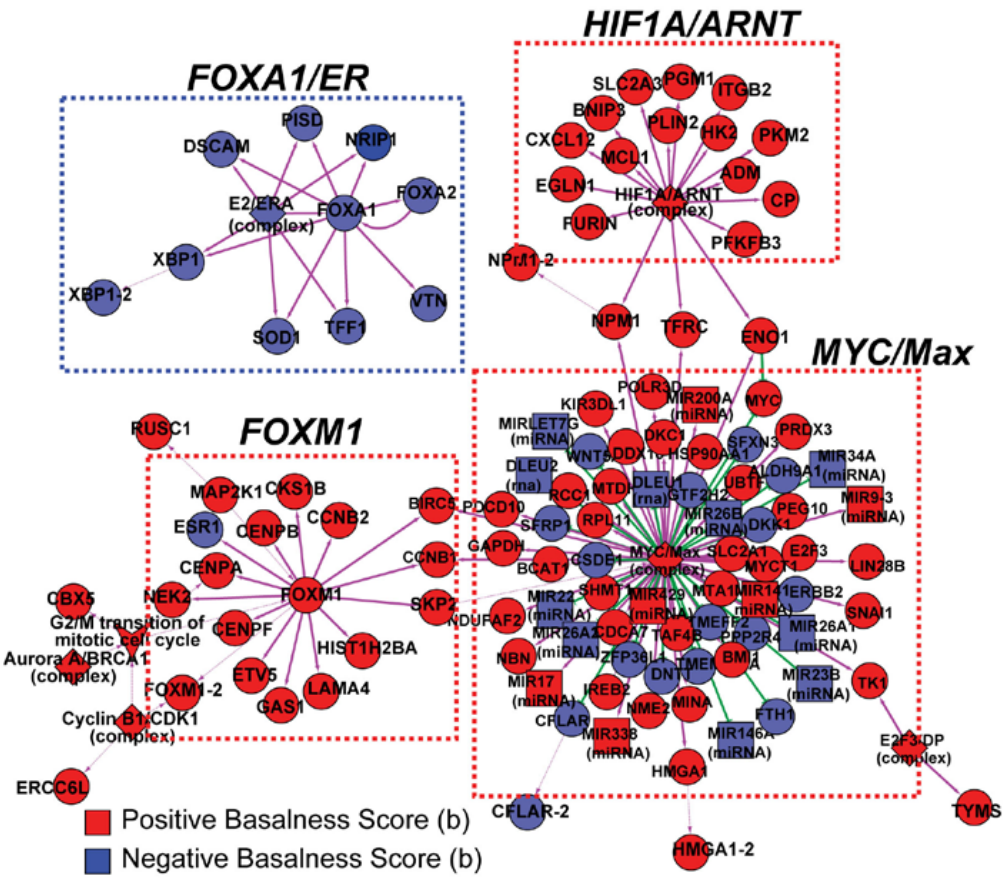

Figure 1.5. Integrated pathway analysis using PARADIGM.
PARADIGM analysis reveals common networks in TNBC and Ovarian cancers. TNBC/Ovarian to luminal breast cancer associations are assessed using a basalness score. The analysis shows that HIF1A, FOXM1 and MYC pathways are highly activated in both TNBC and ovarian cancers than in luminal breast cancer. (Figure was extracted from (2012a).)

1.1.4.3 The Implication of Deregulated Epigenetic Pathway in TNBC progression

Alterations in the transcriptional program via activation of oncogenes and/or loss of function of tumor suppressor genes are not the only mechanisms that drive cancer progression. The configuration of the chromatin structure, which dictates the ability of transcription factors, cofactors or enhancers to bind to specific DNA sequences or the degree of which DNA and nucleosomes are compacted into a higher order structure, will

determine how genes are expressed or repressed. Hence, deregulation of signaling pathway is not always dependent on genetic alterations; epigenetic modifications also contribute considerably toward tumor initiation.

Furthermore, there is a critical difference between genetic alterations and epigenetic modifications in term of restoration of gene expressions. Once genetic alteration takes place in a particular DNA sequence in a form of mutation, it will be difficult to restore the changes in its gene product. However, changes in the gene product due to epigenetic modification can be reversed with small molecule inhibitors targeting the histone-modifying enzymes.

Mechanistically, these epigenetic modifications involve series of post translational modifications at nucleosomal level, specifically the histone protein octamer coiled by 146 basepairs of DNA sequence, which made up the core component of a nucleosome (Luger et al. 1997). Among those post translational modifications, the most well characterized epigenetic modifications are acetylation and methylation (Allfrey et al. 1964).

There are two enzymatic families regulating the histone acetylation event: histone acetyltransferase and histone deacetyltransferase. The histone acetyltransferase was first discovered and isolated in yeast (Kleff et al. 1995; Brownell et al. 1996) and it is associated with transcriptional activation. Upon addition of an acetyl group to the positively charged lysine residue of histone proteins, it neutralizes the interaction between the histone proteins with the negatively charged DNA resulting in the disruption of the higher order chromatin structure (Shogren-Knaak et al. 2006). In contrast, histone

deacetyltransferase reverses the acetylation event and is associated with transcriptional repression (Taunton et al. 1996; Yang et al. 1996).

Histone lysine methyltransferase is another enzymatic family that regulates the histone methylation at lysine residue of histone 3 or histone 4 via its conserved catalytic SET domain (Jenuwein et al. 1998). The methylation event usually involves addition of 1-3 methyl groups and depending on its substrate specificity, methylation at H3K4 and H3K79 are associated with transcriptional activation, in contrast to transcriptional repressive activity on H3K9, H3K27 and H4K20 (Martin and Zhang 2005). However, not all histone lysine methyltransferases catalyze the addition of methyl groups through its SET domain. DOT1 protein, which is conserved in both yeast and human with a role in cell cycle regulation, is able to methylate H3K79 and is associated with transcriptional repression (Feng et al. 2002).

Due to their direct consequences in altering the chromatin structure and influencing the gene expression, deregulated epigenetic modifications have been implicated in tumorigenesis. Particularly in breast cancer progression, where an investigation into histone acetylation pattern in 58 breast surgical samples revealed that progression from normal breast to ductal carcinoma in situ and invasive ductal carcinoma was correlated with global reduction in the level of histone acetylation (Suzuki et al. 2009). In a separate study using a larger breast cancer cohort of 880 primary breast carcinomas, the low level of histone acetylation and methylation are further associated with TNBC and Her2-enriched breast cancer subtypes, and it can be used as a predictive marker for early onset of breast cancer (Elsheikh et al. 2009).

1.1.5 Current Treatment for TNBC

Due to the lack of well-defined molecular targets, TNBC patients represent a clinical challenge with no targeted therapy exists in clinical setting currently (Carey et al. 2007; Lehmann et al. 2011a; Isakoff et al. 2015; Telli et al. 2015). Currently, treatment for TNBC patients is restricted to standard adjuvant chemotherapy regimen. However, due to its heterogeneity nature, TNBC breast cancers respond differentially toward chemotherapeutic agents. Hence, knowledge toward the biology of TNBC breast cancers is vital in identifying potential targets and appropriate treatment.

Several clinical trials that aim to target potential receptors selectively expressed in TNBC, based on the immunohistochemical staining, have demonstrated only modest improvement (Carey et al. 2012; Forero-Torres et al. 2015). One of these studies focusing on EGFR, of which expression is upregulated in TNBC breast cancers (Makretsov et al. 2004; Sandhu et al. 2010; Lehmann et al. 2011b; 2012a; Baselga et al. 2013). However, subsequent studies showed that both the response rate and progression free survival in TNBC patients treated with combination of an EGFR inhibitor, cetuximab, and a chemodrug do not differ significantly with those patients treated with a chemodrug alone (Carey et al. 2012; Baselga et al. 2013).

Other than EGFR, vascular endothelial growth factor 1 (VEGF) has also been shown to be upregulated in TNBC (Lehmann et al. 2011b), and it is another possible candidate for the development of targeted therapy. In earlier trials, combination of a chemodrug and an inhibitor for VEGF receptor, Bevacizumab, improved both response rates and time to progression in patients with metastatic TNBC (Miller et al. 2007). However, subsequent studies of this treatment regime failed to improve overall survival in TNBC patients

(Cameron et al. 2013). Another class of targeted therapy inhibiting the activity of tyrosine kinase receptor, sunitib, proved to be disappointing with issue of toxicity and failure to improve progression free survival in TNBC patients (Barrios et al. 2010).

However, there are several promising targets, utilizing the biology of breast cancer, being explored currently. One of them is BRCA deficiency in TNBC breast cancers, which renders the cells unable to mediate homologous recombination DNA repair in response to DNA damage (Moynahan et al. 1999; McCabe et al. 2006). Thus, breast cancer cells with BRCA deficiency have heightened sensitivity toward DNA-damaging agents such as platinum salts, carboplatin and cisplatin, which binds directly to DNA forming DNA-platinum adducts with a consequent in DNA cross-link strand breaks (Bhattacharyya et al. 2000). Several studies have proven the efficacy of this platinum based chemodrug selectively in advanced TNBC breast cancers (Byrski et al. 2008; Sirohi et al. 2008; Silver et al. 2010).

Consequently, BRCA-deficient tumors are highly dependent on poly-AD-ribose polymerase (PARP) for their DNA repair process (McCabe et al. 2006). This observation suggests that inhibition of PARP could potentially increase the susceptibility of cancer cells (Farmer et al. 2005; Fong et al. 2009; Tutt et al. 2010). PARP is part of DNA repair mechanism similar to BRCA however, PARP repairs single-strand DNA breaks as opposed to BRCA, which repairs double-strand DNA breaks (Lord et al. 2006). The sensitivity of PARP inhibition is not necessarily dependent on BRCA deficiency; cancer cells that lack of homologous recombination DNA repair mechanism are also sensitive toward PARP inhibition (Farmer et al. 2005). A trial using a single agent PARP inhibitor, Olaparib, has shown impressive response rate for patients with BRCA-deficient

metastatic breast cancer with minimal toxicity (Tutt et al. 2010). Another ongoing phase 3 trial investigating the benefit of addition of Veliparib, another PARP inhibitor, in combination with carboplatin and a standard chemodrug has shown an initial significant pathologic complete response in TNBC patient (clinicaltrials.gov identifier NCT02032277) (Negri et al. 2013).

1.2 Molecular Biology of EZH2 in Breast Cancer

EZH2 is first identified in the study of eye color patterning in *Drosophila*, in which the protein homolog in *Drosophila*, enhancer of zeste (E(Z)) is able to suppress expression of white gene for eye color (Jack and Judd 1979). Subsequently, the human homolog, EZH2, was identified (Kuzmichev et al. 2002) and both the drosophila and human homologs are found to form a protein complex, and both contain intrinsic methyltransferase activity with an affinity for histone 3 lysine residue 27 (Czermin et al. 2002; Kuzmichev et al. 2002; Muller et al. 2002). The methyltransferase activity is a process of depositing a methyl group to histone tail and depending on the lysine residue; it will have either a repressive or an activation effect. In the case of EZH2, its methyltransferase activity predisposed a gene to a repressive state by condensing the chromatin structure.

In terms of the regulation of EZH2 in the context of breast cancer, there are three well characterized transcription factors that directly regulate the expression of EZH2 through binding to its promoter region; HIF, E2F and RAF/ERK/ELK signaling pathway. The promoter region of *EZH2* contains HIF response element (HRE), and in the event of hypoxia HIF directly transactivates EZH2 expression through binding to HRE (Chang et

al. 2011). E2F, a transcription factor that involves in cell cycle regulation has also been reported to bind to *EZH2* promoter (Ren et al. 2002). In resting cell, E2F is under inhibitory effect of retinoblastoma protein and it is activated upon phosphorylation of retinoblastoma. Activated E2F is then able to bind to its binding motif of EZH2 and leads to its induction. Lastly, study in HER2-enriched breast cancer has reported that RAF signaling has also been implicated in the activation of EZH2 expression (Fujii et al. 2011).

1.2.1 EZH2 as the Catalytic Subunit of PRC2 complex

In human, EZH2 is the catalytic subunit of Polycomb Group proteins (PcG) and together with its non-catalytic partners; Suppressor of Zeste 12 (SUZ12), Embryonic Ectoderm Development (EED) and other histone binding proteins; they form a multiprotein Polycomb Repressive Complex 2 (PRC2) (Jones et al. 1998; Rietzler et al. 1998; Schumacher et al. 1998; Sewalt et al. 1998; Cao et al. 2002; Kuzmichev et al. 2002; Varambally et al. 2002; Bracken et al. 2003; Kleer et al. 2003; Kirmizis et al. 2004; Shi et al. 2007b; Tan et al. 2007; Margueron et al. 2009; Holm et al. 2010; Wagener et al. 2010; Lee et al. 2011a; Holm et al. 2012; Xu et al. 2012; Kim et al. 2013; Yan et al. 2013). EZH2, through its SET domain that contains methyltransferase active site, facilitates repression of its target genes by modifying their chromatin structures via trimethylation of lysine residue 27 on histone 3 (H3K27me3) (Cao et al. 2002; Kuzmichev et al. 2002; Kirmizis et al. 2004). The PRC2 target genes are mostly involved in cell cycle regulation, DNA repair, cell fate and differentiation and cancer (Bracken et

al. 2003; Tonini et al. 2004; Zeidler et al. 2005; Bracken et al. 2006; Rouleau et al. 2007; Chamberlain et al. 2008; Maertens et al. 2009).

EZH2 protein is made up of five functional domains as depicted in Figure 1.6. (Simon and Lange 2008). The N-terminal domain composed of Domain I and II provide a binding site for EED and SUZ12 respectively. The adjacent cysteine rich CXC domain and SET domain are both required for the catalytic function of EZH2 in mediating methyltransferase activity and subsequent repression of its target genes. The EZH2 itself lacks of enzymatic function despite having an intact SET domain and it needs to form a protein complex with at least two of its binding partners, EED and SUZ12 to achieve a robust methyltransferase activity (Cao et al. 2002; Cao and Zhang 2004b; Pasini et al. 2004; Ketel et al. 2005; Montgomery et al. 2005; Nekrasov et al. 2005).

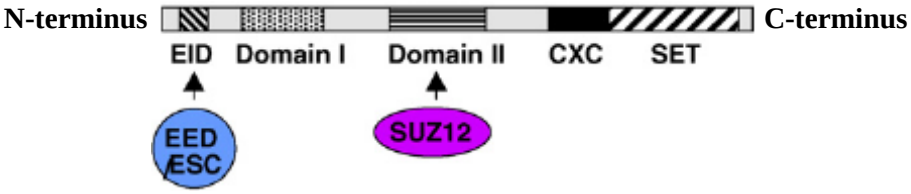

Figure 1.6. Domain organization of EZH2 protein
EZH2 protein contains five functional domains. N-terminal domain I, which includes EED interaction domain (EID), provides a binding site for EED. Domain II serves as binding site for SUZ12. The adjacent cysteine-rich CXC domain and C-terminal SET domain are both required for histone methyltransferase activity. (Image extracted and modified from (Simon and Lange 2008))

1.2.1.1 EED as a Member of PRC2 complex

EED is first identified using a yeast two-hybrid and in-vitro binding assays (Jones et al. 1998; Sewalt et al. 1998), which demonstrate its evolutionary conserved partnership with EZH2 in *Drosophila*, mouse and human (Jones et al. 1998; Rietzler et al. 1998;

Schumacher et al. 1998; Sewalt et al. 1998). The N-terminal domain of EED contains a putative PEST sequence; a peptide sequence that is rich in proline (P), glutamic acid (E), serine (S), and threonine (T); with a role in protein degradation (Sewalt et al. 1998). The adjacent domain contains five WD40 domains and they all participate in the protein-protein interaction with EZH2 (Sewalt et al. 1998). Lastly, the C-terminal domain is the region that recognizes H3K27me3 and binds directly to the histone tail, which activates the methyltransferase activity of PRC2 (Margueron et al. 2009).

Despite its critical role in facilitating methyltransferase activity, aberrant overexpression of EED in human malignancy was not known previously. The first documented studies of EZH2 overexpression in human malignancies, did not observe a concomitant increase of EED expression (Varambally et al. 2002; Kleer et al. 2003). However, a recent study showed that EED is implicated in the EMT process (Oktyabri et al. 2014). Upon stimulation with transforming growth factor-beta (TGF-β), EED expression is upregulated, which mediates a transcriptional repression on the promoter of E-cadherin (*CDH1*), and induces the morphological conversion of cancer cell associated with EMT.

1.2.1.2 SUZ12 as a Member of PRC2 complex

In 1995, Nagase and colleagues isolated a full-length cDNA clone from an acute myeloid leukemia (AML) cell line, KG-1 and designated the predicted gene as *KIAA0160* (Nagase et al. 1995). Subsequently, the predicted gene was associated with a recurrent chromosomal translocation at chromosome 7 in endometrial stromal sarcomas (Koontz et

al. 2001). Due to its position on the breakpoint sites at chromosome 7, recombination of these breakpoints resulting in a fusion of *KIAA0160* with another zinc finger gene, *JAZF1* (Juxtaposed With Another Zinc Finger Gene 1), and *KIAA0160* was renamed as *JJAZ1* (Joined to JAZF1).

In 2001, Birve and colleagues noted that human *SUZ12* was identical to *KIAA0160*, and in their subsequent functional study demonstrated that SUZ12 was required to repressed the homeotic genes in Drosophila (Birve et al. 2001). The involvement of SUZ12 in the PRC2 complex was first reported by Cao and colleagues, where they purified EZH2-EED complex and identified their co-localization with H3K27me3 mark at Ultrabithorax (Ubx) polycomb response element (Cao et al. 2002). They also reported that the EZH2-EED complex required the involvement of SUZ12 to exert a more robust histone methyltransferase activity. Similar to EZH2, aberrant overexpression of SUZ12 has also been implicated in multiple human malignancies, including colon, breast and liver cancer (Kirmizis et al. 2003; Kirmizis et al. 2004; Kuzmichev et al. 2005; Li et al. 2007).

1.2.2 Collaboration of PRC2-Mediated Transcriptional Repression with Other Silencing Enzymes

The repressive H3K27me3, deposited on the histone tail of specific genes, mediated by PRC2 complex only serves as an initiation repressive event, a second layer of a maintenance repressive event is required for a stable repression of a particular gene, and they are either facilitated by PRC1 complex (de Napoles et al. 2004; Wang et al. 2004;

Boyer et al. 2006; Bracken et al. 2006), DNA methyltransferase (Vire et al. 2006; Ohm et al. 2007; Schlesinger et al. 2007; Villa et al. 2007; Widschwendter et al. 2007) or histone deacytelase (HDAC) (van der Vlag and Otte 1999; Garrick et al. 2008) (Figure 1.7).

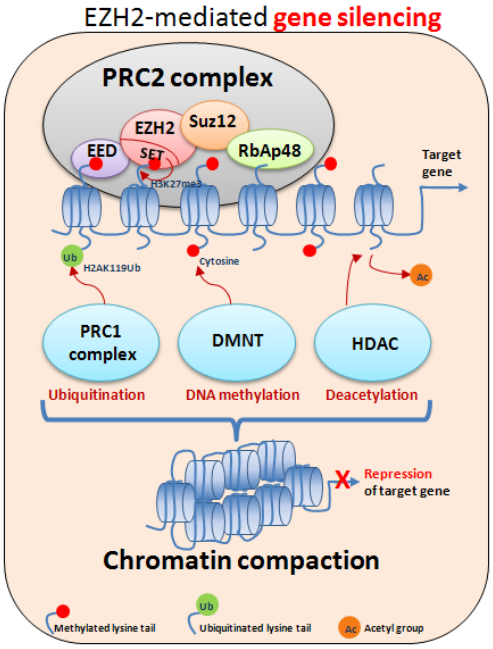

Figure 1.7. PRC2 complex facilitates transcriptional repression.
PRC2 complex through EZH2 catalyzes H3K27 trimethylation which serves as a recruitment marker for either PRC1 complex, DNA methyltransferase (DMNT) or histone deacytelase (HDAC) to facilitate stable repression of certain genes through chromatin compaction. (Image adapted from (Chase and Cross 2011))

1.2.2.1 EZH2/PRC2 Complex Links to PRC1 Complex

Several studies have identified the partnership between PRC2 complex and PRC1 complex in mediating gene silencing. Furthermore, a genome wide analysis has identified co-localization of PRC2 complex, PRC1 complex and the associating repressive H3K27me level in the genes involved in embryonic development and cell fate decisions (Boyer et al. 2006; Bracken et al. 2006). A purification of PcG proteins in HeLa cells has

identified several members of PRC1 complex, they are; polycomb (PC), polyhomeotic (PH), B Lymphoma Mo-MLV Insertion Region 1 Homolog (BMI-1) oncoprotein and ring finger protein 1 (RING1); and despite varying composition of these subunits due to alternative homologues of PcG proteins, the gene silencing activity remains unaffected (Levine et al. 2002).

During initiation of repressive event, PRC2 complex, through its EZH2 subunit, will catalyze H3K27me3 on its target gene. This repressive mark is recognized by the chromodomain of the PC subunit of PRC1 complex, which facilitates the recruitment of PRC1 complex to the target gene and the subsequent gene silencing (Cao et al. 2002; Fischle et al. 2003; Cao and Zhang 2004a; Boyer et al. 2006). The actual mode of gene silencing mechanism has yet to be fully elucidated however, several studies have proposed that PRC1 complex executes its polycomb silencing effect either through; 1) blocking of nucleosomal remodeling (Levine et al. 2002), 2) chromatin condensation (Francis et al. 2004), 3) ubiquitination on histone H2A lysine residue 119 (Cao et al. 2005; Stock et al. 2007) and/or 4) blocking of transcriptional elongation (Guenther et al. 2007; Stock et al. 2007; Zeitlinger et al. 2007).

Despite the overlapping target genes of PRC2 and PRC1 complex, which suggests their concerted effort in mediating polycomb gene silencing, several studies in hematopoietic stem cells (HSC) showed an opposing roles for these 2 complexes (Jacobs et al. 1999; Lessard et al. 1999; Oguro et al. 2006; Majewski et al. 2010). However, whether the same epigenetic regulation could occur in other tissue models remains as an open discussion.

1.2.2.2 EZH2/PRC2 Complex Links to DNA Methylation

PRC2-mediated histone methylation and DNA methylation on CpG islands have long been thought as two separate gene silencing mechanisms. However, a landmark study by Viré and colleagues demonstrated the requirement of both EZH2 through PRC2 complex and DNA methyltransferase to effectively represses EZH2 target genes in osteosarcoma cells (Vire et al. 2006). This observation suggests that EZH2 serves to recruit DNA methyltransferase-1, DNA methyltransferase-3A or DNA methyltransferase-3B and highlights the direct connection between these 2, previously thought to be distinct, gene silencing mechanisms.

A subsequent study comparing both normal and cancer cells reveals that EZH2 target genes i.e. tumor suppressor genes, with low expression of H3K27me3 in normal cells, became hypermethylated at their CpG islands in cancer cells (Ohm et al. 2007). Ohm and Colleagues also proposed that dimethylation at histone 3 lysine residue 9 may contribute to the transition from histone methylation to DNA methyltransferase-mediated CpG methylation. Similar mechanism that involves the collaboration between PRC2-mediated histone methylation and DNA methyltransferase in mediating a more stable gene repression has also been reported in prostate, liver, lung, ovarian, breast and leukemia (Schlesinger et al. 2007; Villa et al. 2007; Widschwendter et al. 2007).

1.2.2.3 EZH2/PRC2 Complex Links to Histone Deacytelase

The relationship between EZH2 and HDAC is first reported by van Der Vlag and colleagues (van der Vlag and Otte 1999). In the yeast two-hybrid system for the cloning

of several cDNAs encoding human PcG protein, they found that only HDAC co-immunoprecipitates with the EED protein and not with other PcG proteins. Furthermore, treatment with HDAC inhibitor, trichostatin A, relieves the PRC2-mediated transcriptional silencing effect suggesting the direct mechanistic link between these 2 distinct global gene silencing systems.

Similar mechanism has also been reported in the regulation of α-globin gene expression (Garrick et al. 2008). In non-erythroid cells, α-globin gene is not expressed due to the presence of PRC2 complex and their associating repressive H3K27me3 mark as well as hypoacetylation of its promoter region. Upon treatment with trichostatin A, PRC2 complex is depleted accompanied by re-expression of α-globin gene.

1.2.3 Non-PRC2 Complex Function of EZH2

There are growing evidences of histone methyltransferase independent function of EZH2 in multiple malignancies, suggesting a role of EZH2 beyond its PRC2-mediated repressive activity (Cha et al. 2005; Shi et al. 2007b; Tan et al. 2007; Holm et al. 2010; Lee et al. 2011b; Wei et al. 2011a; He et al. 2012; Holm et al. 2012; Lee et al. 2012; Xu et al. 2012; Jung et al. 2013b; Jung et al. 2013a; Kim et al. 2013; Yan et al. 2013; Gonzalez et al. 2014b; Gonzalez et al. 2014a). In this instance, oncogenic EZH2 exhibits a transcriptional co-activation function, and the switch from PRC2 dependent function to independent function often involves a post translational modification.

A study in castration-resistant prostate cancer showed that phosphorylation of EZH2 at its serine residue (phospho-EZH2 (S21)) by protein kinase B, also known as Akt,

mediates its interaction with androgen receptor (AR) and subsequent gene activation (Xu et al. 2012). A subsequent study indicated that phosphorylation of EZH2 inhibits its methyltransferase activity preventing the binding of phosphorylated EZH2 to histone 3 (Cha et al. 2005). Paradoxically, phospho-EZH2 (S21) methylates AR instead and leads to activation of target genes involved in prostate cancer progression, without the requirement of any of PRC2 complex subunits. It is worth noting that despite high expression of EZH2 in prostate cancer however, there is no concomitant increase of global H3K27me3 level, indicating a role of EZH2 independent of its repressive PRC2 complex function.

A separate study in glioblastoma-multiforme demonstrated that by phospho-EZH2 (S21) is also capable of methylating signal transducer and activator of transcription 3 (STAT3), and it leads to its subsequent protein stability through increased phosphorylation of STAT3 at its tyrosine residue (Kim et al. 2013). These observations suggest that phospho-EZH2 (S21) could be the potential molecular switch for EZH2 from a canonical epigenetic repressor to a non-canonical transcriptional coactivator.

Components of cell cycle dependent signaling have also been implicated in the phosphorylation of EZH2 particularly cyclin-dependent kinase 1 (CDK1) and cyclin-dependent kinase 2 (CDK2), albeit with several conflicting results. Wei and colleagues reported that phosphorylation of EZH2 by CDK1 at threonine residue (phospho-EZH2 (Thr487)) inhibits its methyltransferase activity by disrupting the interaction between EZH2 and its PRC2 complex subunits (Wei et al. 2011b). However, Wu and colleagues showed that the same phosphorylation residue promotes ubiquitination of EZH2 and leads to its subsequent protein degradation by proteasome (Wu and Zhang 2011). It is

possible that these functional discrepancies are due to the different cell type used or the different target genes being investigated.

In luminal breast cancers, EZH2 has been shown to interact with ER and β-catenin, and together this complex enhances the target genes involved in estrogen and Wnt pathways (Shi et al. 2007a). Interestingly, they also reported a transactivation activity of EZH2 at its N-terminal domains suggesting that EZH2 could function as a transcription factor.

Our group has also previously reported the PRC2 independent function of EZH2 in breast cancer using TNBC as our study model (Lee et al. 2011b). We identified novel partners of EZH2 with components of nuclear factor kappa B (NF-κB), RelA and RelB. This complex helps to activate NF-κB target genes independent of PRC2 complex subunits. At the same time, we have also found that both EZH2/PRC2 complex and EZH2/RelA/RelB complex co-exist in TNBC and it is quite possibly that they each have different target genes with a distinct regulation from each other's. Subsequently, Gonzalez and colleagues also showed the same EZH2/RelA/RelB complex in TNBC with an addition of RNA polymerase II and SET1 protein (Gonzalez et al. 2014a). They demonstrated that this complex is involved in directly activating *NOTCH1* expression resulting in expansion of TNBC stem cells.

The Wnt signaling and EZH2 axis has also been studied in colon cancer, which identified a novel partner of EZH2, DNA repair protein proliferating cell nuclear antigen (PCNA)-associated factor (PAF) (Jung et al. 2013b). Together EZH2, PAF, β-catenin, RNA polymerase II and others mediators transactivate Wnt target genes.

Other than non-PRC2 complex function of EZH2 describes above, a non-canonical methyltransferase activity of EZH2 has also been reported to methylate non-histone proteins. EZH2 has been reported to methylate transcription factor GATA binding protein 4 (GATA4) at its lysine residue (me-GATA4 (K299)) during fetal heart development (He et al. 2012). me-GATA4 (K299) leads to its dissociation with histone acetyltransferase, P300, which prevents it acetylation and subsequent reduction in transcriptional activity. In another study, EZH2 is reported to methylate a tumor suppressor protein, retinoic acid-related orphan nuclear receptor α (RORα), in luminal breast cancer (Lee et al. 2012). The methylated RORα is first recognized by DCAF1 adaptor (damage-specific DNA binding protein 1 (DDB1)/cullin4 (CUL4)-associated factor 1) and is subsequently ubiquitinated and degraded by DDB1/CUL4 E3 ubiquitin ligase.

Taken together, the role of EZH2 during both normal and development and tumorigenesis is more complex and intricate than previously thought. With its multifunctional regulatory roles as a transcriptional activator, transcriptional co-activator and even non-histone protein methyltransferase differs depending on cell types and target genes, it underscores the uniqueness of genomic and epigenetics regulations, and a possible convergence of these two fields mediated by EZH2.

1.2.4 EZH2 as an oncogenic driver in TNBC

Our previous results have demonstrated that the EZH2 is consistently overexpressed in both TNBC cell lines and patient samples (Tan et al. 2007; Lee et al. 2011b). Overexpression of EZH2 has also been reported in numerous solid and hematological

tumors, with a positive correlation between the level of EZH2 with tumor grade, metastasis propensity and poor survival rates (Varambally et al. 2002; Bracken et al. 2003; Kleer et al. 2003; Wagener et al. 2010; Xu et al. 2012; Kim et al. 2013; Yan et al. 2013). Interestingly, several studies have identified an inverse correlation between expression of EZH2 and the level of repressive H3K27me3 particularly in TNBC (Holm et al. 2010; Holm et al. 2012). By comparing tissue microarrays collected from 3 different studies, herein termed as dataset 1, dataset II and GEX dataset (Figure 1.8), Holm and colleagues found that high expression of EZH2 but low level of H3K27me3 repressive mark are only observed TNBC subtype.

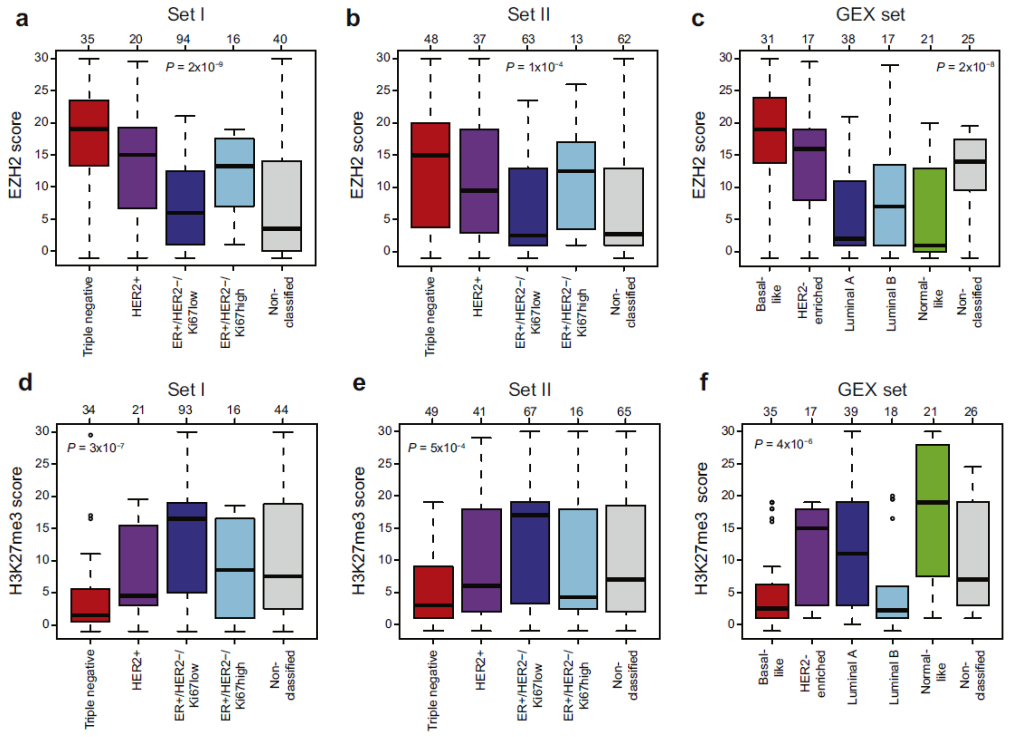

Figure 1.8. Expression of EZH2 and H3K27me3 Levels across Multiple IDC Subtypes in 3 Different Data Sets

(*A-C*) Protein expression of EZH2 stratified by IDC subtypes in dataset I, dataset II and GEX dataset. (*D-F*) Abundance of H3K27me3 levels stratified by IDC subtypes in dataset 1, dataset II and GEX dataset. The tumor sample size for each subtype is shown at the top and ANOVA was used as a statistical analysis with *P-values* shown for each datasets. (Image extracted from (Holm et al. 2012))

When the tumors were further stratified based on the expression of EZH2 and abundance of repressive H3K27me3, Holm and colleagues demonstrated that tumors with high level of EZH2 but low abundance of repressive H3K27me3 is a predictive marker for poor prognosis in breast cancer patients (Figure 1.9). This observation suggested that the epigenetic characteristics of PRC2 complex is reduced especially in TNBC subtype and it contributes to a poor survival rates. In addition, the high expression of EZH2 observed in TNBC subtype could lead to non-canonical functions that directly contribute to the development of a more aggressive breast cancer, independently of its canonical repressive epigenetic role.

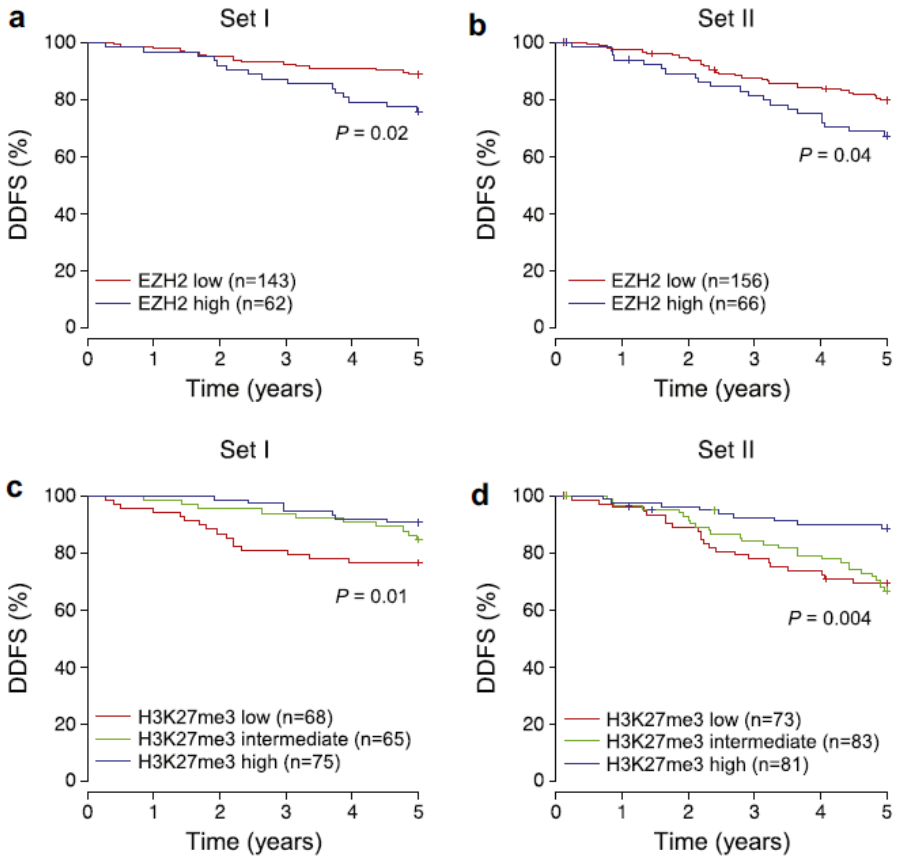

Figure 1.9. Survival Analysis in Breast Cancer patients
Kaplan-Meier curves measuring 5 years of distant disease free survival (DDFS) in breast cancer patients are stratified by abundance of EZH2 in (*A*) dataset I and (*B*) dataset II and abundance of H3K27me3 in (*C*) dataset I and (*D*) dataset II. Log-rank tests was used as a statistical analysis with *P-values* shown for each datasets. (Image extracted from (Holm et al. 2012))

As an oncogene, EZH2 has been implicated in breast cancer progression ranging from proliferation, invasion and stem cell maintenance. Among those well-defined EZH2 target genes associated breast tumorigenesis are *RAD51*, *RUNX3*, *FOXC1*, *CDH1* and *CDKN1C* (Cao et al. 2008; Fujii et al. 2008; Yang et al. 2009; Chang et al. 2011; Du et al. 2012). *RAD51* encodes for RAD51 recombinase protein with a role in DNA double strand break repair (Yuan et al. 1998). Chang and colleagues reported that RAD51 protein expression is under PRC2-mediated repressive activity where promoter of *RAD51*

is enriched for repressive H3K27me3 mark (Chang et al. 2011). Reduction of RAD51 expression promotes breast cancer stem cell expansion through activation of RAF/pERK/β-catenin signaling.

A study in luminal breast cancer cell line showed that both EZH2 and HDAC1 binds to the promoter of *RUNX3* (Runt-related transcription factor 3), and either reduction of EZH2 or pharmacological inhibition of HDAC1 through trichostatin A induces the expression of RUNX3 (Fujii et al. 2008). The role of RUNX3 as a tumor suppressor protein is well established in gastric cancer, and its gene is frequently deleted or transcriptionally repressed during cancer progression (Brenner et al. 2004). Suppression of *RUNX3* in luminal breast cancer through regulation of EZH2 and HDAC1 leads to subsequent induction of cell proliferation as a consequence of reduced downstream target of RUNX3, cyclin-dependent kinase inhibitor $p21^{WAF/Cip1}$.

EZH2 through its repressive PRC2 complex activity has been shown to downregulate the expression of forkhead box protein C1 (FOXC1) transcription factor in TNBC cell line (Du et al. 2012). FOXC1 is known for its role in cell differentiation and particularly during eye development (Mortemousque et al. 2004; Aldinger et al. 2009). Reduction of FOXC1 in TNBC cell lines helps promote cancer cell migration and invasion in-vitro and metastasis in-vivo. Overexpression of EZH2 is also shown to repress the expression of E-cadherin, which leads to enhanced invasion in breast cancer (Cao et al. 2008). However, a more effective silencing of E-cadherin also requires the involvement of HDAC activity, further emphasizing the PRC2 complex-HDAC axis as a mode of transcriptional silencing mechanism.

Our group has previously reported the direct regulation of EZH2 through its PRC2-mediated gene silencing effect on *CDKN1C* (Yang et al. 2009). We identified the enrichment of EZH2 in the promoter of *CDKN1C*, which coincides with the repressive H3K27me3 levels across multiple breast cancer cell lines. *CDKN1C* encodes for a cyclin-dependent kinase inhibitor protein $p57^{KIP2}$ protein, and it is known for its role as a tumor suppressor (Lee et al. 1995; Matsuoka et al. 1995). Consistent with its role, we also observed reduced expression of $p57^{KIP2}$ across multiple breast cancer cell lines. However, upon treatment with EZH2 inhibitor, 3-deazaneplanocin A (DZNep), the level of H3K27me3 on the promoter of *CDKN1C* is reduced followed by increased expression of $p57^{KIP2}$, further highlighting the direct link between repressive PRC2 complex and transcriptional repression in CDKN1C.

Loss of BRCA1, which is highly associated with breast cancer progression, has also been linked to overexpression of EZH2, and currently there are two proposed mechanism on how EZH2 causes the decrease in BRCA1 expression in TNBC (Gonzalez et al. 2009; Gonzalez et al. 2011). In 2009, Gonzalez and colleagues showed that overexpression of EZH2, which is frequently observed in ER-negative breast cancers, blocks the phosphorylation of BRCA1 at its serine residue (phospho-BRCA1 (Ser1423)) (Gonzalez et al. 2009). The blocking of phospho-BRCA1 (Ser1423) leads to induction of several gene expressions involved in G2/M progression hence, overexpression of EZH2 is associated with increase proliferation in breast cancer. Unfortunately, the group did not address the biological significance of phospho-BRCA1 (Ser1423), instead they demonstrated that increased BRCA1 is associated with increased phospho-BRCA1 (Ser1423) upon EZH2 knock down and vice versa.

Two years later, Gonzales and colleagues again reported that EZH2 mediates the loss of BRCA1 expression by preventing its nuclear localization in breast cancer cell line (Gonzalez et al. 2011). In order to achieve this effect, EZH2 activates Akt-1 and together they prevents nuclear translocation of phospho-BRCA1 (Ser1423) resulting in subsequent aberrant mitoses and genomic instability. Even though, they were able to provide neither a suppression mechanism of EZH2/Akt-1 on BRCA1 nor an activation mechanism of EZH2 on Akt-1 however, there is a clear association between high EZH2 and loss of BRCA1 activity in majority of breast cancers.

1.3 Molecular Biology of FOXM1 in Breast Cancer

Despite overexpression of EZH2 in numerous malignancies, multiple observations show the requirement of EZH2 to form a direct interaction with other molecules in order to exert its oncogenic property. Considering the cellular complexity, it is not unexpected for more than 2 molecules modulating a specific molecular event in concert. Particularly in invasion and metastasis pathways, which attribute to the higher risk of relapse in TNBC compared to other breast cancer subtypes. Another oncogenic driver known to be associated with TNBC is forkhead box protein M1 (FOXM1), where mitotic gene network mediated by FOXM1 is highly enriched in TNBC compared to Luminal breast cancers (2012a).

Similar to EZH2, overexpression of FOXM1 has been reported across multiple human malignancies and it has also been identified as one of the most upregulated oncogenes in tumors (Okabe et al. 2001; Pilarsky et al. 2004; Dai et al. 2007; Ahmad et

al. 2010; Bhat et al. 2011; Lok et al. 2011; Wang et al. 2011; Yau et al. 2011; 2012a; Gong and Huang 2012; Halasi and Gartel 2012; Uddin et al. 2012; Xia et al. 2012; Chen et al. 2013; Li et al. 2013; Xue et al. 2014; Li et al. 2015). Although FOXM1 is a transcription factor best known for its regulation in mitotic progression (Laoukili et al. 2008) however, hyperactivation of FOXM1 has been linked to invasion pathway and is associated with a higher metastatic potential (Korver et al. 1997; Dai et al. 2007; Ahmad et al. 2010; Lok et al. 2011; Yau et al. 2011; Gong and Huang 2012; Uddin et al. 2012; Xia et al. 2012; Chen et al. 2013; Li et al. 2013; Xue et al. 2014).

1.3.1 The Evolution of Forkhead Box Gene Family

FOXM1 belongs to an evolutionary conserved forkhead box (Fox) gene family, which is characterized by a common DNA binding domain termed the forkhead box domain or winged-helix domain (Weigel et al. 1989). The Fox gene family consists of 19 subfamilies designated by an English alphabet i.e. FoxA-FoxS, with its subclasses designated by an Arabic numeral i.e. FoxA1, FoxA2 and FoxA3 (Kaestner et al. 2000).

The conserved forkhead box DNA binding domain consists of an approximately 100 amino-acid residues was first identified in *Drosophila*, where no known protein motif of similar sequence was found at that time (Weigel et al. 1989). The encoding cDNA sequence was later cloned in a rat model, where its function in transcriptional regulation was further characterized and is now known as FoxA1 (Lai et al. 1990).

Since the discovery of FoxA1 as a homeotic gene in *Drosophila* development, numerous Fox-related genes have been identified in various species, and with each gene nomenclaturally assigned by their independent discoverers, it eventually posed a

challenge in keeping up with their discoveries and literatures (Kaestner et al. 2000). To address this issue, a proposal for a unifying symbol and a standardizing nomenclature based on a phylogenetic analysis on Fox-related genes in various species was implemented by a winged helix/forkhead nomenclature committee in 2000 (Kaestner et al. 2000).

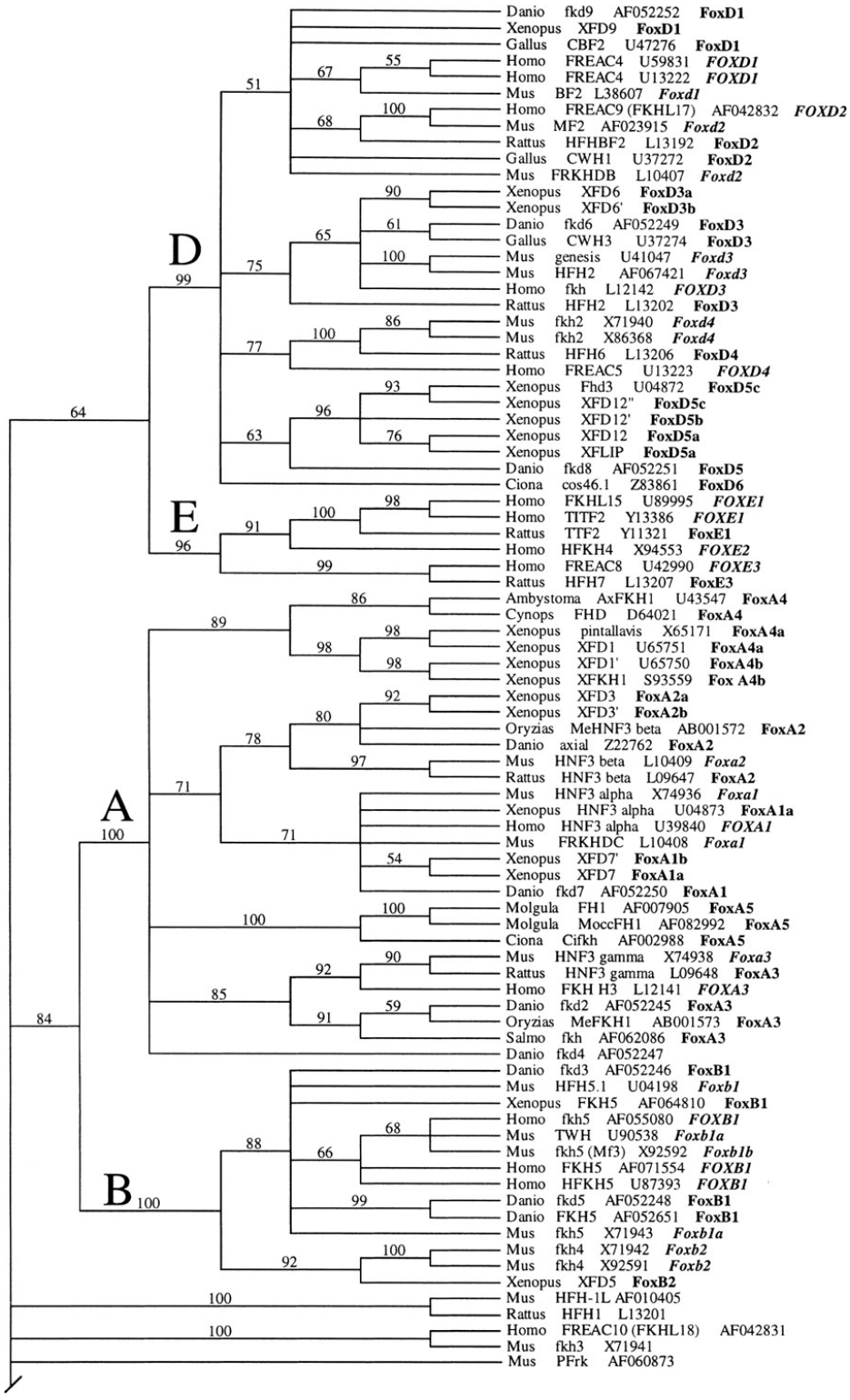
Danio fkd9 AF052252 FoxD1
Xenopus XFD9 FoxD1
Gallus CBF2 U47276 FoxD1
Homo FREAC4 U59831 FOXD1
Homo FREAC4 U13222 FOXD1
Mus BF2 L38607 Foxd1
Homo FREAC9 (FKHL17) AF042832 FOXD2
Mus MF2 AF023915 Foxd2
Rattus HFHBF2 L13192 FoxD2
Gallus CWH1 U37272 FoxD2
Mus FRKHDB L10407 Foxd2
Xenopus XFD6 FoxD3a
Xenopus XFD6' FoxD3b
Danio fkd6 AF052249 FoxD3
Gallus CWH3 U37274 FoxD3
Mus genesis U41047 Foxd3
Mus HFH2 AF067421 Foxd3
Homo fkh L12142 FOXD3
Rattus HFH2 L13202 FoxD3
Mus fkh2 X71940 Foxd4
Mus fkh2 X86368 Foxd4
Rattus HFH6 L13206 FoxD4
Homo FREAC5 U13223 FOXD4
Xenopus Fhd3 U04872 FoxD5c
Xenopus XFD12" FoxD5c
Xenopus XFD12' FoxD5b
Xenopus XFD12 FoxD5a
Xenopus XFLIP FoxD5a
Danio fkd8 AF052251 FoxD5
Ciona cos46.1 Z83861 FoxD6
Homo FKHL15 U89995 FOXE1
Homo TITF2 Y13386 FOXE1
Rattus TTF2 Y11321 FoxE1
Homo HFKH4 X94553 FOXE2
Homo FREAC8 U42990 FOXE3
Rattus HFH7 L13207 FoxE3
Ambystoma AxFKH1 U43547 FoxA4
Cynops FHD D64021 FoxA4
Xenopus pintallavis X65171 FoxA4a
Xenopus XFD1 U65751 FoxA4a
Xenopus XFD1' U65750 FoxA4b
Xenopus XFKH1 S93559 Fox A4b
Xenopus XFD3 FoxA2a
Xenopus XFD3' FoxA2b
Oryzias MeHNF3 beta AB001572 FoxA2
Danio axial Z22762 FoxA2
Mus HNF3 beta L10409 Foxa2
Rattus HNF3 beta L09647 FoxA2
Mus HNF3 alpha X74936 Foxa1
Xenopus HNF3 alpha U04873 FoxA1a
Homo HNF3 alpha U39840 FOXA1
Mus FRKHDC L10408 Foxa1
Xenopus XFD7' FoxA1b
Xenopus XFD7 FoxA1a
Danio fkd7 AF052250 FoxA1
Molgula FH1 AF007905 FoxA5
Molgula MoccFH1 AF082992 FoxA5
Ciona Cifkh AF002988 FoxA5
Mus HNF3 gamma X74938 Foxa3
Rattus HNF3 gamma L09648 FoxA3
Homo FKH H3 L12141 FOXA3
Danio fkd2 AF052245 FoxA3
Oryzias MeFKH1 AB001573 FoxA3
Salmo fkh AF062086 FoxA3
Danio fkd4 AF052247
Danio fkd3 AF052246 FoxB1
Mus HFH5.1 U04198 Foxb1
Xenopus FKH5 AF064810 FoxB1
Homo fkh5 AF055080 FOXB1
Mus TWH U90538 Foxb1a
Mus fkh5 (Mf3) X92592 Foxb1b
Homo FKH5 AF071554 FOXB1
Homo HFKH5 U87393 FOXB1
Danio fkd5 AF052248 FoxB1
Danio FKH5 AF052651 FoxB1
Mus fkh5 X71943 Foxb1a
Mus fkh4 X71942 Foxb2
Mus fkh4 X92591 Foxb2
Xenopus XFD5 FoxB2
Mus HFH-1L AF010405
Rattus HFH1 L13201
Homo FREAC10 (FKHL18) AF042831
Mus fkh3 X71941
Mus PFrk AF060873
D
E
A
B

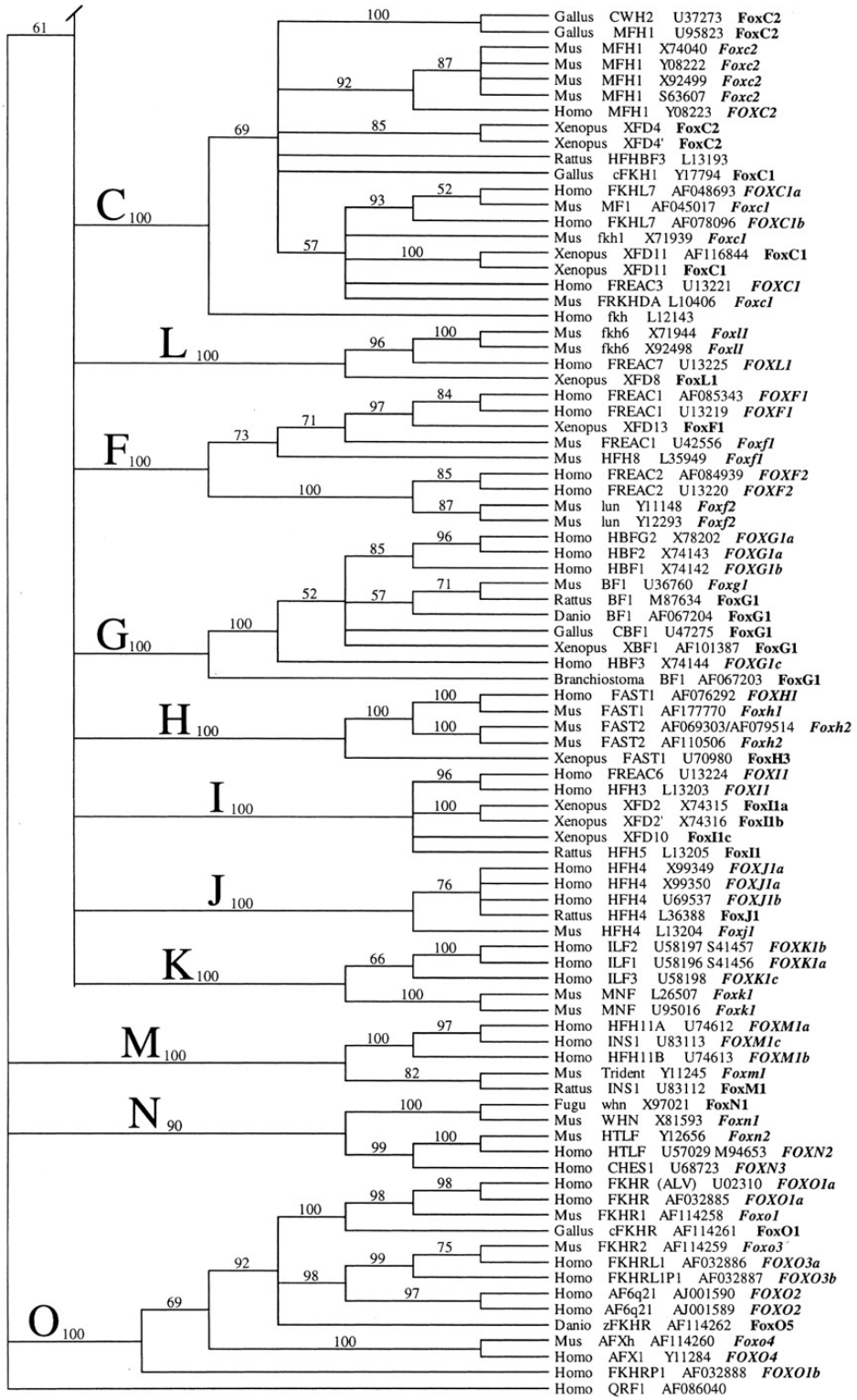

Figure 1.10. Fox Protein Family Tree

Phylogenetic analysis of Fox proteins in various species based on the amino acid sequence of the forkhead box domain. Bootstrap percentages are indicated in the interior branches (Image extracted from committee (Kaestner et al. 2000)

Due to the evolutionary conserved forkhead box DNA binding domain in different species, functional redundancy is often found in several Fox proteins. Particularly during lung morphogenesis in a developing mouse embryo, both FoxA1 and FoxA2 are co-expressed in respiratory epithelial cells and the deletion of either one of the genes could be compensated by the other subclass (Wan et al. 2005). On the other hand, gene duplication event over long evolutionary period could result in a newly evolved gene with a distinct function from its ancestral gene. A study in FOXP2 orthologs in human, chimpanzee, gorilla, orang-utan, macaque and mouse uncovered an intraspecific variation of FOXP2 gene sequence and nucleotide polymorphism specifically in human, which favors language acquisition and vocal learner particularly in human species.

Several Fox proteins have also been implicated in human malignancies such as FoxA, FoxC, FoxM, FoxO and FoxP proteins. Deregulated FoxA1 has been linked to breast cancer progression, where it acts as a co-factor for ER in luminal breast cancer (Carroll et al. 2005) and is required for cyclin D regulation with a consequent role in breast cancer proliferation (Eeckhoute et al. 2006). Other than high proliferative capacity, another fundamental component of malignancy is invasive capacity, and overexpression of FoxC2 in murine mammary carcinoma cells has been reported to play a crucial role in cancer cell invasion and metastasis by mediating EMT pathway furthermore, expression of FoxC2 is correlated with TNBC subtype in human breast cancer (Mani et al. 2007). Cancer cell invasion and metastasis can also be promoted through evasion of immune cell, and deregulated expression of FoxP3 promotes evasion of tumor immune surveillance through regulating T regulatory cells (Liu et al. 2007). In contrast, FoxO proteins are known for their roles as a tumor suppressor, where activation of both

FoxO3a and FoxO4 proteins induce cell cycle arrest (Kops et al. 2002). Furthermore, a broad somatic deletion of *FOXO1*, *FOXO3A* and *FOXO4* induced a progressive tumor development characterized by thymic lymphomas and hemangiomas in a mouse model, highlighting not only the role of FoxO protein as a bonafide tumor suppressor, but also functional redundancy of FoxO subfamily (Paik et al. 2007).

1.3.2 Different Isoforms of FOXM1

In term of its structural gene arrangement, human *FOXM1* gene consists of 10 exons and two of its exons, exon A1 and A2 (also termed as exon Va and VIIa respectively), are alternatively spliced at its transcript level generating 3 protein isoforms; FoxM1a, FOXM1b and FOXM1c (Figure 1.10) (Korver et al. 1997; Yao et al. 1997; Ye et al. 1997). At protein level, FOXM1 contains 3 functional domains; N-terminal autorepressor domain (NRD), forkhead DNA Binding domain (FKH) and C-terminal transactivation domain (TAD) (Laoukili et al. 2008). The largest protein isoform, FOXM1a, retains both alternative exons and one of the exon, exon A2, is inserted within the C-terminal TAD, which disrupts its transactivation function (Ye et al. 1997). Hence, FOXM1a is reported to be transcriptionally inactive and may also act as a dominant-negative since it still retains a functional FKH domain and able to bind to its target genes.

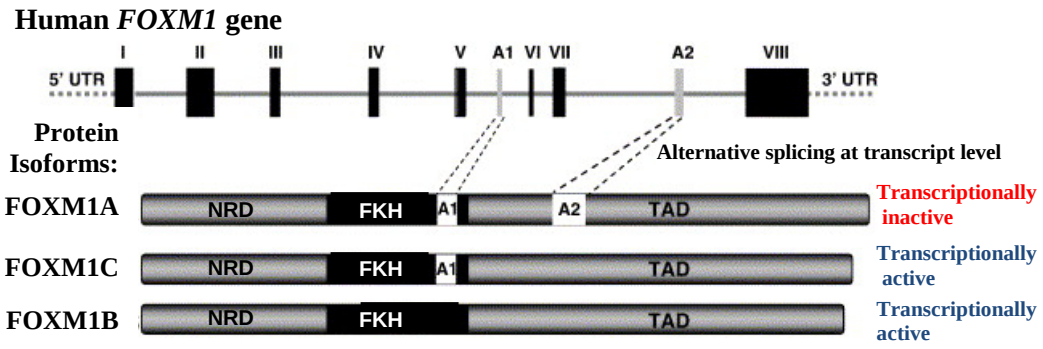

Figure 1.11. Domain Organization of FOXM1
FOXM1 gene consists of 10 exons with two of its exons; exon A1 and A2, alternatively spliced to generate 3 FOXM1 protein isoforms. FOXM1a retains both alternative exons, particularly in its transactivation TAD domain, rendering it transcriptionally inactive. While both FOXM1b and FOXM1c have functional transactivation and DNA binding FKH domains, rendering them transcriptionally active. (Image extracted and modified from (Laoukili et al. 2007))

Both FOXM1b and FOXM1c lack of the alternative exon A2 in their C-terminal TAD however, FOXM1c still retains the alternative exon A1 within its FKH domain (Ye et al. 1997). Due to functional C-terminal TAD, both FOXM1b and FOXM1c are transcriptionally active. Considering the role of FOXM1 protein as a transcription factor, these natural splice variants may have a role in modulating the activity of FOXM1 under different conditions. Although there is no intensive study done on functional regulation of FOXM1a isoform (Ma et al. 2005) however, it is likely that the transcriptionally inactive FOXM1a isoform may compete with transcriptionally active FOXM1b and FOXM1c isoforms in order to maintain a balanced gene regulation during normal development,

It is worth noting that FOXM1b isoform is specifically expressed in human testis and skin while FOXM1c isoform is ubiquitously expressed in several primary and secondary cell lines as well as in embryonic tissues, suggesting that the tissue-specific alternative splicing might have a regulatory significance (Yao et al. 1997; Chaudhary et al. 2000;

Teh et al. 2002; Ma et al. 2005; Wierstra and Alves 2006b; Wierstra and Alves 2006a). It is likely that the presence of the alternative exon A1 in the FKH domain of FOXM1 will determine the DNA binding specificity and preferential of different FOXM1 isoforms to its target genes.

Furthermore, several studies have shown that the alternative exon A1 contains RB binding motif hence, FOXM1c isoform is under negative regulation of RB and requires RAF/MEK/MAPK signaling for its activation (Ma et al. 2005; Wierstra and Alves 2006a; Wierstra and Alves 2006b; Lam et al. 2013). The stimulation by RAF/MEK/MAPK signaling helps in the processing of FOXM1c resulting into a more active and truncated form of FOXM1c isoform (Lam et al. 2013). On the other hand, FOXM1b that lack of the alternative exon A1 is not under the inhibitory effect of RB binding and hence, it does not require the proteolytic processing for its activation (Lam et al. 2013). As a consequence, FOXM1b isoform is upregulated in cancer cells with a higher transforming potential compared to FOXM1c despite both having similar transactivity potential.

1.3.3 Post Translational Regulation on FOXM1

Due to its key role in cell cycle progression and to prevent unscheduled entry into the cell cycle, both expression and activity of FOXM1 are strictly controlled and varied during cell cycle progression (Laoukili et al. 2008; Yau et al. 2011). The transcript level and protein expression of FOXM1 are not detectable in resting cells however, they are upregulated when cells are poised to enter cell cycle. The highest expression of FOXM1 is found during late G1 phase and early S phase, and its expression is subsequently

sustained throughout the remainder of cell cycle progression (Figure 1.11) (Korver et al. 1997; Yau et al. 2011).

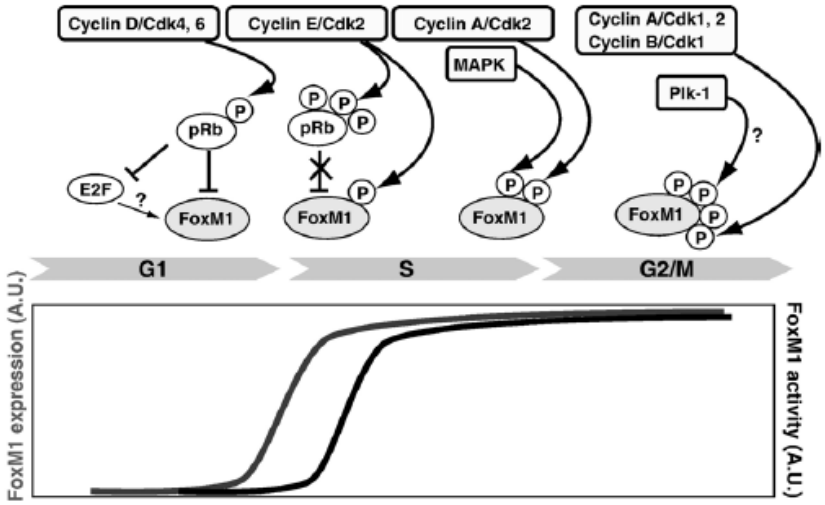

Figure 1.12. Post Translational Modification of FOXM1 Protein During Cell Cycle Progression

Regulation of FOXM1 expression and activity are subjected to different layer of post translational modifications by Cyclin-CDK2 and other proteins at each cell cycle phase. At G1 and S phase, Cyclin D-Cdk4/6 and Cyclin E-Cdk2 inactivate retinoblastoma protein through phosphorylation, relieving the inhibitory effect on FOXM1 protein posed by retinoblastoma protein. It is at this phase that the initiation of the phosphorylated FOXM1 protein takes place. At late S phase, both Cyclin A-Cdk2 and mitogen-activated protein kinase (MAPK) signaling cascade helps to further phosphorylate FOXM1 protein. FOXM1 protein reaches its full activation at G2/M phase mediated by the corresponding mitotic kinases and possibly polo-like kinase-1 (Plk-1) protein. (Image extracted from (Laoukili et al. 2007))

1.3.3.1 Post Translational Modification by Cyclin-CDKs

In order to exert its role as a transcription factor, FOXM1 requires further post translational modification for its activation. As cell cycle progresses, there will be a successive and cyclical expression, activation and inhibition of different cyclins and its interacting kinases; Cyclin D-CDK4/6 at G1 phase, Cyclin E-CDK2 at late G1 phase, Cyclin A-CDK2 at S phase, Cyclin A-CDK1 at G2 phase and lastly Cyclin B-CDK1 at mitotic phase (Figure 1.9) (Dehay and Kennedy 2007). These cyclin-CDKs will in turn

phosphorylate FOXM1 resulting in gradual increment in phosphorylated FOXM1 level and it reaches its maximum activity at mitotic phase (Laoukili et al. 2008). Major and colleagues reported that phosphorylated FOXM1 mediates the recruitment of transcriptional co-activator p300/CREB binding protein (CBP) and in turn helps with enhancement of FOXM1 transcriptional activity (Major et al. 2004; Chen et al. 2009).

1.3.3.2 Positive and Negative Autoregulation

Other than post translational regulation by cyclin-CDKs, FOXM1 also controls it own expression by having both positive and negative autoregulations (Laoukili et al. 2008; Halasi and Gartel 2009). A study in osteosarcoma cell line showed that exogenous expression of FOXM1 is able to induce endogenous level of FOXM1 at both transcript and protein levels (Halasi and Gartel 2009). This positive feedback regulation is not seen in other members of Forkhead family, suggesting that FOXM1 preferentially induces its own expression by binding to its own promoter. On the other hand, Laoukili and colleagues showed that the N-terminal NRD of FOXM1 protein acts as an autorepressor domain, inhibiting the activity of FOXM1 protein during G1 and S phases (Laoukili et al. 2008). In contrast, deletion or mutated RXL/LXL motifs on NRD results in constitutively active form of FOXM1 protein, relieved from its autoinhibitory regulation.

Taken together, the expression and activity of FOXM1 are strictly and timely regulated in response to cell cycle progression during normal development. Any mutation in mitotic kinases, proliferative signaling pathways or even in FOXM1 protein itself

could potentially contribute to aberrant expression and activity of FOXM1, which are often implicated in the onset of cancer progression.

1.3.4 Cellular Function of FOXM1 in Cell Proliferation

As a proliferation associated transcription factor, not only FOXM1 regulates genes important for cell cycle progression, but also genes essential for chromosome stability and DNA repair to ensure a proper execution of cellular proliferation (Ye et al. 1999; Wang et al. 2002; Kalinichenko et al. 2004; Krupczak-Hollis et al. 2004; Laoukili et al. 2005; Wonsey and Follettie 2005; Halasi and Gartel 2012). A study in *FOXM1* knockout mice showed that FOXM1 deficiency leads to various organ defects due to decreased proliferation of progenitor cell (Krupczak-Hollis et al. 2004), suggesting its critical role in cell proliferation. Cellular cell proliferation is tightly linked to cell cycle progression and consistent with this, FOXM1 deficiency also results in reduced expression of cell cycle-associated genes especially for those mediating S, G2 and M phases of the cell cycle (Wang et al. 2002; Kalinichenko et al. 2004; Krupczak-Hollis et al. 2004).

In contrast to FOXM1 knockout mice experiment, Ye and colleagues generated FOXM1 overexpression transgenic mice and showed that not only numerous genes associated with mitotic phase are upregulated in response to the transgenic overexpression, but also a premature onset of DNA replication and mitosis are observed (Ye et al. 1999). Interestingly, the transgenic overexpression effect does not cause any abnormal increased in proliferative capacity for non-proliferative tissue, suggesting that the effect of FOXM1 is only apparent for cells with high proliferative index.

Several microarray analyses identified FOXM1-regulated cluster genes centering on G2/M-phase associated genes, further refining the function of FOXM1 as a mitotic phase regulator (Laoukili et al. 2005; Wonsey and Follettie 2005). With their chromatin Immunoprecipitation (ChIP) assay, Laoukili and colleagues demonstrated direct binding of FOXM1 to the promoters of those G2/M-phase associated genes i.e. *CCNB1* and *CENPF*, further confirming the role of FOXM1 as a mitotic regulator (Laoukili et al. 2005).

In contrast, loss of FOXM1 leads to a delay in G2 phase progression, chromosome mis-segregation, mitotic spindle defect and ultimately resulting in mitotic catastrophe (Laoukili et al. 2005; Wonsey and Follettie 2005). More importantly, the expression profiling also uncovers several new set of FOXM1 target genes other than cell cycle-related genes involved in metabolism, extracellular matrix remodeling and other transcriptional regulation (Laoukili et al. 2005; Wonsey and Follettie 2005). Collectively, the above mentioned studies suggest a pleiotropic regulation of FOXM1 beyond cell proliferation.

1.3.5 Cellular Function of FOXM1 during Oxidative Stress

Reactive oxygen species (ROS) is a natural biological event produced regularly during aerobic condition in mammalian cells (Benz and Yau 2008). ROS is generated in mitochondria in several forms, which includes superoxide radical (O^{2-}), hydrogen peroxide (H_2O_2), hydroxyl radical ($^{\cdot}OH$) and singlet oxygen. To maintain physiological condition favorable for normal cell developments, mammalian cells are equipped with

antioxidant defense mechanism to scavenge for the excessive ROS, and FOXM1 has been implicated in this process (Park et al. 2009; Halasi et al. 2013).

Following induction of ROS, FOXM1 regulates the expression of several antioxidant gene expressions i.e. Superoxide Dismutase, Catalase and Peroxiredoxin 3 (Park et al. 2009). This negative feedback loop mediated by FOXM1 in response to ROS production helps to protect and to promote survival of both normal proliferating and tumor cells from oxidative stress. Moreover, Park and colleagues also identified oncogenic Ras is implicated in this oxidative stress response (Park et al. 2009). Oncogenic Ras induces cellular levels of ROS, which in turn leads to activation of FOXM1 expression as a negative feedback response.

Tumor cells expressing oncogenic Ras with elevated expression of FOXM1 during oxidative stress, which correlates with the production of antioxidant enzymes, are resistance to premature senescence and apopotosis (Park et al. 2009). As a biological consequence, tumor cells are addicted to FOXM1 for their survival during oxidative stress. Depletion of FOXM1 either by small interfering RNA knockdown or pharmacological inhibition of FOXM1 using bortezomib or thiostrepton, reverses the protective role from oxidative stress conferred by FOXM1 (Halasi et al. 2013).

1.3.6 Cellular Function of FOXM1 in Mediating Drug Resistance

Overexpression of FOXM1 has also been implicated in acquired chemoresistance, particularly in breast cancers (Carr et al. 2010; Kwok et al. 2010). To investigate the role of FOXM1 in acquired drug resistance, Kwok and colleagues generated a cisplatin-

resistant breast cancer cell line (Kwok et al. 2010). They demonstrated that elevated expression of FOXM1, at both transcript and protein levels, is seen in resistant cell line and it correlates with upregulation of genes involved in DNA repair mechanism, particularly BRCA2 and X-ray cross-complementing group 1 (XRCC1). Ablation of FOXM1, either through small interfering RNA knockdown or thistrepton treatment, abrogates the DNA damage repair pathway, and causes proliferative arrest and cell death in resistant cell line (Kwok et al. 2010).

In another study, overexpression of FOXM1 confers drug resistance in several HER2-enriched cell lines in response to Herceptin and paclitaxel (Carr et al. 2010). Herceptin is a targeted treatment designed for HER2-enriched breast cancer. However, only a modest response is observed in a single agent Herceptin treatment and hence, it is often used in combination with other microtubule stabilizing drugs (Burris 2000). On the other hand, paclitaxel is known to bind to tubulin and prevent dissociation of tubulin dimers during cell division, causing mitotic failure and subsequent cell death (Xiao et al. 2006). FOXM1 confers drug resistance in the context of Herceptin and paclitaxel by upregulating one of its direct target, a tubulin destabilizing protein Stathmin (Carr et al. 2010). By doing so, FOXM1 indirectly causes alteration in microtubule formation and protects the cancer cell from paclitaxel-induced apoptosis.

Further supports for the role of FOXM1 in mediating drug resistance in breast cancer come from works done by Millour and colleagues (Millour et al. 2010; Millour et al. 2011). In 2010, they investigated the role of FOXM1 in conferring endocrine resistance in luminal breast cancer and found that FOXM1 is under direct regulation of ERα (Millour et al. 2010). ERα binds to *FOXM1* promoter region and transactivates *FOXM1*

expression, which in turns leads to upregulation of FOXM1 downstream target Cyclin D1. The ERα-FOXM1-Cyclin D1 generates a positive feedback loop further enhancing the activity of FOXM1 and provides the underlying mechanism for endocrine resistant phenotype in luminal breast cancer (Millour et al. 2010).

In the subsequent year, they investigated the link between epirubicin resistant phenotype and FOXM1 in luminal breast cancer (Millour et al. 2011). Epirubicin is an anthracycline based chemodrug that acts by intercalating DNA strands causing DNA damage and cytotoxic cell death (Cantoni et al. 1989). Millour and colleagues found that epirubicin activates ataxia-telangiectasia mutated (ATM) and promotes E2F activity in resistant cell line (Millour et al. 2011). FOXM1 contains E2F binding site within its promoter region and hence, activation of E2F leads to upregulation of FOXM1 expression. In contrast, inhibition of ATM can resensitize the resistant cell line by downregulating expression of both E2F and FOXM1, leading to cell death.

1.3.7 Cellular Function of FOXM1 in Tumorigenicity

Tumorigenicity involves series of events culminating in tumor metastasis; starting from the initial vascularization of primary tumor, followed by increased cell motility and invasion of the basement membrane via secretion of MMPs, and lastly the EMT transition aiding in the dissemination of the invasive cancer cell to distant organ (Shook and Keller 2003; Hanahan and Weinberg 2011). Several studies have linked FOXM1 to early onset of tumorigenicity.

1.3.7.1 FOXM1 Links to Angiogenesis

The availability for oxygen and nutrients are crucial during cancer progression and this process is term as angiogenesis, which describes the formation of new blood vessels necessary for tumor growth. Many studies have identified VEGF as the principal mediator for angiogenesis, and FOXM1 has a direct role in activating VEGF through direct binding to forkhead binding elements within *VEGF* promoter (Zhang et al. 2008; Li et al. 2009; Karadedou et al. 2012). There is also a positive correlation between FOXM1, VEGF and distant metastasis in multiple human malignancies and inhibition of FOXM1 will significantly reduce the expression of VEGF (Wang et al. 2007; Zhang et al. 2008; Li et al. 2009; Ahmad et al. 2010).

1.3.7.2 FOXM1 Links to Cell Migration and Invasion

Enzymatic activity of MMPs has been linked to cancer cell migration and invasion and interestingly, FOXM1 expression directly correlates with MMP2, MMP7, MMP9 and MMP12 expressions (Dai et al. 2007; Wang et al. 2007; Wang et al. 2008; Balli et al. 2012; Xia et al. 2012). Wang and colleagues showed that suppression of FOXM1 in pancreatic cancer leads to downregulation of MMP2 and MMP9 expressions, which correlates with reduction in cancer cell angiogenesis, migration and invasion (Wang et al. 2007).

Similar observation has also been reported in glioblastoma, where Dai and colleagues showed that FOXM1 binds directly to the promoter region of *MMP2* regulating its transcriptional activation and protein expression (Dai et al. 2007). While in

lung cancer, Wang and colleagues showed that indirect activation of MMP9 by FOXM1 is through modulating the activity of one of its downstream target c-Jun N-terminal protein kinase 1 (JNK1) (Wang et al. 2008).

FOXM1 has also been shown to bind to the promoter region of *MMP7* and this regulation together with RhoC, and Rho-kinase 1 (ROCK1) mediates the cancer migration and invasion in hepatitis B virus (HBV)-associated hepatocellular carcinoma (HCC) (Xia et al. 2012). FOXM1 also serves as a poor prognostic marker for recurrence and survival of patients with HBV-HCC after surgical resection.

Interestingly, FOXM1 has also been implicated in tumor-associated macrophage during lung inflammation and tumor formation (Balli et al. 2012). Balli and colleagues showed that expression of FOXM1 in macrophage plays a critical role during tumor-associated pulmonary inflammation. It helps recruit macrophages to the tumor site, which in turn support the proliferation and promote lung tumor growth. Mice with macrophage-specific *FOXM1* deletion has reduced tumor size and number, which is consistent with reduced migration of tumor-associated macrophage, and one of the migration-related target genes implicated in this process is MMP12 (Balli et al. 2012).

1.3.7.3 FOXM1 Links to EMT

Despite a strong correlation between FOXM1 expression and poor prognosis in HCC, overexpression of FOXM1 could only marginally affect HCC progression (Park et al. 2011). It is because FOXM1 activity is under repression by its negative regulator, tumor suppressor $p14^{ARF}$. By generating transgenic mouse with Arf-null background,

Park and colleagues demonstrated a significant increase in FOXM1 and Akt expressions (Park et al. 2011). The Arf-/- HCC cells also displayed a low expression of E-cadherin but high expression of Vimentin and Snail, a classic signature of EMT-like phenotypes.

Paradoxically, FOXM1C has been reported to bind to the promoter region of *CDH1* and transactivates the expression of this tumor suppressor gene (Wierstra 2011). This finding suggests a new role of FOXM1 as a tumor suppressor. However, it is worth noting that the particular study was performed using normal kidney cells (Wierstra 2011), which has different gene regulation and signaling pathway compared with tumor cells (Park et al. 2011). It is likely that as a biological consequence, FOXM1 regulation differs during normal cell development and during cancer progression, which could explain the discrepancy between these 2 studies.

A study in pancreatic cancer showed that overexpression of FOXM1 mediates the acquisition of both EMT-like and cancer stem cell phenotypes (Bao et al. 2011). And these phenotypes can be reversed with the treatment of genistein, a natural chemo-preventive agent. In a separate study, FOXM1 mediates the acquisition of EMT-like phenotype by directly transactivate Caveolin-1 (Huang et al. 2012). Caveolin-1 is a structural protein of calveolar membrane domains, and there is a correlation between its overexpression and FOXM1 upregulation in pancreatic cancer cells and tumor tissues. Collectively, the above mentioned study defines FOXM1 as an important oncogenic driver during cancer progression, and that deregulated signaling of FOXM1 and its downstream targets promotes cancer development and eventually tumor metastasis.

1.4 Aims of Thesis Research

Identifying the gene expression patterns associated with shorter time to progression, invasive capacity, and metastatic propensity among different subtype of breast cancers, especially in TNBC, will be critical in predicting the clinical course of disease. Due to its highly heterogeneous nature and existence of different biological subgroups of TNBC (Lehmann et al. 2011b), it is necessary to identify molecular biomarkers associated with TNBC in order to improve both our understanding and ability to predict the overall severity of the disease. The ability to predict the overall severity of breast cancer will aids in the improvement of stratification of patients and a better disease management by ensuring that the patients will receive appropriate treatment.

In the initial phase of this study, both expressions of EZH2 and FOXM1 were identified to be highly upregulated in TNBC and were associated with poor prognosis. Particularly in FOXM1, where its hyperactivation has been shown to be significantly correlated with TNBC-like subtype and is associated with a high degree of proliferation rate (Ye et al. 1997). The aim of this study was to examine whether both EZH2 and FOXM1 works in concert in driving high proliferative capacity, which is one of the many characteristics of aggressive TNBC. By depleting EZH2 in TNBC cell lines, we identified reduction in the proliferating cancer cells. Similarly, depletion of FOXM1 also yielded similar phenotype to the case of EZH2 depletion. Therefore, we sought to dissect the possible crosstalk between EZH2 and FOXM1 in regulating proliferation pathway in TNBC.

In addition, FOXM1 exerts a tumorigenic role beyond cell cycle regulation as illustrated by Yau and colleagues in their study on two cohorts of breast cancer patients

differing in their ER status (Yau et al. 2011). Despite an elevated level of FOXM1 in ER- breast cancers, especially in TNBC, FOXM1 does not contribute to the tumor proliferative capacity directly instead; it is a reflection of its metastatic potential. This observation is further supported by the effect of FOXM1 depletion in neuroblastoma, pancreatic cancer, hepatocellular carcinoma and breast cancer where the cancer cells are viable and proliferating but with a severe consequence of reduction in tumorigenicity (Bhat et al. 2011; Wang et al. 2011; Halasi and Gartel 2012; Liu et al. 2012). Thus, the aim of the second phase of this study was to identify the molecular mechanistic that causes the switch in the role of FOXM1 from a proliferation regulator to an invasion regulator, and how EZH2 may assist in the switch. By integrating the key finding gathered from the first phase of study, where a novel interaction of EZH2 and FOXM1 was identified, we subsequently uncovered an antagonistic relationship between a canonical EZH2/PRC2 complex and a non-canonical EZH2/FOXM1 complex in promoting invasion pathway in TNBC.

This thesis highlights the plasticity of EZH2 activity during TNBC progression. Depending on its interacting partners, EZH2 may act as an epigenetic repressor or as a transcriptional co-activator. Whether the dual antagonistic role of EZH2 could be influenced by a biological stimulus e.g metabolic stress, oxidative stress, immuno-cytotoxic stress, etc would be an interesting future avenue to explore.

CHAPTER 2: MATERIALS AND METHODS

2.1 Cell Culture and drug treatment

All cell lines used in this study were obtained from the American Type Culture Collection and grown at 37 °C with 5% CO_2. MDA-MB-231, HS578T and BT549 were maintained in Dulbecco's modified Eagle's medium (DMEM) (Invitrogen) supplemented with 10% fetal bovine serum (FBS) (Invitrogen). SUM159PT was maintained in Ham's F-12 medium (Invitrogen) supplemented with 5% FBS, 5μg/mL insulin (Invitrogen) and 1μg/mL hydrocortisone (Invitrogen). MCF10A was maintained in mammary epithelial growth medium (MEGM) (Invitrogen) supplemented with 5% horse serum (Invitrogen), 20ng/mL EGF (Invitrogen), 0.5mg/mL hydrocortisone, 100ng/mL cholera toxin (Invitrogen) and 10μg/mL insulin. All media were supplemented with 5000U/mL penicillin/streptomycin (Invitrogen).

For drug treatment, cells were treated with DZNep and GSK126, purchased from Pharmaron Inc. (Beijing, China), for 24 hours and 72 hours respectively. The concentrations of the drugs were listed in the respective experimental figures. All of the tissue culture works were carried out under aseptic techniques inside a biological safety cabinet II.

2.2 Freezing and Thawing of Cultured Cell Lines

For cryopreservation, cells were trypsinized and centrifuged at 1000 rpm for 3 minutes. After discarding supernatant, cell pellets were resuspended with freezing media (For MCF10A: 90% culture media supplemented with 10% DMSO; for other cell lines: 90% FBS and 10% DMSO) and aliquoted into each cryovials with a concentration of

$1x10^6$/mL. The cryovials were placed inside Mr. Frosty cylinder (NALGENE) filled with 99% iso-propanol and stored at -80°C freezer. After 24 hours of incubation, the cryovials were transferred into a liquid nitrogen tank (-196°C) for a long term storage.

For thawing out frozen cells, the cryovials were thawed rapidly by full submersion inside 37°C water bath. The freshly thawed cells were resuspended with its respective complete media at 5mL/cryovial. The cells were further centrifuge at 1000 rpm for 3 minutes and seeded into T25 flasks (NALGENE). The cells were grown for 1 week post thawing before further experiments were performed. All of the cell lines used in the experiments were grown and maintained for less than 20 times passages.

2.3 Transfection of Small Interfering RNA (siRNA)

Transfection of siRNA was conducted using Lipofectamine RNAiMax (Invitrogen) according to the manufacturer's instructions. The initial steps involved individual preparation of siRNA and RNAiMax solution by diluting 20μM of siRNA and 2μL of RNAiMax with 100μL OPTI-MEM (Invitrogen). The two solutions were mixed together with equal parts and incubated for 20 minutes at room temperature. The medium of seeded cells, which were grown in a 6-well plate 18 hours prior to the transfection, was refreshed with 800μL complete medium before addition of the 200μL transfection mixture. After 6 hours, the transfection medium was replaced with 2mL of complete medium, and the cells were allowed to grow and harvested 48 hours post transfection for RNA extraction or 72 hours post transfection for protein extraction.

Target-specific siRNA and non-targeting control siRNA were purchased from Integrated DNA Technologies Pte. Ltd. (IDT) Singapore with the following target sequences:

Gene	siRNA Sequence
EZH2 (CDS)	5'-GACUCUGAAUGCAGUUGCU-3'
EZH2 (5'UTR)	5'- CGGUGGGACUCAGAAGGCA-3'
FOXM1 (CDS)	5'-GGACCACUUUCCCUACUUU-3'
EED #1	HSC.RNAI.N003797.12.1_ (IDT)
EED #2	HSC.RNAI.NOO3797.12.2_ (IDT)
SUZ12 #1	HSC.RNAI.NO15355.12.1_ (IDT)
SUZ12 #2	HSC.RNAI.N015355.12.2_ (IDT)

Table 2.1. siRNA sequences used for transfection of siRNA in cell lines.

2.4 Transfection of Plasmid Vectors

To generate plasmid vectors, target genes from their respective transient expression plasmids were subcloned into the PMN retroviral expression vector (a gift from Dr Linda Penn's lab, University Health Network, Canada). EZH2 WT plasmid had been described previously (Lee et al. 2011b) and FOXM1 WT plasmid was a gift from Prof. Eric Lam (Imperial College London, U.K.).

Transfection of plasmid vector was conducted using Lipofectamine 2000 (Invitrogen) according to the manufacturer's instructions. The initial steps involved individual preparation of plasmid vector and Lipofectamine 2000 solution by diluting 4μg of plasmid and 10μL of RNAiMax with 100μL OPTI-MEM (Invitrogen). The two

solutions were mixed together with equal parts and incubated for 20 minutes at room temperature. The medium of seeded monolayer platinum-A retroviral packaging cells (CELL BIOLAB), which were grown in a 6-well plate coated with collagen I (BD BIOCOAT) 18 hours prior to the transfection, was refreshed with 800μL complete medium before addition of the 200μL transfection mixture. After 24 hours, the transfection medium was replaced with 2.5mL of complete medium. After 48 hours post transfection, the conditioned medium from the transfected platinum-A cells contained retroviruses packaged with our target genes and this in turn was harvested and filtered through 0.45μm filter unit. The target cells, which were seeded in a 6-well plate 24 hours prior viral infection, were overlaid with 2mL conditioned media and 1mL complete media containing 3μL of 8μg/mL polybrene, followed by centrifugation at 1800 rpm for 90 minutes. After 48 hours post viral infection, the viral infected cells were sorted based on green fluorescent protein (GFP) over-expression and the sorted cells were subcultured and used for subsequent experiments.

2.5 RNA Extraction

Total RNA was isolated from various cell lines using Trizol (Invitrogen) and extracted with the RNAeasy Mini Kit (Qiagen). Cell pellets were collected by trypsinizing and harvesting monolayer cells. 1mL Trizol (Invitrogen) was added to the cell pellet, followed by addition of 200μL chloroform. The mixture was resuspended gently and followed by centrifugation at 12,000 rcf for 15 minutes at 4ºC to separate nucleic acids from proteins and other cell debris. After centrifugation, the top clear liquid

phase containing nucleic acids was transferred to a fresh tube followed by addition of 70% ethanol to precipitate the nucleic acids content.

To purify the RNA content, RNAeasy mini kit (Qiagen) was used. The mixture of nucleic acids and ethanol was transferred to the RNAeasy mini kit column to allow for RNA binding. The column was further centrifuged at 8,000 rcf for 30 seconds before washing once with 750µL RW1 buffer and twice with 500µL RPE buffer. At final step, the purified nucleic acids were eluted with 30µL RNAse-free water and their concentration and purity were assessed using Nanodrop ND-1000.

2.6 Complementary DNA Conversion and Quantitative Real-Time PCR (qRT-PCR)

To reverse transcribe and convert RNA samples into single-stranded complementary DNA (cDNA) samples, a High Capacity cDNA Reverse Transcription Kit (Applied Biosystems) was used. The initial step involved preparation of 750ng of RNA samples in 25µL nuclease-free water. A 25µL master mix solution containing 5µL RT buffer, 5µL random primers, 2µL dNTP mix, 2.5µL MultiScribe^{TM} reverse transcriptase and 10.5µL nuclease-free water, was prepared separately. Both the diluted RNA solution and the master mix were combined together and subjected to PCR amplification using thermo cycler at 25ºC for 10 minutes, followed 37ºC for 2 hours.

To perform qRT-PCR, cDNA samples obtained above were further diluted in a 10x dilution factor to yield a total volume 4.4µL/reaction, followed by dispensing into an individual well of 96-well reaction plate (Thermo Fisher MicroAmp® Fast Optical). A separate primer master mix was prepared by combining 0.4µL 10µM gene-specific

primer mix, 5ul 2X KAPA SYBR® FAST qPCR master mix (Kapa Biosystems) and 0.2μL KAPPA SYBR® FAST ROX dye (Kapa Biosystems). Lastly, 5.6μL primer master mix was mixed together with the cDNA sample inside each individual well of 96-well, and the sample was amplified and quantified with PRISM 7500 Fast Real-Time PCR system (Applied Biosystems). All reactions were performed in triplicate using the following primer sequences and actin level was used as an internal control:

Gene	Forward primer	Reverse primer
ACTB	GCACAGAGCCTCGCCTT	GTTGTCGACGACGAGCG
AURKB	AGGAGAACTCCTACCCCTGG	AGATGGGGTGACAGGCTCTT
CCNB1	TGGAAAAGTTGGCTCCAAAG	GATTTTGCAGAGCAAGGCAT
CDC2	CCCTCCTGGTCAGTACATGGA	GTTGAGTAACGAGCTGACCCC
CDC20	ATTCGCATCTGGAATGTGTG	TGTAATGGGGAGACCAGAGG
CENPF	AAGCCCAGCTCATTTTGTTC	GCGCCAGAACTGTACTCTCC
EZH2	AGTGTGACCCTGACCTCTGT	AGATGGTGCCAGCAATAGAT
FOXM1	AGGTGTTTAAGCAGCAGAAACG	GCTAGCAGCACCTTGGGGGCAA
MMP1	CCTCGCTGGGAGCAAACA	TTGGCAAATCTGGCGTGTAAT
MMP2	TGAGCTATGGACCTTGGGAGAA	CCATCGGCGTTCCCATAC
MMP7	GTTGTATGGGGAACTGCTGA	GTTTCCTGGCCCATCAAATG
MMP9	GGACGATGCCTGCAACGT	CAAATACAGCTGGTTCCCAATCT
UBE2C	AGCAGGAGCTGATGACCCT	GGCGTGAGGAACTTCACTGT

Table 2.2. Primer sequences used for qRT-PCR analysis of target genes.

2.7 Microarray Gene Expression Analysis

Total RNA was isolated from MDA-MB-231 using Trizol (Invitrogen) and extracted with the RNAeasy Mini Kit (Qiagen) as described above. Reverse transcription was performed using the RNA Amplification kit (Ambion) and microarray hybridization was performed using the Illumina Gene Expression Sentrix BeadChip HumanRef-8_V2 according to the manufacturer's instructions.

Briefly, 500ng RNA samples were reverse transcribed into cDNA samples and further processed into double- stranded cDNA samples. After cDNA purification step, biotinylated cRNA was generated and further purified before the hybridization step onto BeadChip. The biotinylated cRNA was further stained with streptavidin- Cy3 after washing. Lastly, the processed BeadChip was scanned using Illumina BeadArray Reader and images were stored with their repective barcodes. The scanned images were processed using Illumina GenomeStudio^{TM} and the generated data were analysed using GeneSpringGX^{TM} (Agilent Technologies) by selecting Illumina single color as an experimental type and median expression as a normalization control. Fold changes were analyzed by pairwise comparisons to internal controls. The normalized fold change data were further subjected to further bioinformatics analyses.

2.8 Gene Ontology Analysis using Ingenuity Pathway Analysis (IPA)

To determine differentially regulated genes after EZH2 depletion in MDA-MB-231 cell line, a two-fold cut-off was employed and the genes were further separated into upregulated and downregulated genesets. The downregulated geneset was then imported

into Ingenuity Pathway Analysis (IPA) software for gene ontology analysis. From the analysis; gene network, biological functions and upstream regulator analysis enriched in the imported geneset were obtained. The gene network and upstream regulator analysis were exported from IPA.

2.9 Clinical Dataset Analysis using TCGA and Oncomine Databases

To determine expression levels EZH2, FOXM1 and their co-target genes expressions in breast cancer patients, normalized mRNA expression data derived from the Agilent expression platform, "BRCA.exp.547.med.txt.", was obtained from TCGA breast cancer online portal (https://tcga-data.nci.nih.gov/docs/publications/brca_2012/)RNA-Seq). PAM50 subtype classifications were available for 547 of the primary breast invasive carcinoma tumor samples and these samples were further classified into four intrinsic subtypes of breast cancers: 98 TNBC, 58 HER2-enriched, 232 Luminal A and 129 Luminal B breast cancer patients. To generate heatmaps, median-normalized data were represented in $\log_2$ values and were processed by Cluster (Eisen, 1998, Stanford University) and visualized by Treeview (Eisen, 1998, Stanford University).

To further establish the correlation between EZH2 and FOXM1 expressions, two microarray data sets from Curtis (Curtis et al. 2012) was downloaded from Oncomine (https://www.oncomine.org/). Pearson Correlation was calculated between gene expression values of EZH2 and FOXM1 in these two data sets.

2.10 Histone Extraction, Protein Extraction and Immunoblots

For histone extraction, cells were lysed in Triton-X extraction buffer (1XPBS, 0.5% Triton-X-100 and 2mM PMSF) for 10 minutes. The histone pellet was collected by centrifugation at 5000 rpm for 10 minutes at 4ºC, followed by an overnight acid digestion in 0.2N HCl at 4°C. The next day, the histone was harvested by centrifugation at 13,000 rpm for 10 minutes at 4ºC and its concentration was determined by Nanodrop ND-1000.

For protein lysate, cells were lysed in radioimmunoprecipitation assay (RIPA) buffer (50mM Tris-HCl pH7.4, 1mM EDTA, 150mM NaCl, 1% Igepal CA630, 0.5% sodium deoxycholate, 1mM Na2VO4, 20mM NaF, 1mM PMSF, and mini-Complete protease inhibitor (Roche)) and incubated on ice for 1 hour, with 15 minutes interval of 15 seconds vortex. The lysate was further sonicated for 15 seconds using an XL2000 Microson Ultrasonic Processor (Misonix) followed by centrifugation at 13,000 rpm for 15 minutes at 4ºC. The supernantant containing protein lysate was transferred to a new tube and the protein concentration was determined using Bradford Assay (Bio-rad). Using bovine serum albumin (BSA) with a known concentration, a serial dilution was performed as the standard and on the other hand, the protein sample was diluted into a 20x dilution factor. Both the standard and diluted protein sample were mixed with Bradford reagent and incubated at room temperature for 7 minutes before being measured using Tecan Xfluor™ software.

Equal amount of histone extract (3µg) or protein extract (30µg) were separated on SDS-polyacrylamide gels and transferred to PVDF membranes. The membranes were blocked with 5% milk or 5% BSA according to the antibody requirements and immunoblots were probed with the following antibodies: anti-EED (07-368), anti-H3K27me3 (07-449) and anti-SUZ12 (07-379) were purchased from Upstate Biotechnology. Anti-Cyclin B (sc-245)

and anti-FOXM1 (sc-500) were purchased from Santa Cruz. Anti-Aurora A (CST-4718), anti-CDC2 (CST-9112), anti-EZH2 (CST-3147) and anti-PLK1 (CST-4513) were purchased from Cell Signaling. Anti-p-EZH2 Thr487 (Ab-109398) and anti-Actin were purchased from Abcam and Sigma-Aldrich respectively.

2.11 Co-Immunoprecipitation (coIP)

Co-Immunoprecipitation was performed by a whole cell lysis with 1ml of Immunoprecipitation (IP) lysis buffer (20mM Tris-HCl, pH 7.4, 2mM EDTA, 25mM NaF, 1% Triton X-100, and mini-Complete protease inhibitor (Roche)) incubated on ice for 1 hour. The lysates were centrifuged at 13,000 rpm for 10 minutes at 4ºC and the supernatants were transferred to fresh a tube. The samples were further diluted with 500µL IP lysis buffer and precleared with 30µL Protein A agarose beads (Roche) for 2 hour. After 2 hours, the samples were collected by centrifugation at 13,000 rpm for 30 seconds at 4ºC. The samples were further immunoprecipitated with 3µg antibody pull down and Protein A/G agarose bead (Roche) by rotating in a cold room for overnight. The next day, the agarose beads were washed three times with washing buffer (50 mM Tris-HCl, pH 8.0, 150 mM NaCl, 1% Nonidet P-40, 0.5% sodium deoxycholate, and 0.1% SDS). The immune complexes were eluted with sample buffer containing 1% SDS and DTT (Cell Signaling) for 5 min at 95°C. The sample was separated by SDS-polyacrylamide gels and transferred to PVDF membranes for immunobloting. Antibodies used for pull down were: non-specific IgG (sc-2025 or sc-2027) and anti-FOXM1 (sc-500

or sc-502) purchased from Santa Cruz. Anti-EZH2 (39901 or 39875) was purchased from Active Motif.

2.12 Chromatin Immunoprecipitation (ChIP) and Sequential ChIP

Chromatin Immunoprecipitation was performed by harvesting 3 x 10^6 cells using trypsinization, followed by a cell fixing with 81µL 37% formaldehyde (Sigma-Aldrich). The fixing was quenched with 192µL 2M glycine and the cells were washed twice with ice cold 1XPBS. Cell pellets were then lysed with 300µl SDS lysis buffer (1% SDS, 10mM EDTA, 50mM Tris-HCl pH 8.0) and sonicated for 2 minutes and 40 seconds (10 seconds pulse on and 30 seconds pulse off). The cell lysate was transferred to 15mL Falcon tubes and top-up with Dilution buffer (0.01% SDS, 1% Triton X-100, 1mM EDTA, 10mM Tris-HCl pH 7.4, 140mM NaCl) to 3mL. Samples were then precleared with 30µL Protein G Dynal Beads (Life technologies) and 2µg Rabbit IgG for 4 hours with rotation at 4ºC. Pre-cleared chromatin was immunoprecipitated with 3µg specific primary antibodies and rotated overnight at 4ºC. The next day, 30µL Protein G Dynal Beads were added into the immunocomplexes and further incubated for 2 hours. The Beads were subsequently washed thrice with the Dilution buffer, and the immunoprecipitated chromatins were eluted with 100µL SDS Elution Buffer (1%SDS, 10mM EDTA, 50mM Tris-HCl pH 7.5) and shook at 68ºC for 10 minutes. The supernatants were recovered using magnetic rack and transferred to fresh tubes for an overnight decrosslinking at 68ºC. Purification of immunoprecipitated DNA was performed using PCR purification kit (Qiagen) following manufacturer's protocol.

Sequential ChIP was performed with similar procedures as ChIP assay above except that the elution step was performed with 240μL 10mM DTT (Cell Signaling) and shook at 37ºC for 30 minutes. The eluate was subsequently subjected to second IP using the same protocol as mentioned above. Antibodies used for ChIP were as followed: anti-EZH2 (39901, Active Motif), anti-FOXM1 (sc-500, Santa Cruz), anti-EED (09-733, Millipore), anti-H3K27me3 (9744, Cell Signaling) and a non-specific IgG (sc-2027, Santa Cruz). The immunoprecipitated DNA and input DNA were quantified by qPCR analysis with the following ChIP promoter primer sequences:

Primer		**Forward primer**	**Reverse primer**
Gene	**ID**		
AURKB		GGGGTCCAAGGCACTGCTAC	GGGGCGGGAGATTTGAAAAG
CCNB1		CGCGATCGCCCTGGAAACGCA	CCCAGCAGAAACCAACAGCCGT
FOXM1		CCGGAGCTTTCAGTTTGTTC	CGGAATGCCGAGACAAGG
MMP2	P1	TGCTGGAGTTCCCCATCA	GCATGTTAAAGGAAGCACCCA
	P2	AACCAGTCTTGCCCAATTTC	CCTTCTGCAAATGTGTAAGCC
	P3	AAAACGGACAAAGAGTTGGC	TGTTTACCGAAGCCCCTCC
	P4	ATGTTGTCTTGTGAGCGTGC	AACAAGGGAGCAGATATCCC
MMP7	P1	CAAAATGACATGAATCCACC	ATATCAGTAGTTGTGTGGGC
	P2	GGTAAGATGACTGTTAAGGT	ATATCCAATAAAGGACTGTT
	P3	ATACCTATGAGAGCAGTCAT	CATCGTTATTGGCAGGAAGC
	P4	ATTGCATATTCCTGGGCGGT	CATTAGAAACATGTGTAGGG
ACTB		AGTGTGGTCCTGCGACTTCTAAG	CCTGGGCTTGAGAGGTAGAGTGT

Table 2.3. ChIP primer sequences used for qRT-PCR analysis of target gene promoters.

Quantification of promoter binding enrichment was defined as the percentage of the whole cell lysate relative to the input DNA. The fold enrichment was calculated by normalizing the specific antibody enriched against the nonspecific IgG-enriched chromatin. All ChIP promoter primer sequences were synthesized and purchased from AITbiotech Singapore. The ChIP promoter primer sequences for proliferation-associated genes (*FOXM1*, *CCNB1* and *AURKB*) (Sanders et al. 2013) and for invasion-associated genes (*MMP2* (primer ID: P2) and *MMP7* (primer ID: P2)) (Xia et al. 2012) were made as previously reported respectively.

2.13 Beta-Galactosidase Senescence Marker

To investigate for the presence of senescence, cells were stained with β-galactosidase staining kit (Cell Biolabs) according to the manufacturer's protocol. Briefly, cells were seeded into a 6-well plate (Corning) and fixed with 1X Fixing solution 48 hours post siRNA transfection. After washing the fixed cells with 1X PBS, the cells was overlaid with freshly prepared cell staining working solution supplemented with X-gal and incubated at 37ºC protected from light for overnight. Cells were further washed with 1X PBS before viewing under a light microscope (NIKON Eclipse TS100).

2.14 Cell Proliferation Assay

To measure the rate of cellular proliferation, cells were assayed with CellTiter-Glo (CTG) (Promega) according to the manufacturer's protocol. Cells were lysed with CTG

solution and chemiluminescent signal was detected with a microplate reader (TECAN). For siRNA transfection, cells were seeded into a 96-well white polystyrene plate (Corning) 24 hours post transfection and allowed to grow for 7 days, with measurement taken every 2 days. For drug treatment, cells were treated 24 hours after cell seeding and the measurement was taken the following day for 9 days. The growth rate was calculated by normalizing CTG values obtained with those taken on day 1 and plotted against time.

2.15 Mitotic Index

To measure the percentage of cells in mitotic phase, cells were harvested and fixed in 70% ethanol. Fixed cells were then resuspended with permeabilizing solution (PBS, 0.1% bovine serum albumin, 0.25% Triton X-100) and incubated for 15 minutes. Cells were further stained with 10μL Alexa Fluor® 555 Rat anti-Histone H3 pS28 (BD Pharmingen), 100μg/mL RNase (Invitrogen) and 50μg/mL Propidium Iodide (PI) (Sigma-Aldrich). The flow-cytometric analysis for DNA content was performed using FACSCalibur (Becton Dickinson Instrument). Cell cycle fractions and cells positive for p-H3 were quantified using the CellQuest software (Becton Dickinson).

2.16 Transwell Invasion Assay

For invasion assay, a 24-well Falcon FluoroBlok Transwell insert (BD Biosciences) with a pore size of 8μm was overlaid with 250μg/mL of growth factor-reduced Matrigel (BD Biosciences) for 6 hours at 37°C. For MDA-MB-231, 2.5 x 10^4 cells were seeded in

each insert with DMEM supplemented with 0.5% FBS. For MCF10A, 5 x 10^4 cells were seeded in each insert with MEGM supplemented with 0.5% horse serum. Chemoattractants used were the complete medium used for each cell lines and were added outside the chamber. Invaded cells were fixed after an indicated incubation time using 3.7% formaldehyde (Sigma-Aldrich) and stained with 25μg/mL PI. Ten fields per insert were scanned and average invaded cells were counted in triplicate using Cellomics ArrayScan.

2.17 Statistical Analysis

The experimental results presented in the figures are representative of at least three independent observations. The data are presented as the mean values ± SEM. Comparisons between groups were evaluated by Student's *t* test. For multiple comparisons involving more than 2 groups, One-way ANOVA or Two-way ANOVA were employed depending on the intrinsic experimental data to be analyzed. Values of at least $*P \leq 0.05$ were considered to be statistically significant or as indicated in each figure legends. All statistical tests and generation of graphs were done using Graphpad Prism Version 5.

CHAPTER 3: EZH2 AND FOXM1 REGULATION IN PROLIFERATION PATHWAY

3.1 Identification of EZH2 Dependent Co-regulatory Gene Network in TNBC

To explore the possibility of non-PRC2 complex function of EZH2 independent of its repressive H3K27me3 activity, we exploited EZH2 positively-regulated transcriptome in a TNBC cell line. This was achieved by depleting EZH2 expression using siRNA in MDA-MB-231 cell line, followed by cDNA microarray hybridization. Subsequent gene expression analysis led to the identification of 445 genes (Appendix 1) that were downregulated upon EZH2 depletion (with fold change ≥ 2, FDR $\approx$1% and $p < 0.01$) (Figure 3.1A, left) and this group of genes was thought to be under positive regulation of EZH2, though their downregulation could also be due to an indirect effect. Nevertheless, to gain further insights into the role of histone methyltransferase independent function of EZH2, we performed Gene Ontology analysis using IPA on the 445 EZH2-positively regulated genes and identified several gene networks (Figure 3.1A, right). Most networks identified by IPA were associated cell cycle, DNA repair, cellular movement and inflammatory response. Consistent with our previous report that showed the axis of inflammatory response is well interconnected with positive EZH2 regulation on NF-κB pathway (Lee et al. 2011b), our IPA analysis has also identified the enrichment for this particular gene regulatory network.

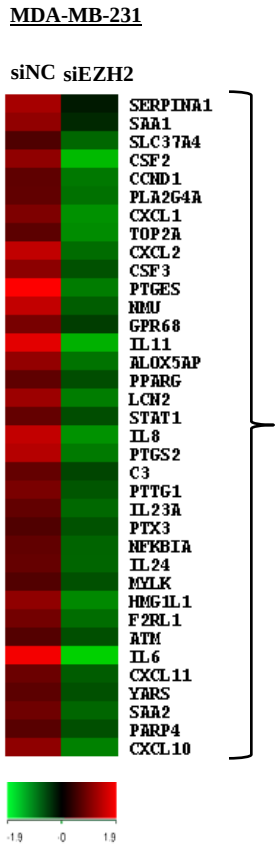

ID	Associated Network Functions	Score
1	Cell cycle, cellular assembly or organization, DNA replication, recombination and repair	48
2	Cancer, organismal injury and abnormalities, reproductive system disease	48
3	Cell cycle, cellular movement, cancer	48
4	Inflammatory response, cancer, cellular movement	48
5	Developmental disorder, hematological disease, hereditary disorder	48

Figure 3.1 EZH2 positively correlates with FOXM1 and its associated gene network in aggressive breast cancer.
Gene heatmap showing the downregulation of genes following EZH2 depletion in MDA-MB-231 cells (left) and their associated GO analysis by IPA (right).

On the other hand, the notion of EZH2 as the sole regulator for these gene networks identified by IPA might be an oversimplification. Coupled with previous studies of identification of novel non-PRC2 partners of EZH2 (Cha et al. 2005; Shi et al. 2007b; Tan et al. 2007; Holm et al. 2010; Lee et al. 2011b; He et al. 2012; Holm et al. 2012; Lee et al. 2012; Xu et al. 2012; Jung et al. 2013b; Jung et al. 2013a; Kim et al. 2013; Yan et al. 2013; Gonzalez et al. 2014b; Gonzalez et al. 2014a), it is very likely for EZH2 to work in concert with other molecule in regulating these newly identified EZH2-positively regulated gene networks. To determine candidate upstream regulators that potentially co-regulates with EZH2, we further utilized IPA for upstream regulator analysis and identified top 10 candidate regulators (Figure 3.2). As expected, the top hit is EZH2,

further reflecting the robustness of IPA analysis in predicting upstream regulators under EZH2 depletion condition.

No.	Upstream Regulators	*P-value*
1	EZH2	4.23E-15
2	E2F1	1.11E-10
3	PPARA	3.68E-08
4	FOXM1	2.84E-07
5	NFYA	1.35E-04
6	ATF2	2.71E-04
7	JUN	3.04E-04
8	IRF6	3.19E-04
9	NFKB1	3.75E-04
10	E2F2	6.29E-04

Figure 3.2 IPA upstream regulator analysis.
IPA analysis identifies top 10 candidate regulators mediating EZH2-positively regulated gene networks. *P-value* is indicated for respective candidate regulators.

From the previous analysis of 453 breast carcinomas, TNBC subtype was reported to be highly enriched for a mitotic gene network mediated by either c-Myc or FOXM1 activation (2012a). Since FOXM1 is identified as one of the potential upstream regulator by IPA analysis and to explore the possibility of coregulation between EZH2 and FOXM1, we performed a hierarchical clustering using microarray dataset from TCGA breast cancer cohort. Strikingly, EZH2, FOXM1 and FOXM1 target genes associated with mitotic progression were highly enriched in TNBC subtype (Figure 3.3A).

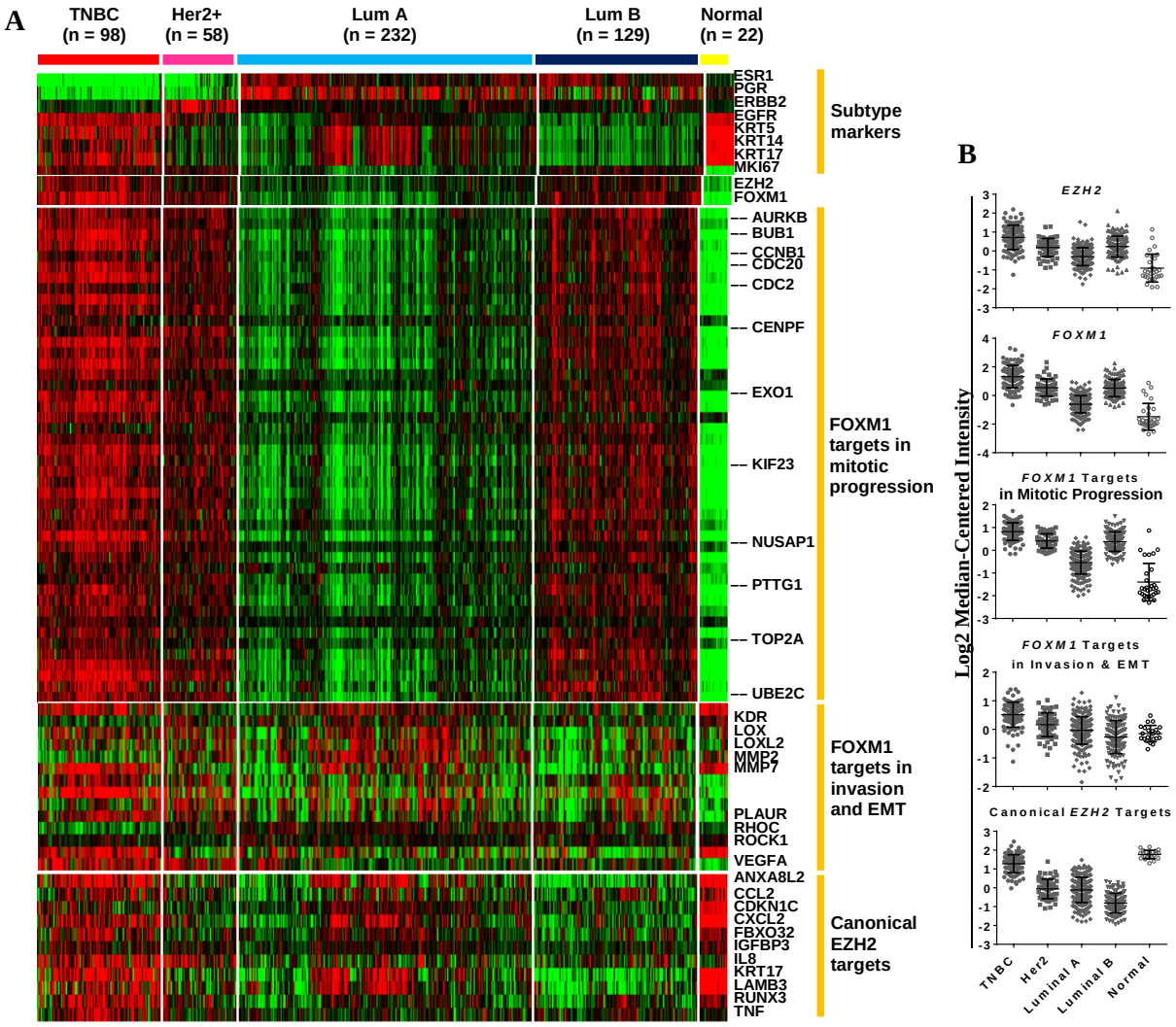

Figure 3.3 Hierarchical Clustering in Breast Cancer Patients.
(A) Hierarchical clustering downloaded from TCGA database showing four subtypes of tumors are colored as: TNBC, red; Her2-enriched, pink; Luminal A, light blue; and Luminal B, dark blue. Normal breast tissue is colored as yellow as a comparison. (*B*) Quantification of each gene expressions from the gene clusters (right) as log2 median-centered intensity.

Although similar observation was also seen in Her2-enriched and Luminal B subtypes however, the commonly known PRC2 targets were downregulated in these two subtypes as opposed to TNBC. This finding indicates with interest that despite the overexpression of EZH2, the repressive H3K27me3 activity is reduced only in TNBC,

further demonstrating the histone methyltransferase independent function of EZH2 is associated with TNBC subtype.

Other than cell cycle regulator, FOXM1 is also known for its role during early onset of cancer metastasis and 3 pathways have been reported to be associated with FOXM1 role; angiogenesis, cell migration and invasion, and EMT (Dai et al. 2007; Wang et al. 2007; Wang et al. 2008; Zhang et al. 2008; Li et al. 2009; Ahmad et al. 2010; Bao et al. 2011; Park et al. 2011; Balli et al. 2012; Huang et al. 2012; Karadedou et al. 2012; Xia et al. 2012). We also observed enrichment for these subsets of genes in TNBC, further reflecting the invasive nature of this particular breast cancer subtype.

To further establish coregulation of EZH2 and FOXM1, we analyzed 2 independent data sets from Curtis (Figure 3.4A) and TCGA (Figure 3.4B) downloaded from Oncomine. Pearson's correlation calculation showed statistically significant correlation between expression of EZH2 and FOXM1 in these 2 breast cancer cohorts. Collectively, our data indicate that coregulation of EZH2 and FOXM1 is specific to invasive TNBC subtype and it does not require repressive histone methyltransferase activity of EZH2.

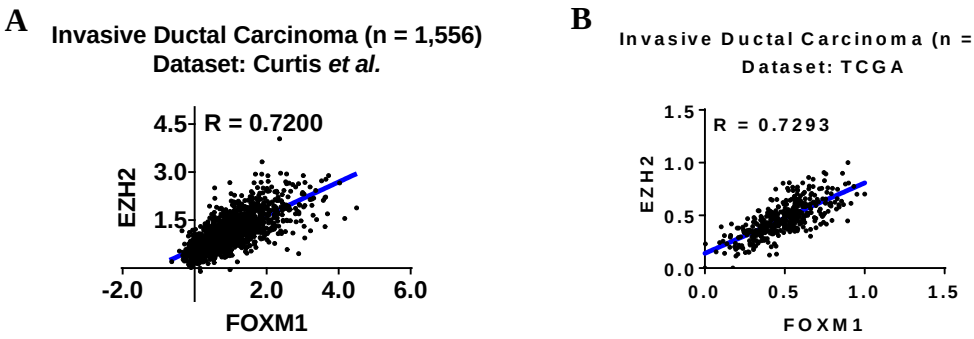

Figure 3.4 Pearson's correlation in 2 breast cancer cohorts.
Pearson's correlation calculation showing a significant correlation between EZH2 and FOXM1 in (*A*) Curtis breast cancer dataset and (*B*) TCGA breast cancer dataset. Both datasets are downloaded from Oncomine database and R-value is indicated for respective cohorts.

3.2 EZH2 Positively Modulates FOXM1 and Its Target Gene Expressions for Mitotic Progression

To further validate our microarray data, we sought to deplete EZH2 by siRNA in MDA-MB-231 cell line and determined its effect on FOXM1 and its target genes expressions by immunoblots and qRT-PCR analyses. Depletion of EZH2 and the associated H3K27me3 activity by siRNA caused the downregulation of not only FOXM1 but also its commonly known mitotic targets at both protein (Figure 3.5A) and mRNA (Figure 3.5B) levels in MDA-MB-231 cell line. At the same time, we also performed FOXM1 depletion as a comparison. True to its function as a mitotic regulator, we also observed reduction in its mitotic targets similar to the effects seen in EZH2 depletion.

Interestingly, depletion of either EZH2 or FOXM1 caused downregulation of FOXM1 and EZH2 respectively at both protein and mRNA levels, which raised two possibilities; 1) EZH2 and FOXM1 regulates each other protein stability, 2) EZH2 and FOXM1 regulates each other transcriptional activity. This question would be addressed by performing EZH2 ChIP and FOXM1 ChIP and determining their occupancy on each other promoters in the later part of this thesis.

Nevertheless, our initial validation showed coregulation of EZH2 and FOXM1 on FOXM1 mitotic targets. Although there was a possibility that the downregulation of those mitotic targets by EZH2 depletion could be an indirect effect mediated in part by downregulation of FOXM1. In our subsequent ChIP experiments, we would prove that indeed EZH2 regulation on FOXM1 mitotic targets was an indirect effect through modulating FOXM1.

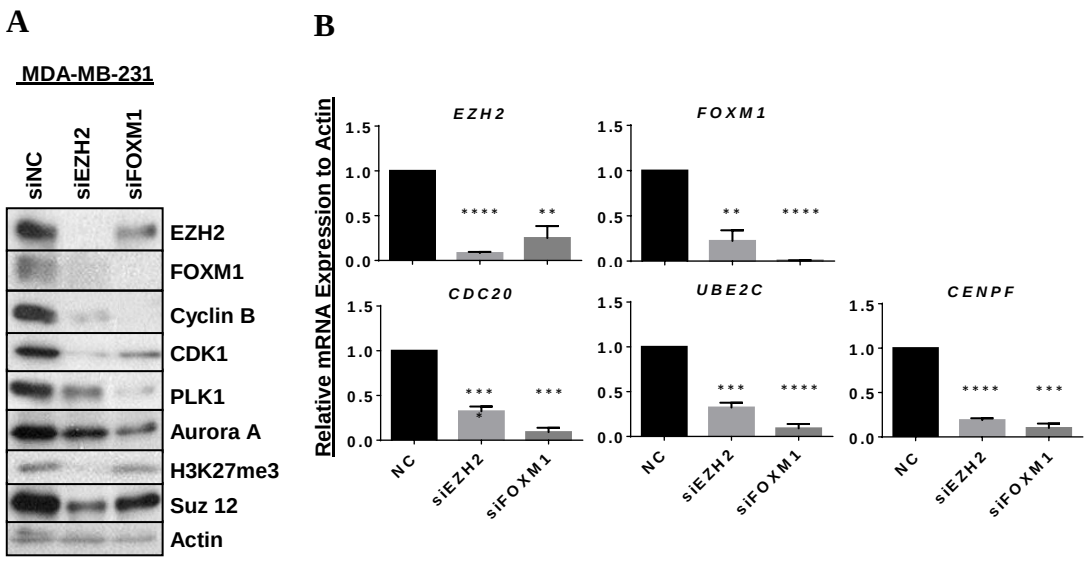

Figure 3.5 EZH2 positively modulates FOXM1 and its target gene expressions.
(*A*) Immunoblots and (*B*) qRT-PCR analysis of MDA-MB-231 cells upon EZH2 or FOXM1 depletion utilizing siRNA knockdown system. Student *t* test was used as a statistical analysis and all the data in the graph bars represented ± SEM; ***P-value* ≤ 0.01, ****P-value* ≤ 0.001, *****P-value* ≤ 0.0001

To eliminate the possibility of cell type-specific effect, we also performed EZH2 depletion in multiple TNBC cell lines i.e. SUM159PT, HS578T and BT549; using multiple EZH2 siRNA sequences (Figure 3.6A). Consistent with the effect seen in MDA-MB-231, all of the TNBC cell lines also demonstrated downregulation of FOXM1 and Cyclin B1 upon EZH2 depletion. The incomplete knockdown effect by siRNA targeting the 5'UTR region of EZH2 was due to the difficulty to achieve an efficient knockdown for this particular region. 5'UTR region is often G-C rich and some region may bind to RNA-binding proteins, collectively these factors contribute to reduce knockdown efficiency as siRNA may not be able to form a complete base-pairing at this region.

To validate the specificity of our siRNA effects, we again utilized the siEZH2 UTR in MDA-MB-231 cell line and thus, has no effect on the exogenous wild-type (WT)

EZH2, which was ectopically expressed in this particular TNBC cell line. This plasmid rescue experiment effectively restored the endogenous EZH2 depletion effects (Figure 3.6B). The exogenous WT EZH2 not only restored EZH2 and FOXM1 levels, but also the mitotic target of FOXM1, Cyclin B1. This rescued data indicated that our EZH2 depletion effects seen on the mitotic targets of FOXM1 was specific to EZH2 modulation and our WT EZH2 plasmid was able to rescue the depletion effectively.

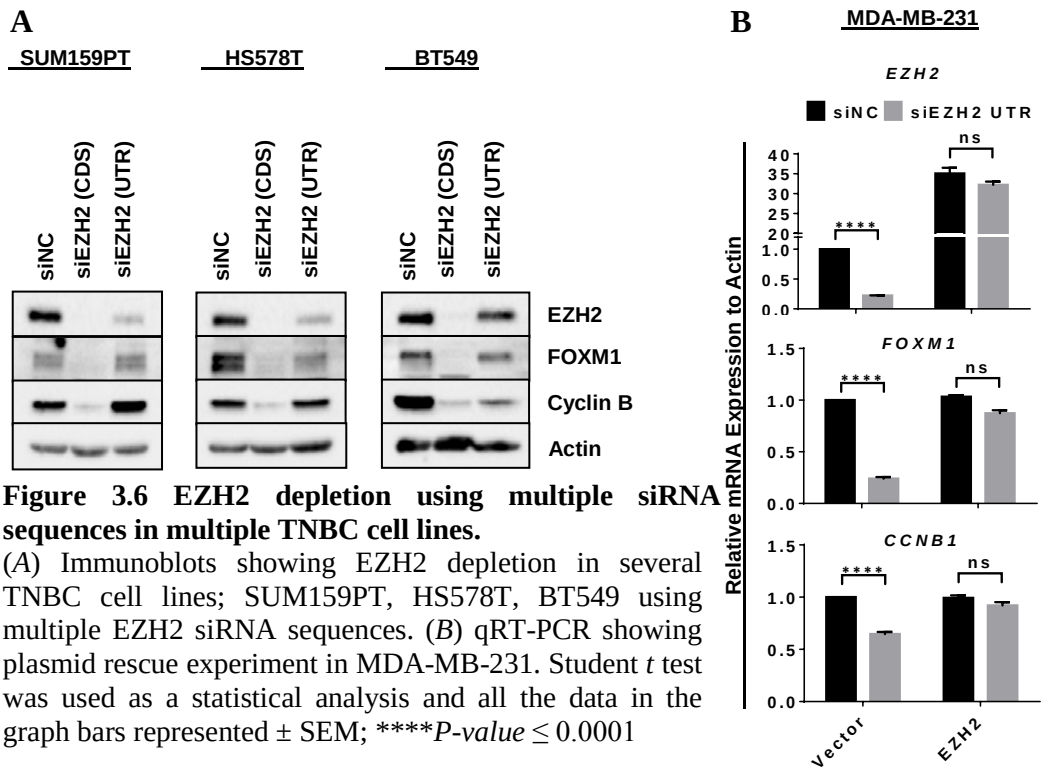

Figure 3.6 EZH2 depletion using multiple siRNA sequences in multiple TNBC cell lines.
(*A*) Immunoblots showing EZH2 depletion in several TNBC cell lines; SUM159PT, HS578T, BT549 using multiple EZH2 siRNA sequences. (*B*) qRT-PCR showing plasmid rescue experiment in MDA-MB-231. Student *t* test was used as a statistical analysis and all the data in the graph bars represented ± SEM; ****$P\text{-}value \leq 0.0001$

It was worth noting that ectopic expression of WT EZH2 did not induce upregulation of FOXM1 expression, although depletion of EZH2 (Figure 3.5 and 3.6) led to reduction of FOXM1 at both protein and mRNA levels in multiple TNBC cell lines, suggesting that EZH2 might regulate protein stability of FOXM1. To explore this possibility, we

measured the retention of FOXM1 protein after Nocodazole release. It has been reported that the maximum expression and the highest activity of FOXM1 is at mitotic phase (Laoukili et al. 2008) and FOXM1 protein is gradually degraded past this point until the next cell cycle begins.

We next stimulated MDA-MB-231 cell to undergo mitotic phase using Nocodazole treatment before releasing the mitotic cells in a Cycloheximide supplemented medium, followed by several cell harvests for protein extraction in interval. Cycloheximide is a global protein inhibitor and it was used in this protein stability assay to prevent any confounding factor from other proteins that may have effects on FOXM1 stability. By comparing ectopic expression of WT EZH2 in MDA-MB-231 with empty vector using immunoblots and densitometry analysis, we observed a marked increase in FOXM1 protein stability in the WT EZH2 overexpression cell (Figure 3.7A). Although the Nocodazole release experiment suggested that EZH2 had a positive role in maintaining FOXM1 protein stability however, we could not exclude the possibility of EZH2 regulation at FOXM1 transcript level. It is possible that the overexpression of FOXM1 commonly seen in TNBC has reached its maximum tumorigenicity level and it could not be further induced, despite the overabundance of its positive regulator. In accordance to this theory, we also observed no significant difference in term of mitotic index between overexpressed WT EZH2 and empty vector in MDA-MB-231 (Figure 3.7B), despite the retention of FOXM1 seen in the former cell construct.

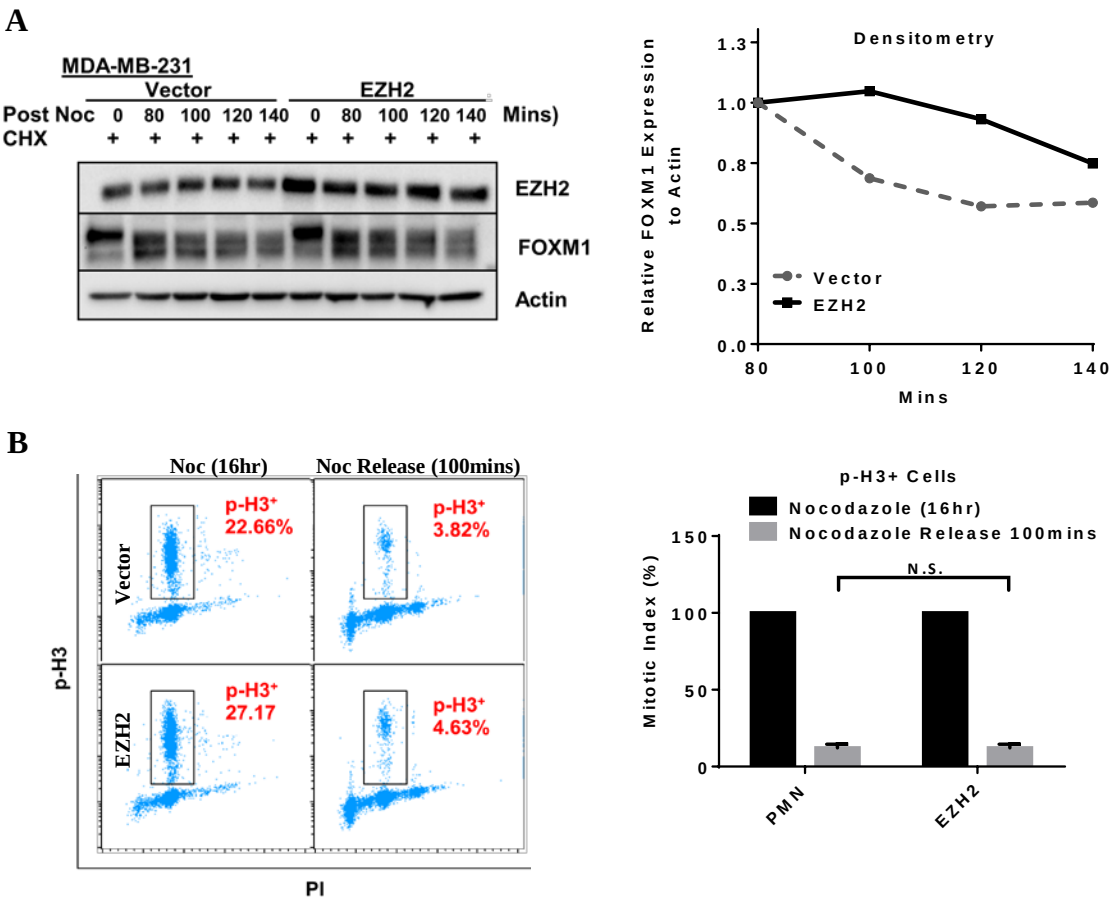

Figure 3.7 EZH2 promotes FOXM1 protein stability.
(*A*) Immunoblot and densitometry analysis in Nocodazole release experiment showed retention of FOXM1 protein in overexpressed WT EZH2 in MDA-MB-231 cell compared to empty vector. (*B*) Mitotic index in Nocodazole release experiment comparing overexpressed WT EZH2 and empty vector in MDA-MB-231 cell. Student *t* test was used as statistical analysis and all the data in the graph bars represented ± SEM.

On the other hand, depletion of PRC2 members; SUZ12 and EED, had no effect on the expression of FOXM1 and its mitotic target genes at both protein (Figure 3.8A) and mRNA levels (Figure 3.8B). We utilized multiple siRNA sequences for the SUZ12 and EED depletions to eliminate the possibility of sequence-specific effect for our immunoblots. Since both siRNA sequences targeting either SUZ12 or EED achieved

similar knockdown efficiency at protein level, we randomly chose one siRNA sequence for each gene to be used for qRT-PCR analyses.

It was noteworthy that the downregulation of EZH2 protein (Figure 3.8A) but not its mRNA level (Figure 3.8B) was observed in either SUZ12 or EED depletion, which is consistent with previous reports (Cao and Zhang 2004b; Pasini et al. 2004; Montgomery et al. 2005). Similarly, Depletion of EED caused downregulation of SUZ12 proteins (figure 3.8A) but not its mRNA level (Figure 3.8B) and vice versa. In order for PRC2 complex to exert a robust methyltransferase activity, at least 3 subunits have to be present and intact, and they are EZH2, EED and SUZ12 (Cao et al. 2002; Cao and Zhang 2004b; Pasini et al. 2004; Ketel et al. 2005; Montgomery et al. 2005; Nekrasov et al. 2005). Disruption of either one of these proteins will affect the stability of PRC2 complex as a whole, which was demonstrated in our immunoblots knockdown experiments in MDA-MB-231 cell line. Taken together, our data suggested that the methyltransferase activity of PRC2 complex was not required for the regulation of FOXM1 and its mitotic targets in TNBC model.

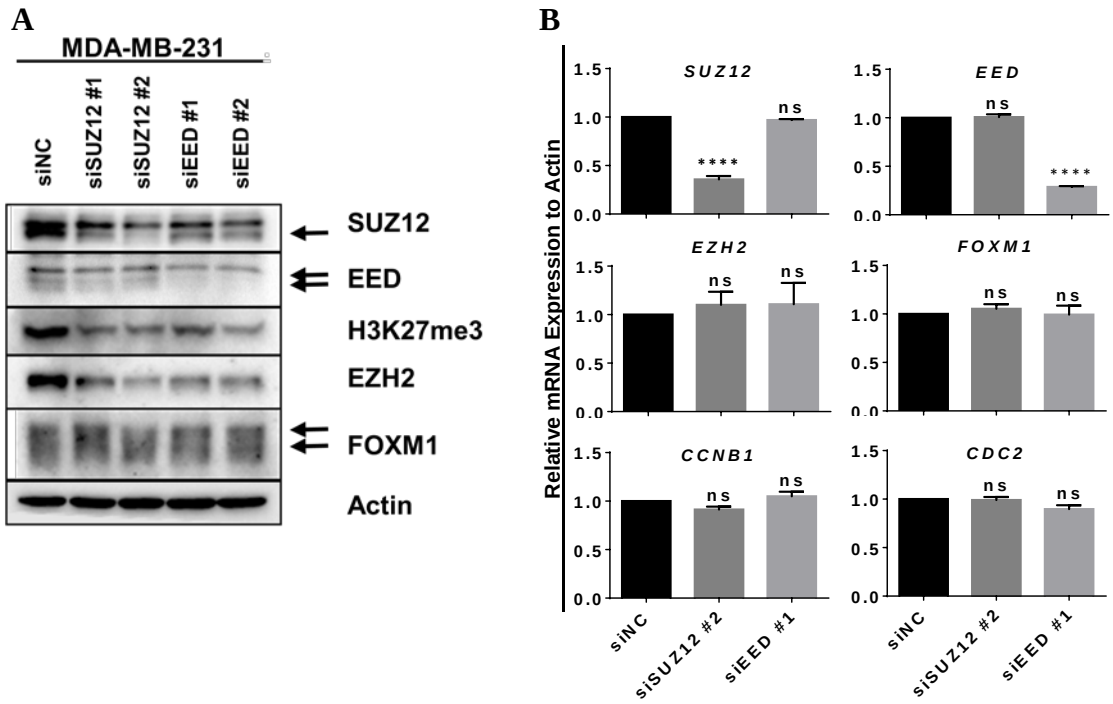

Figure 3.8 EZH2 positively modulates FOXM1 and its target gene expressions.
(*A*) Immunoblots and (*B*) qRT-PCR analysis of MDA-MB-231 cells upon SUZ12 or EED depletion utilizing siRNA knockdown system. Student *t* test was used as statistical analysis and all the data in the graph bars represented ± SEM; ****$P\text{-value} \leq 0.0001$

3.3 Depletion of EZH2 or FOXM1 Shares Similar Biological Consequences in Cell Proliferation

Both EZH2 and FOXM1 have been reported to regulate cell cycle progression in multiple malignancies (Korver et al. 1997; Varambally et al. 2002; Bracken et al. 2003; Kleer et al. 2003; Shi et al. 2007b; Ahmad et al. 2010; Derfoul et al. 2011; Yau et al. 2011; Bao et al. 2012; Gong and Huang 2012; Uddin et al. 2012; Jung et al. 2013a; Yan et al. 2013). We next asked whether biological consequences resulting from depletion of EZH2 or FOXM1 in TNBC would also affect cell proliferation and in particular, mitotic progression. We first compared EZH2 and FOXM1 effects in cell proliferation using MDA-MB-231 cell line and found that after siRNA depletion, both EZH2-depleted cells

and FOXM1-depleted cells underwent senescence as shown by the presence of blue-stained cells using β-galactosidase senescence assay when compared to siNC control (Figure 3.9A top panel). On the other hand, no blue-stained senescent cells were observed in either EED-depleted cells, or SUZ12-depleted cells (Figure 3.9A bottom panel).

Subsequent investigation for the cell growth rate using CTG proliferation assay was consistent with the observation seen in senescence assay, where the inhibitory effect in cell growth was only observed in EZH2-depleted cells and FOXM1-depleted cells, but was not observed in EED-depleted cells and SUZ12-depleted cells (Figure 3.9B). Especially at day 7, where there was a significant reduction in growth rate for EZH2-depleted cells and FOXM1-depleted cells when compared to siNC control cell cells. However, both EED-depleted cells and SUZ12-depleted cells had a similar growth rate as siNC control cells. Taken together, our phenotypic assays suggesting a histone methyltransferase independent activity of EZH2, where depletion of either subunits of PRC2 complex had no effect on both growth arrest and cell proliferation in general.

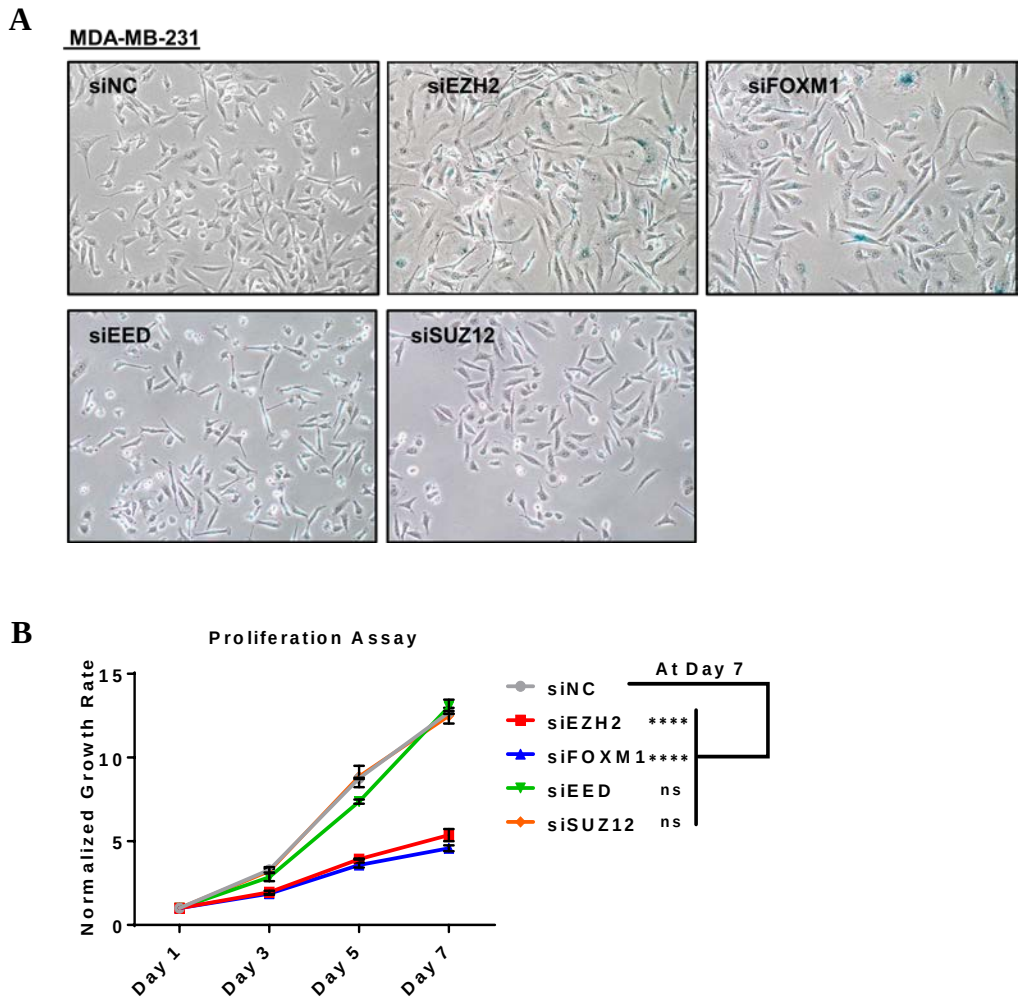

Figure 3.9 EZH2 and FOXM1 role in cell proliferation.
(*A*) Beta-galactosidase staining for senescence marker in MDA-MB-231. Blue staining in EZH2-depleted cells and FOXM1-depleted cells indicated presence of senescence. (*B*) MDA-MB-231 cells depleted for EZH2, FOXM1, EED or SUZ12 were seeded in a 96-well format and their proliferation rates were measured every alternate day for 7 days. The proliferation rate for each knockdown cell was individually compared to non-targeting siRNA (siNC) cells. Two way ANOVA was used as statistical analysis and all the data in the graph bars represented ± SEM; ****$P\text{-value} \leq 0.0001$

To investigate whether the inhibitory effects seen in cell proliferation, in particularly mitotic phase, could be rescued by ectopic expression of WT FOXM1, we performed endogenous EZH2 depletion in WT FOXM1 overexpressed MDA-MB-231 cell line followed by mitotic index. During mitosis, histone H3 is phosphorylated at its serine

residue 28 (H3 pS28) (Tapia et al. 2006) and by fixing and staining cells with antibody specific for H3 pS28, we were able to quantify for mitotic cells using FACS analysis. From our mitotic index analysis, ectopic expression of WT FOXM1 could modestly rescue the inhibitory effect in mitotic progression due to endogenous EZH2 depletion (Figure 3.10A), further demonstrating the role of FOXM1 in regulating this biological pathway.

The rescued effects were also seen at mRNA levels, with a modest rescued expression seen for CDK1 (gene name *CDC2*) and Cyclin B after ectopic expression of WT FOXM1 (Figure 3.10B). Both CDK1 and Cyclin B are known for their active roles in mitotic progression (Dehay and Kennedy 2007) yet FOXM1, a well known mitotic regulator, was not able to effectively rescue the EZH2-mediated depletion phenotype. Since activation of FOXM1 is dependent on its post translational modification, it is possible that the ectopic expression of WT FOXM1 may not be able to fully recapitulate the endogenous activity of FOXM1, which has been downregulated due to EZH2 depletion. Hence, both CDK1 and Cyclin B expressions could not be fully restored to their basal levels.

Furthermore, our FOXM1 plasmid still retains the N-terminal NRD, which acts as an autorepressor of FOXM1 activity (Laoukili et al. 2008) and as such, the ectopic WT FOXM1 plasmid may not be able to readily direct its activity in-vitro. Interestingly, ectopic expression WT FOXM1 could modestly induce mRNA level of EZH2 (Figure 3.10B), further suggesting the possibility of FOXM1 in transactivating *EZH2* gene expression. Nevertheless, both of our rescued phenotypic data and qRT-PCR analysis

indicated that the EZH2-FOXM1 axis might potentially regulate biological pathway other than cell proliferation in MDA-MB-231 cell.

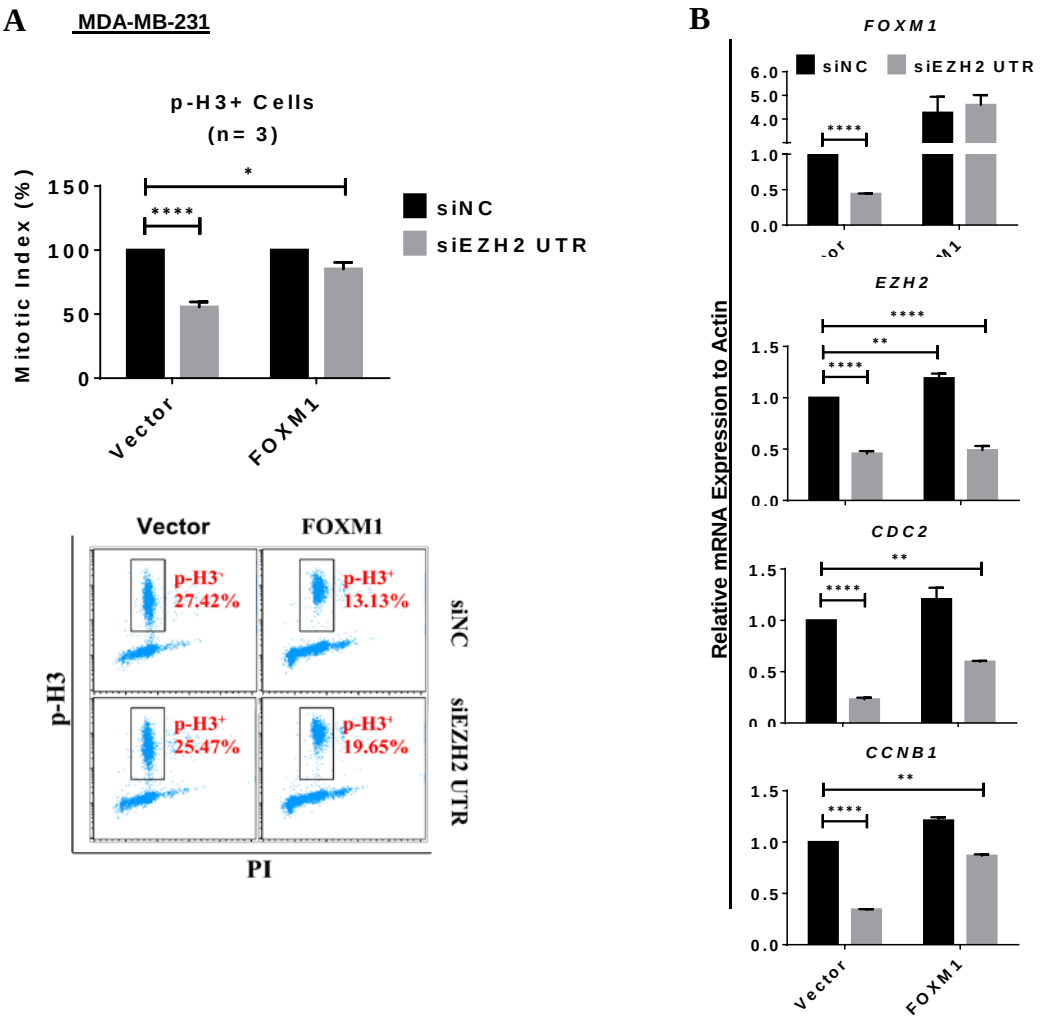

Figure 3.10 Functional rescue experiments for mitotic progression.
EZH2 depletion in MDA-MB-231-FOXM1 overexpression cells were analyzed for (*A*) mitotic index and (*B*) qRT-PCR. For mitotic index, cells were synchronized for mitotic phase using 100ng/ml Nocodazole, incubated for 16 hours and harvested for FACS analysis. Percentages of cells positive for p-H3 (S28) were indicated. Two way ANOVA was used as a statistical analysis and all the data in the graph bars represented ± SEM; **P-value* ≤ 0.05, ***P-value* ≤ 0.01, *****P-value* ≤ 0.0001

3.4 EZH2 Forms a Protein Complex with FOXM1 Independent of PRC2 Members

Since depletion of either EZH2 or FOXM1 not only affected each other expressions (Figure 3.5), but also exhibited similar biological consequence in reduction of cell proliferation (Figure 3.9), we next explored the possibility that EZH2 might form a direct physical interaction with FOXM1. In endogenous coIP performed in MDA-MB-231, EZH2 was co-precipitated with FOXM1 and members of PRC2 complex, EED and SUZ12 (Figure 3.11A left). However, on the other direction of pull-down assay, FOXM1 was found to be co-precipitated with EZH2 but not with EED or SUZ12 (Figure 3.11A right). These results indicated that EZH2 forms 2 separate protein complexes; a canonical PRC2 complex and a non-canonical EZH2/FOXM1 complex in TNBC. This data was consistent with our previous report (Lee et al. 2011a), where we observed 2 groups of gene sets differentially regulated by EZH2 upon EZH2 depletion – EZH2-negatively regulated gene set and EZH2-positively regulated gene set. Previous work identified the non-canonical EZH2/RelA/RelB complex and in this current work, the non-canonical EZH2/FOXM1 complex.

To investigate whether similar observation could also be replicated in other TNBC cell lines, we performed coIP in SUM159PT and HS578T. Consistent with the observation seen in MDA-MB-231, we also observed EZH2/FOXM1 protein complex in both SUM159PT (Figure 3.11B) and HS578T (Figure 3.11C), further validating the bi-directional non-canonical EZH2/FOXM1 complex in TNBC. This finding raised several questions; 1) whether the non-canonical EZH2/FOXM1 complex had any role in breast cancer progression and 2) whether the methyltransferase activity was still required for the

physical interaction. These two questions would be subsequently addressed in the later part of this thesis.

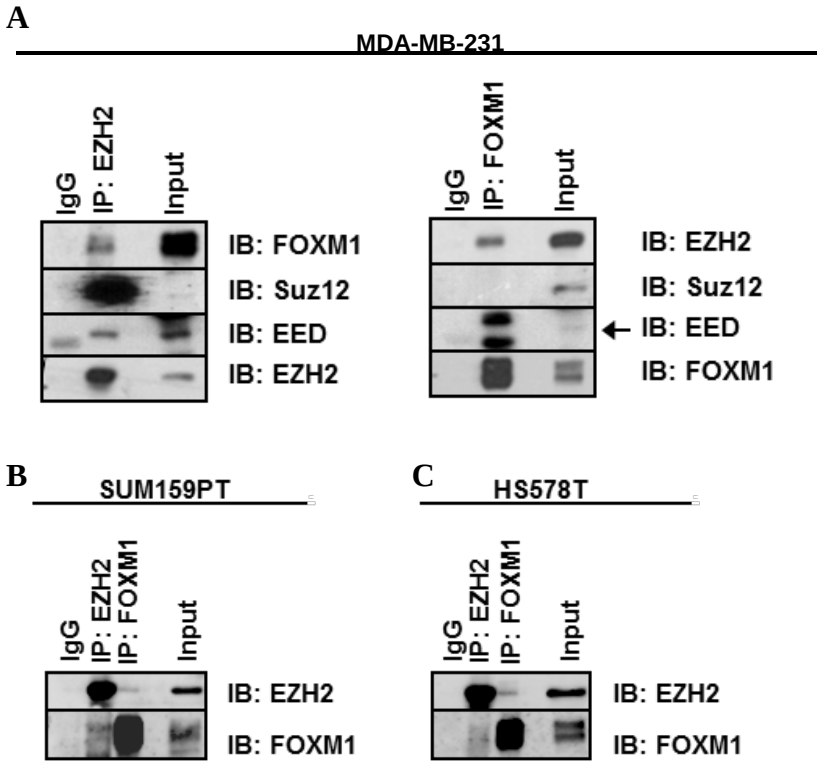

Figure 3.11 EZH2 forms both canonical EZH2/PRC2 complex and non-canonical EZH2/FOXM1 complex in TNBC.
immunoblot analysis showing bi-directional coIP of (*A*) MDA-MB-231, (*B*) SUM159PT and (*C*) HS578T cell lysates using indicated pull down antibodies followed by immunoblot analysis.

3.5 FOXM1 Occupies Promoters of its Target Genes in Mitotic Progression

With known role in cell cycle progression for both EZH2 and FOXM1 (Korver et al. 1997; Varambally et al. 2002; Bracken et al. 2003; Kleer et al. 2003; Shi et al. 2007b; Ahmad et al. 2010; Derfoul et al. 2011; Yau et al. 2011; Bao et al. 2012; Gong and Huang 2012; Uddin et al. 2012; Jung et al. 2013a; Yan et al. 2013), coupled with similar

inhibitory effects in cell proliferation at both gene expressions (Figure 3.5) and phenotypic analysis (Figure 3.9), we attempted to explore the potential of these two molecules in binding to the promoter of FOXM1 targets in mitotic progression using ChIP assay.

We first conducted single ChIP pull down for EZH2 and FOXM1 and investigated their occupancies on promoters of two known mitotic targets of FOXM1; Cyclin B and Aurora Kinase B. We also included *CNR1* promoter as a positive control for EZH2 ChIP pull down and *ACTB* promoter as a negative control. We detected significant enrichment of FOXM1 on *CCNB1* and *AURKB* promoters (Figure 3.12), further supporting the known role of FOXM1 on these mitotic targets. Furthermore, we also detected significant enrichment of EZH2 to its own target promoter. In contrast, we did not detect any enrichment of EZH2 on these promoters. These initial observations suggested that only FOXM1 directly regulated its mitotic targets and not EZH2.

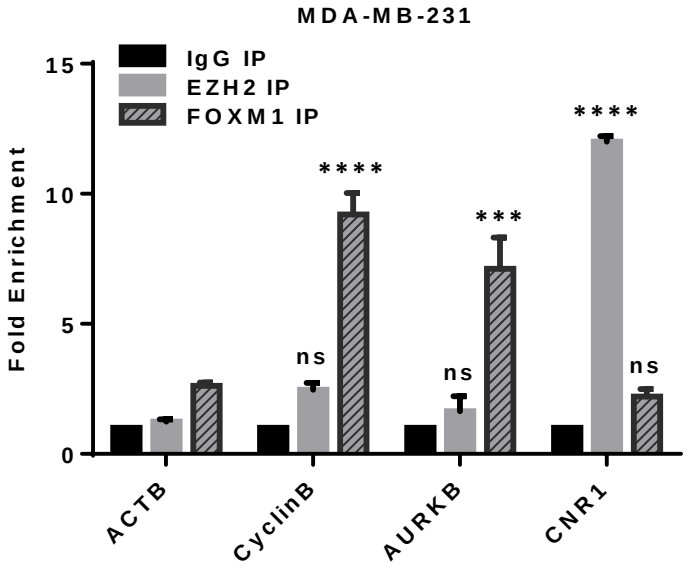

Figure 3.12 FOXM1 enrichment on *CCNB1, AURKB* and its own promoters.
ChIP qPCR of EZH2 and FOXM1 on the promoters of *ACTB*, *FOXM1*, *CCNB1* and *AURKB*. *ACTB* as a negative control was used as a statistical comparison with each ChIP pull down. Quantification of enrichment was determined as fold enrichment over IgG. Two way ANOVA was used as a statistical analysis and all the data in the graph bars represented ± SEM; ****$P\text{-value} \leq 0.0001$

The inhibitory effect seen in cell proliferation under EZH2 depletion could be an indirect effect of downregulated FOXM1 expression under this condition. Collectively our data showed that FOXM1 is a bona fide mitotic regulator in TNBC model. However, our identification of non-canonical EZH2/FOXM1 complex suggested that FOXM1 might have a role beyond the mitotic regulation, which in part mediated by EZH2.

On the other hand, the EZH2/FOXM1 complex could be an “interaction artefact” by the virtue of cellular proximity. There was a concern that any two or even more molecules could form a physical interaction at cellular level when they are in close proximity. Usually, such interaction is transient and does not exert any cellular function. However, our coIP assay was performed endogenously without the involvement of any

crosslinking agent. Hence, our experimental design had eliminated the possibility of "interaction artefact". Whether the non-canonical EZH2/FOXM1 identified in our initial investigation had a role in other cellular pathway would be the topic of our second phase of study.

CHAPTER 4: EZH2 AND FOXM1 REGULATION IN INVASION PATHWAY

4.1 Depletion of EZH2 or FOXM1 Shares Similar Biological Consequences in Cancer Cell Invasion

Other than cell cycle progression, both EZH2 and FOXM1 have been reported to regulate invasion and metastasis in multiple malignancies (Kleer et al. 2003; Dai et al. 2007; Cao et al. 2008; Ahmad et al. 2010; Derfoul et al. 2011; Lok et al. 2011; Yau et al. 2011; Gong and Huang 2012; Ren et al. 2012; Shin and Kim 2012; Xia et al. 2012; Xu et al. 2012; Chen et al. 2013; Jung et al. 2013a; Kim et al. 2013; Li et al. 2013; Xue et al. 2014). We next asked whether biological consequences resulting from depletion of EZH2 or FOXM1 in TNBC would also affect cancer cell invasion and migration. We first compared EZH2 and FOXM1 effects in promoting invasive capacity using MDA-MB-231 cell line and found that after siRNA depletion, both EZH2-depleted cells and FOXM1-depleted cells had reduced invasive capacity when compared to siNC control (Figure 4.1).

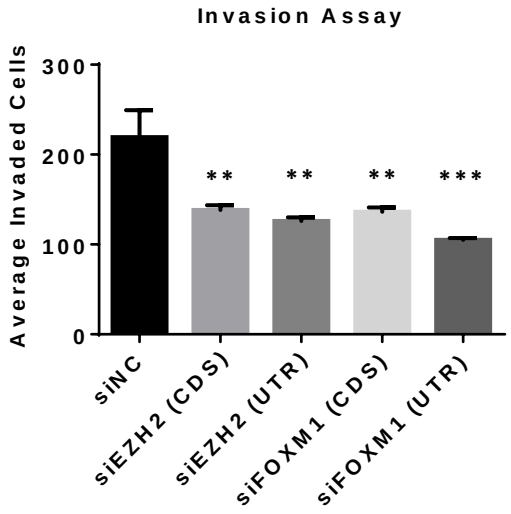

Figure 4.1 EZH2 and FOXM1 role in cancer cell invasion.
Transwell Fluoroblok invasion assay in MDA-MB-231 cells depleted for EZH2 and FOXM1 using multiple siRNA sequences. Cells were seeded in a matrigel coated 24-well format and invading cells were stained with PI after 48 hours of incubation. The number of invading cells was measured using high content screening analysis and the average values were taken. Each sample was done in triplicate and one way ANOVA was used as statistical analysis. All the data in the graph bars represented ± SEM; ***P-value* ≤ 0.01, ****P-value* ≤ 0.001

To investigate whether the inhibitory effects seen in invasion pathway could be rescued by ectopic expression of WT FOXM1, we performed endogenous EZH2 depletion in WT FOXM1 overexpressed MDA-MB-231 cell line followed by invasion assay. From our analysis, ectopic expression of WT FOXM1 could effectively rescue the EZH2 depletion phenotype in invasion back to its basal level (Figure 4.2), in contrast to the modest rescued phenotype seen in mitotic progression (Figure 3.10). Taken together, our data indicated that the EZH2-FOXM1 axis is more effective in regulating invasion pathway than cell cycle progression in TNBC.

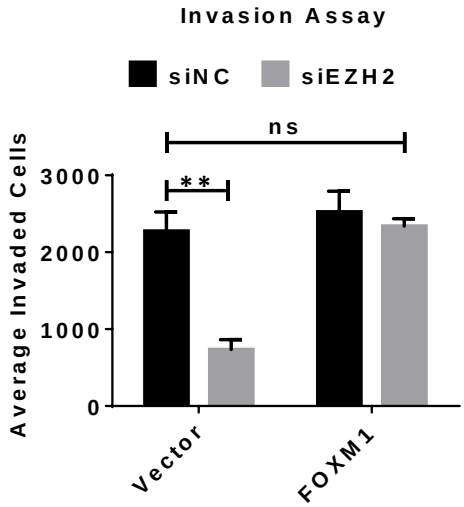

Figure 4.2 Functional rescue experiments for invasion pathway.
EZH2 depletion in MDA-MB-231-FOXM1 overexpression cells were analyzed for invasive capacity. Invasion assay was taken after 48 hours incubation. Two way ANOVA was used as a statistical analysis and all the data in the graph bars represented ± SEM; ***P-value* ≤ 0.01

4.2 MMP-mediated Invasion Pathway in TNBC

As described earlier, there are two biological processes most commonly known to contribute to invasive capacity of highly aggressive TNBC; EMT (Shook and Keller 2003; Mani et al. 2008; Visvader and Lindeman 2008; Bao et al. 2011; Hanahan and Weinberg 2011; Park et al. 2011; Huang et al. 2012) and MMP (Boire et al. 2005; Dai et al. 2007; Wang et al. 2007; Wang et al. 2008; Balli et al. 2012; Shin and Kim 2012; Wieczorek et al. 2012; Xia et al. 2012). To determine which of these two biological processes are directly under the regulation of EZH2-FOXM1 axis, we sought to investigate the mRNA levels of several well known EMT-associated transcription factors and MMP families under EZH2 or FOXM1 depletion condition.

We first investigated the possibility of EZH2-FOXM1 regulation in EMT pathway, and by comparing either EZH2 or FOXM1 depletion with siNC control in MDA-MB-

231, we unexpectedly found that all of transcription factors associated with EMT was upregulated (Figure 4.3A). The properties of EMT are commonly associated with embryogenesis (Nieto et al. 1994; Carver et al. 2001), wound healing (Lepilina et al. 2006; Arnoux et al. 2008) and in the case of human pathology, cancer metastasis (Mani et al. 2008; Visvader and Lindeman 2008; Bao et al. 2011; Park et al. 2011; Huang et al. 2012). Conversely, the reduction in senescence (Figure 3.9A) and cell proliferation (Figure 3.9B) observed under EZH2 or FOXM1 depletion, which constituted to regression of cancer progression, should be inversely correlated with growth promoting properties of EMT. Paradoxically, our study suggested the potential convergence of these two polar opposite biological processes – senescence and EMT.

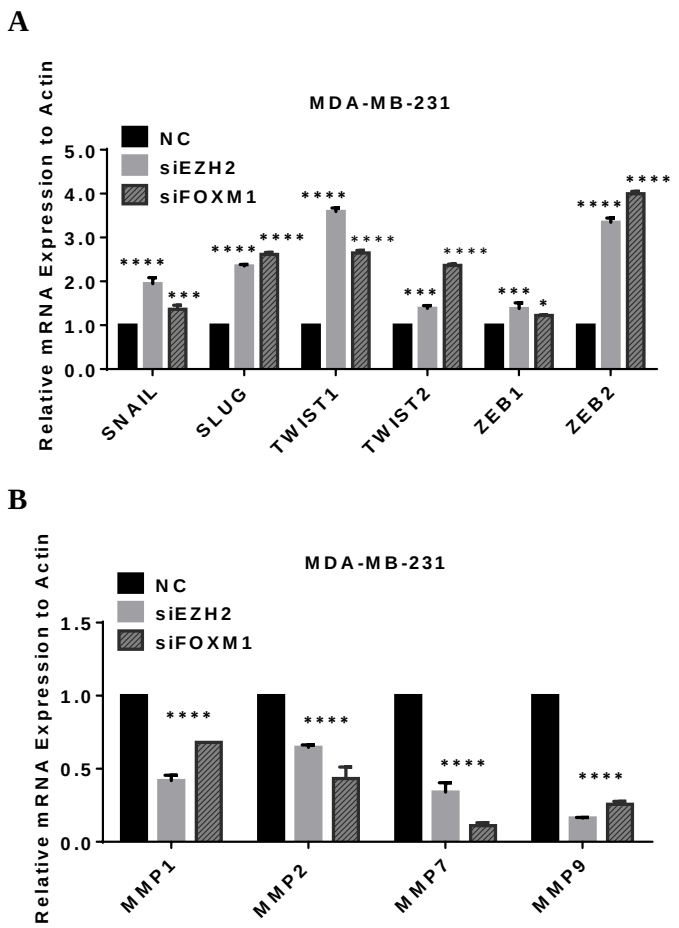

Figure 4.3 Positive regulation of EZH2 and FOXM1 in MMP-mediated invasion. qRT-PCR analysis of MDA-MB-231 cells upon EZH2 or FOXM1 depletion for (*A*) EMT-associated transcription factors and (*B*) MMP families. Two way ANOVA was used as statistical analysis by comparing either EZH2 or FOXM1 depletion with siNC and all the data in the graph bars represented ± SEM; **P-value* ≤ 0.05, ****P-value* ≤ 0.001, *****P-value* ≤ 0.0001

However, the finding of a positive relationship between senescence and EMT was not unprecedented. Several studies have shown that senescent cells are often responded to the cellular stress by secreting several interleukins such as IL-6, IL-8 and CXCL-1 (Acosta et al. 2008; Coppe et al. 2008; Kuilman et al. 2008). These interleukins in turn stimulate the proliferation of malignant epithelial cell through EMT, linking a robust inflammatory network with both senescence and EMT. Coincide with this reported

studies, we had also identified the enrichment for inflammatory network under EZH2 depletion using IPA analysis (Figure 3.1).

Although senescence-induced EMT would be an attractive hypothesis to pursue however, it was not consistent with the reduced invasive capacity observed in our study (Figure 4.1). It was possible that the upregulation of senescence-induced EMT markers by either EZH2 or FOXM1 depletion was a reflection of the morphological changes in the shape of the cell. As shown in figure 3.9A, the β-galactosidase positive EZH2-depleted cells and FOXM1-depleted cells had a morphologically elongated cell shape compared to siNC (and β-galactosidase negative EED-depleted and SUZ12-depleted cells), reminiscing the classical shape of messenchymal cells.

Since the "collateral effect" of senescence-induced EMT marker did not activate the EMT machinery, as evident by the contradictorily reduced invasive capacity of either EZH2-depleted cells or FOXM1-depleted cells, we investigated the mRNA levels of several MMP families with reported role in cancer metastasis (Figure 4.3B). As anticipated, depletion of either EZH2 or FOXM1 caused downregulation of MMP1, MMP2, MMP7 and MMP9, which was consistent with the reduced invasive capacity observed (Figure 4.1). Furthermore, in an attempt to recapitulate the invasion assay condition, where the cells were seeded in a serum free medium for 48 hours, the RNA extraction for qRT-PCR analysis of EMT markers and MMP families was also performed in a similar serum free condition to minimize the confounding factor due to the presence of the serum.

4.3 Nutrient Deprivation Increases MMP-mediated Invasion Pathway

As a comparison, we also investigated the mRNA levels for MMP2 and MMP7 under both complete and serum free medium (Figure 4.4). Both MMP2 and MMP7 are direct targets of FOXM1 during cancer invasion, where FOXM1 binds to both promoters and transactivates their expressions (Dai et al. 2007; Wang et al. 2007; Xia et al. 2012). Hence, they would be appropriate downstream targets to investigate for the crosstalk of EZH2 and FOXM1 in MMP-mediated invasion in TNBC.

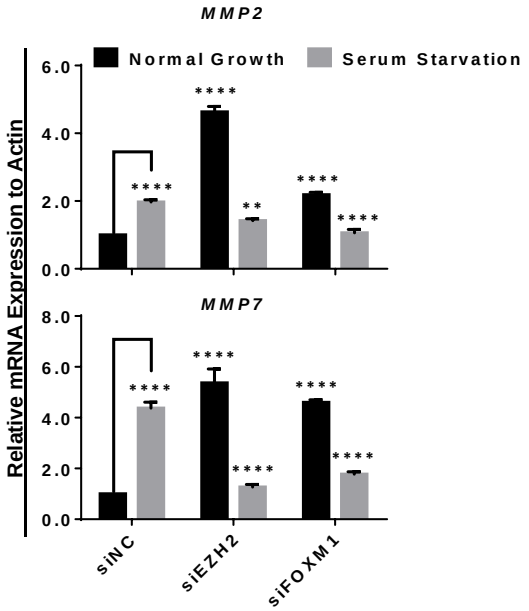

Figure 4.4 Positive regulation of EZH2 and FOXM1 in MMP-mediated invasion during serum starvation.
qRT-PCR analysis of MDA-MB-231 cells upon EZH2 or FOXM1 depletion for MMP2 and MMP7 under complete and serum free medium growth. Unless specified otherwise, two way ANOVA was used as statistical analysis by comparing either EZH2 or FOXM1 depletion with siNC and all the data in the graph bars represented ± SEM; ***P-value* ≤ 0.01, ******P-value* ≤ 0.0001

As expected, the mRNA levels for MMP2 and MMP7 were upregulated for both EZH2-depleted cells and FOXM1-depleted cells grown under complete medium (Figure

4.4), further affirming our initial concern for the confounding effect by serum. However, both EZH2-depleted cells and FOXM1-depleted cells grown under serum free condition exhibited downregulation of MMP2 and MMP7 mRNA levels, consistent with reduced invasive capacity observed in invasion assay (Figure 4.1). Interestingly, we observed a significant 2-fold and 4-fold upregulations for MMP2 and MMP7 mRNA levels respectively for cells grown under serum free medium (Figure 4.4 comparing siNC normal growth with siNC serum starvation). It was likely that the serum starvation condition might have altered the cellular metabolic state, and as a response toward this metabolic stress the cancer cells converged the stress signaling to increased migration and invasion, potentially by recruiting EZH2, FOXM1 and other co-activator to promoters of *MMP* target genes for transcriptional activation.

4.4 Nutrient Deprivation Decreases PRC2 Activity on *MMP*s Promoters

To examine this theory, we first performed ChIP analysis in MDA-MB-231 cell and detected significant enrichment of EZH2 and FOXM1 on *MMP2* and *MMP7* promoters under normal growth compared to *ACTB* promoter (Figure 4.5A). Moreover, following FOXM1 depletion, the enrichment of EZH2 and FOXM1 associated with *MMP2* and *MMP7* promoters decreased significantly (Figure 4.5B). The changes in promoter occupancies following FOXM1 depletion corresponded well to the downregulation of MMP2 and MMP7 mRNA levels upon FOXM1 depletion (Figure 4.3B and 4.4). These observations not only validated our ChIP assay on EZH2 and FOXM1 occupancies on the

promoters of *MMP* target genes, but also provided a possible co-recruitment of EZH2 and FOXM1 as suggested by our initial coIP data (Figure 3.11).

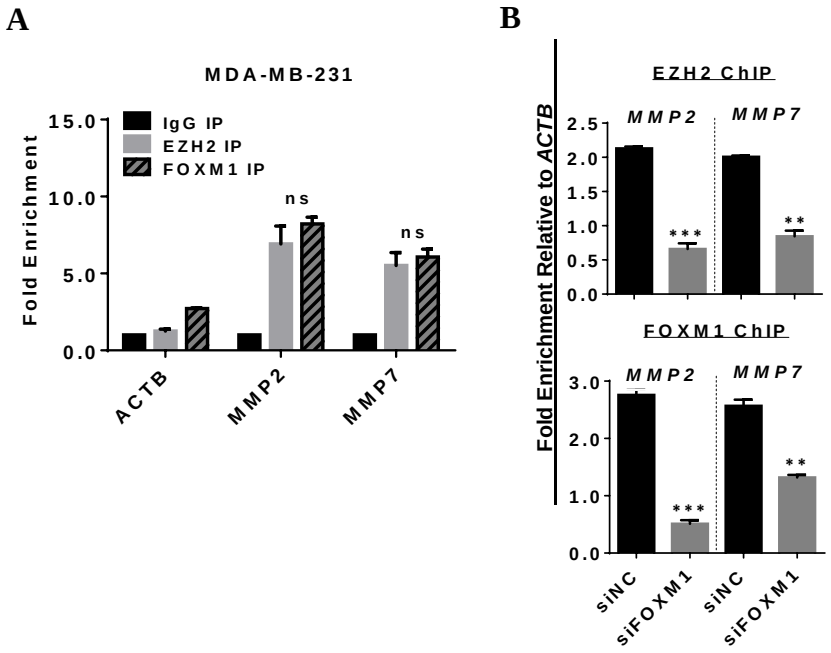

Figure 4.5 EZH2 and FOXM1 co-enrichment on *MMP2* and *MMP7* promoters.
ChIP qPCR of EZH2 and FOXM1 on the promoters of *ACTB*, *MMP2* and *MMP7* (*A*) under normal growth condition and (*B*) FOXM1 depletion. *ACTB* as a negative control was used as a statistical comparison with each ChIP pull down. Quantification of enrichment was determined as fold enrichment over IgG. Two way ANOVA was used as a statistical analysis and all the data in the graph bars represented ± SEM; ***P-value* ≤ 0.01, ****P-value* ≤ 0.001

In concordance with increased invasive capacity following serum starvation condition, where mRNA levels of MMP2 and MMP7 were upregulated (Figure 4.4), and several evidences that support accelerated MMP-mediated invasion of cancer cells especially during starvation (Kousidou et al. 2004; Suzuki et al. 2004; Storz et al. 2009), we performed ChIP assay comparing normal growth and serum starvation to justify for the effect of EZH2, FOXM1 and EED on promoters of *MMP2* and *MMP7*.

Based on the ChIP data, we did not observe any significant difference in the recruitment of EZH2, FOXM1 and EED on the promoter of *MMP2* and *MMP7* during starvation (Figure 4.6A top and bottom panels respectively). In contrast, there was a significant reduction in the H3K27me3 mark on both promoters during starvation. Although there was a reduction in the recruitment of EED on both promoters, which was consistent with the qRT-PCR analysis for reduced mRNA level of EED as well as SUZ12 during starvation (Figure 4.6B), however those factors were too inconsequential to contribute to the significant reduction in the H3K27me3 level on MMP promoters.

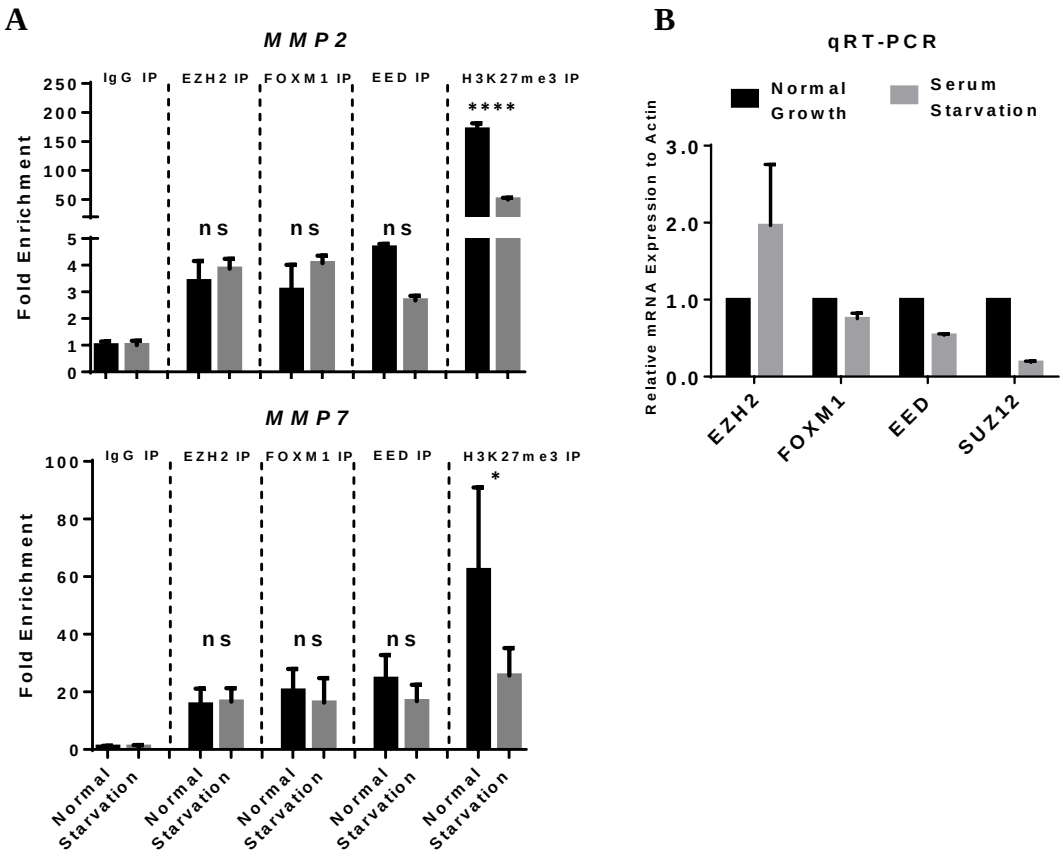

Figure 4.6 Comparison of promoter occupancy during normal growth and starvation. (*A*) ChIP qPCR of EZH2, FOXM1, EED and H3K27me3 on the promoters of *MMP2* (top) and *MMP7* (bottom) in MDA-MB-231 cells. Normal growth and starvation condition were indicated at x axis label. Quantification of enrichment was determined as fold enrichment over IgG. Two way ANOVA was used as a statistical analysis and all the data in the graph bars represented ± SEM; **P-value* ≤ 0.05, *****P-value* ≤ 0.0001. (B) qRT-PCR analysis comparing mRNA level of EZH2, FOXM1 and EED during normal growth and starvation

4.5 Depletion of PRC2 Subunits Promotes MMP-mediated Invasion Pathway

So far our data from coIP experiments indicated that EZH2 formed 2 different complexes in TNBC; canonical EZH2/PRC2 complex and non-canonical EZH2/FOXM1 complex (Figure 3.11). The non-canonical EZH2/FOXM1 complex had a positive role in regulating invasion pathway in TNBC and it was imperative to investigate whether the EZH2/PRC2 complex contributed to this pathway as well. We first examined the effect of

EED or SUZ12 depletions in invasion pathway and surprisingly, we found that both EED-depleted cells and SUZ-12-depleted cells promoted invasion in TNBC (Figure 4.7A). Furthermore, mRNA levels for invasive markers, MMP2 and MMP7, were upregulated upon either EED or SUZ12 depletion. Unlike EZH2 or FOXM1 depletion, the upregulation of these invasive markers mediated by either EED or SUZ12 depletion was not affected by the growth condition.

It was worth noting that EED depletion conferred a higher upregulation of invasive capacity as evident by the invasion assay (Figure 4.7A) and the qRT-PCR analysis (Figure 4.7B) compared to SUZ12 depletion. Although both EED and SUZ12 mediate the methyltransferase activity of EZH2/PRC2 complex, but they each exert a distinct role during epigenetic repression. EED is responsible in recognizing and binding to the histone tail of H3 (Margueron et al. 2009), while SUZ12 helps to stabilize the EZH2-EED complex resulting in a more robust methyltransferase activity (Cao et al. 2002). Hence, the minor difference between EED depletion and SUZ12 depletion in the light of TNBC invasion could be due to their different roles in mediating repressive methyltransferase activity via PRC2 complex.

Since EED is in direct contact with the histone tail, depletion of EED would be more effective in disrupting the PRC2-mediated repressive function on its target genes. This theory subsequently led to the possibility that both MMP2 and MMP7 were under epigenetic repression by PRC2 complex and upon depletion of PRC2 subunits, their expressions were activated. Paradoxically, our ChIP data indicated potential transcriptional activation of MMP2 and MMP7 expressions via EZH2/FOXM1 complex (Figure 4.5 and 4.6A).

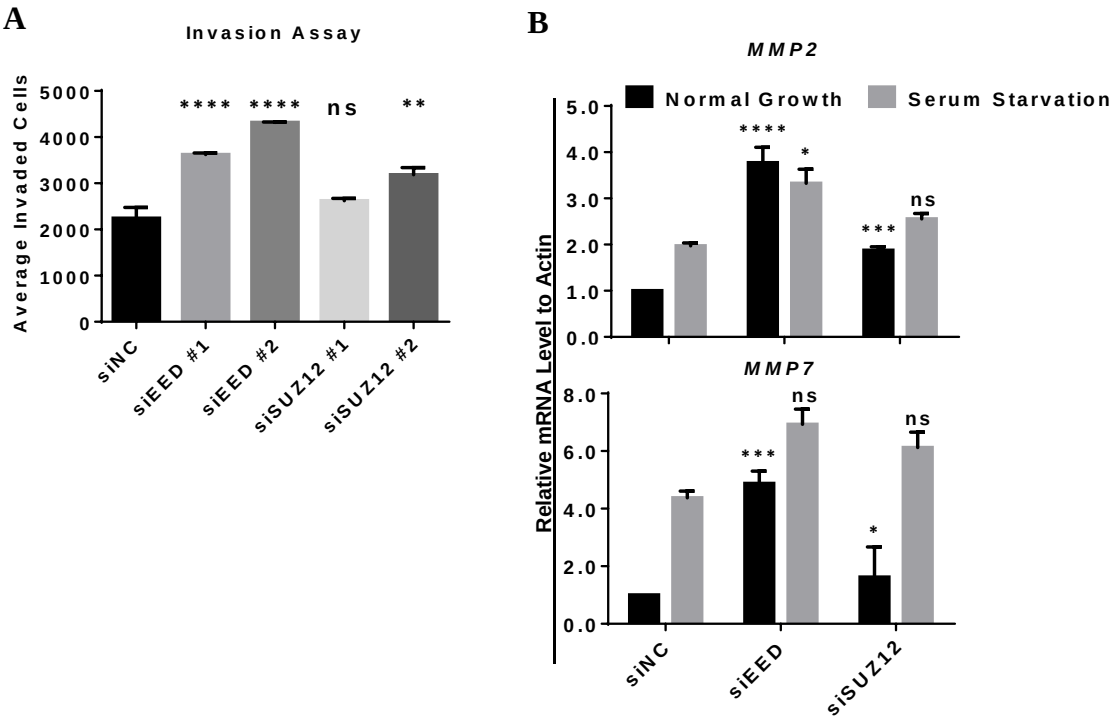

Figure 4.7 Negative regulation of PRC2 complex in cancer cell invasion.
EED or SUZ12 depletion in MDA-MB-231 cell was analyzed for (*A*) invasive capacity and (*B*) qRT-PCR analysis for mRNA level of MMP2 and MMP7 under complete and serum free medium growth. Invasion assay was taken after 48 hours incubation and one way ANOVA was used as statistical analysis. For qRT-PCR analysis, two way ANOVA was used as statistical analysis by comparing either EED or SUZ12 depletion with siNC and all the data in the graph bars represented ± SEM; **P-value* ≤ 0.1, ***P-value* ≤ 0.01, ****P-value* ≤ 0.001, *****P-value* ≤ 0.0001

4.6 Co-occupancy of EZH2/PRC2 Complex and EZH2/FOXM1 Complex on *MMP*s Promoters

To explore the possibility of dual antagonistic role of EZH2/PRC2 complex and EZH2/FOXM1 complex acting on the promoter of *MMP2* and *MMP7*, we first designed series of PCR primers to probe chromatin regions surrounding *MMP2* and *MMP7* transcription start sites (TSS) for the binding of EZH2, FOXM1 and one member of PRC2 complex, EED. Much to our surprise, we found co-occupancies of not only EZH2

and FOXM1 on distal promoter region, but also EED on both *MMP2* and *MMP7* promoters (Figure 4.8A top and bottom panel respectively). Consistent with the binding of EED, we also detected a concomitant enrichment for repressive H3K27me3 level on both promoters.

Albeit the knockdown ChIP data showed dependency of EZH2 and FOXM1 (Figure 4.5B) and primer pairs surrounding the TSS showed EED occupancy on MMP2 and MMP7 promoter (Figure 4.8A), those were insufficient to demonstrate a possible co-occupancy of all three factors on the promoters. Thus we performed an extensive sequential ChIP. After the EED first ChIP, only EZH2 binding was significantly enriched in EED-bound *MMP2* and *MMP7* promoters (Figure 4.8B), indicating that only EZH2 was concurrently bound with EED to these promoters.

At the same time, we also conducted EZH2 first ChIP experiment and found that FOXM1/EED were concurrently bound to these promoters with EZH2 (Figure 4.8C). These results indicated that the recruitment of EZH2/EED and EZH2/FOXM1 to *MMP2* and *MMP7* promoters was interdependent. In contrast, the recruitment of EED was void of FOXM1 binding, where the FOXM1 binding was not significantly enriched in EED-bound *MMP2* and *MMP7* promoters.

These sequential ChIP data further supported the demonstration by CoIP assay, where FOXM1 did not co-precipitate with either EED or SUZ12 (Figure 3.11). The co-occupancy of EZH2, FOXM1, EED and H3K27me3 enrichment seen in Figure 4.8A could be due to the 3-dimensional arrangement of chromatin, it was possible for the

EZH2/FOXM1 complex and EZH2/PRC2 complex to bind to the same region but in a cis-trans fashion.

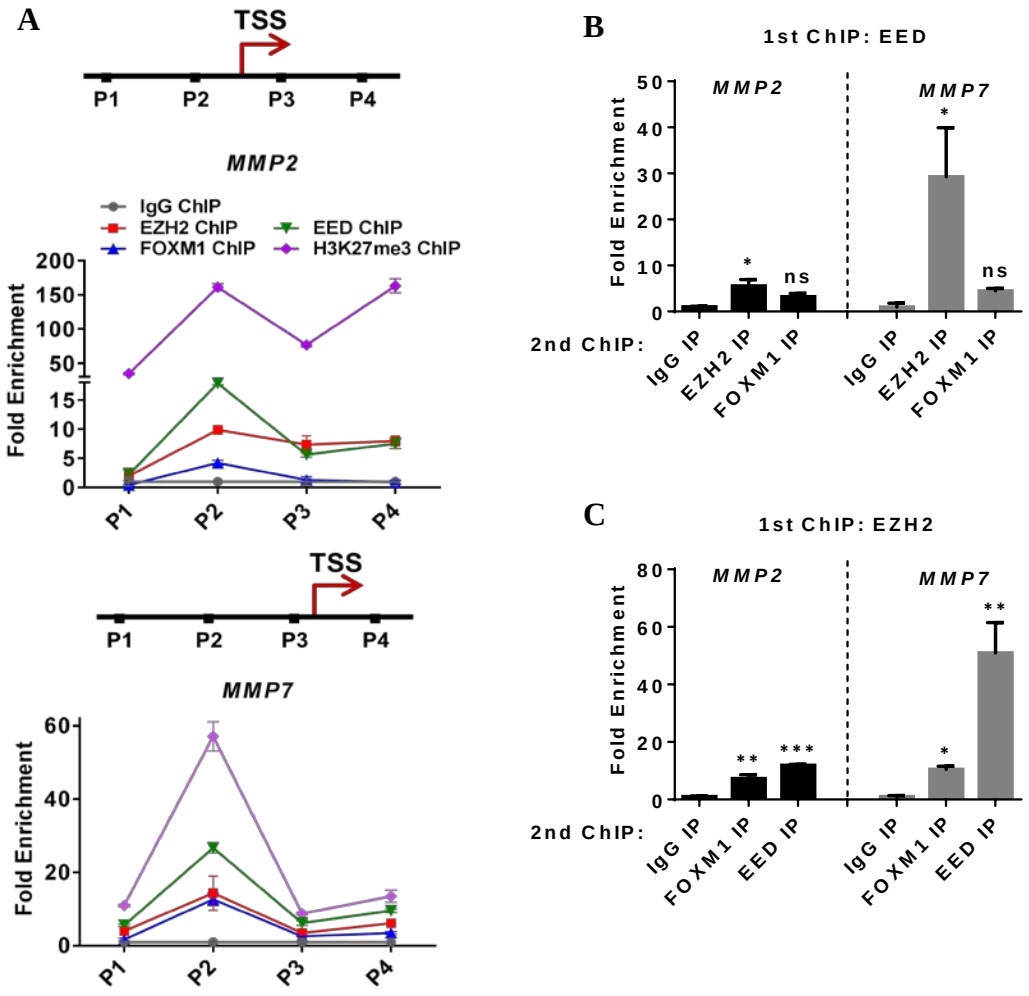

Figure 4.8 Promoter co-occupancy of EZH2, FOXM1 and EED.
(*A*) ChIP qPCR of EZH2, FOXM1, EED and H3K27me3 on the promoters of *MMP2* (top) and *MMP7* (bottom) in MDA-MB-231 cells. P1 to P4 indicate primer pairs used to encompass the genomic regions analyzed for promoter occupancy, TSS (transcription start site). (*B*) and (*C*) Sequential ChIP assay was performed to assess in-vivo co-localization of EZH2, FOXM1 and EED on the promoters of *MMP2* and *MMP7*. First ChIP and second ChIP antibodies were indicated as the chart title and x axis labels, respectively. Quantification of enrichment was determined as fold enrichment over IgG. One way ANOVA was used as a statistical analysis and all the data in the graph bars represented ± SEM; **P-value* ≤ 0.05, ***P-value* ≤ 0.01, ****P-value* ≤ 0.001

Taken together, we concluded that EZH2, through interacting with FOXM1, was required for the activation of a subset of MMP target genes in mediating invasion pathway in TNBC cells. At the same time, EZH2, through interacting with its PRC2 subunits, exerted an antagonistic effect for the same MMP target genes. These observations established potential dual roles of EZH2 acting as a transcriptional activator and transcriptional repressor simultaneously on the promoter of MMP target genes. Upon cellular response toward stress signaling such as nutrient starvation, the repressive EZH2/PRC2 complex was downregulated leading to increased invasive capacity regulated by activator EZH2/FOXM1 complex

4.7 EZH2 and FOXM1 Regulates Each Other at Transcriptional Level

In our early investigation into EZH2 and FOXM1 regulation on each other, we did not observed recruitment of EZH2 to the promoter of *FOXM1* using a single PCR primer pair (Figure 3.12). However, it did not exclude the possibility of EZH2 regulating the transcriptional activity of FOXM1, since depletion of EZH2 caused downregulation of both mRNA and protein levels of FOXM1 (Figure 3.5). On the other hand, mRNA level of EZH2 was upregulated during starvation condition (Figure 4.8B) and we reasoned that it might play a role in the recruitment of EZH2 to *FOXM1* promoter.

To further investigate the possibility of EZH2 occupancy on *FOXM1* promoter, we designed series of PCR primers to probe for chromatin regions surrounding *FOXM1* transcription start sites (TSS) for the binding of EZH2 under both normal growth and starvation condition. As anticipated, we observed enrichment for EZH2 recruitment on

the distal *FOXM1* promoter region approximately 1.1 kbps from TSS only during starvation condition (Figure 4.9A). Since depletion of FOXM1 also led to downregulation of EZH2 (Figure 3.5), we also performed similar ChIP assay using primer pairs surrounding the TSS of *EZH2* for the binding of FOXM1. Similarly to recruitment of EZH2 to *FOXM1* promoter, FOXM1 was also recruited to the promoter of *EZH2* in response to nutrient starvation (Figure 4.9B).

Based on these results, we concluded that EZH2 regulated both protein stability (Figure 3.7) and transcriptional activity of FOXM1, thus depletion of EZH2 caused the downregulation of both protein and mRNA levels of FOXM1. At the same time, FOXM1 also played a role in the transcriptional activity of EZH2, which demonstrated a positive feedback loop between EZH2 and FOXM1 during starvation condition.

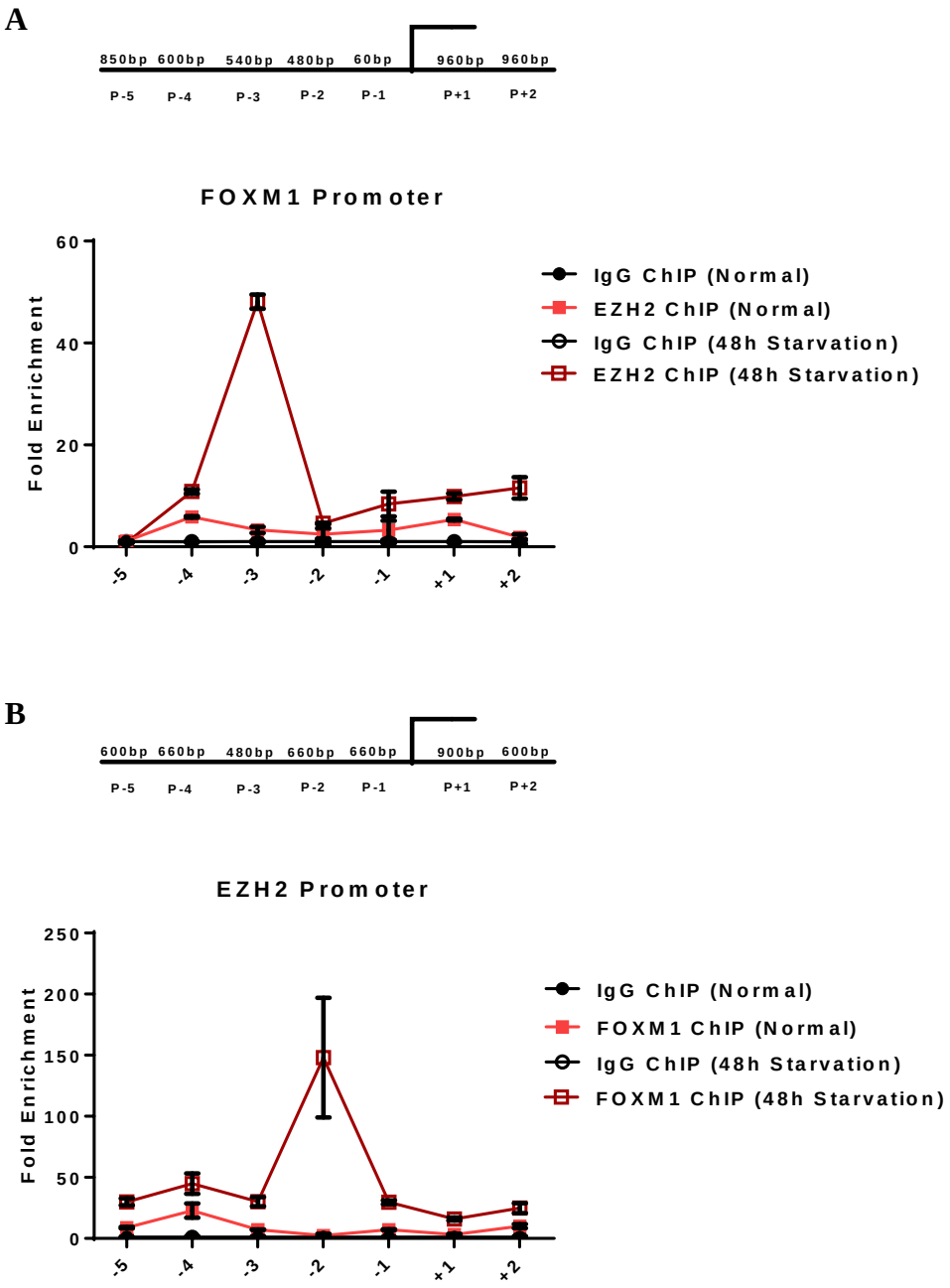

Figure 4.9 ChIP qPCR for whole promoter during normal growth and starvation. ChIP qPCR of EZH2 and FOXM1 recruiment on the promoter of (*A*) *FOXM1* and (*B*) *EZH2* in MDA-MB-231 cells respectively under normal growth and starvation condition. P-5 to P+2 indicated primer pairs used to encompass the genomic regions analyzed for promoter occupancy. Quantification of enrichment was determined as fold enrichment over IgG. All the data in the graph bars represented ± SEM

CHAPTER 5: FUNCTIONAL VALIDATION OF EZH2-FOXM1 REGULATION IN INVASION PATHWAY

5.1 EZH2 or FOXM1-mediated Oncogenic Transformation in Mammary Epithelial Cell

Our study of EZH2 and FOXM1 crosstalk in TNBC had been limited to TNBC cell lines, in particular MDA-MB-231 cell line. Hence, there was a concern that this functional crosstalk could be limited to this particular cell line. In order to ascertain the oncogenic nature of EZH2 and FOXM1 in breast cancer progression, we sought to overexpress EZH2 or FOXM1 in an immortalized human mammary epithelial cell line, MCF10A. Our theory was if both EZH2 and FOXM1 were true oncogenes, they would be able to mediate oncogenic transformation even in a normal mammary epithelial cell.

To this end, we generated a single overexpressed WT EZH2 or WT FOXM1 cell and a double overexpressed WT EZH2-FOXM1 cell in MCF10A. For the double overexpressed WT EZH2-FOXM1-MCF10A, we titrated the plasmid transfection such as each ectopic expression of WT EZH2 and WT FOXM1 were halved of those in the single overexpressed cell lines, to ensure equal expression dosage in the overexpression MCF10A cell, which was evident from both immunoblot (Figure 5.1A) and qRT-PCR (Figure 5.1B) analysis for protein and mRNA levels in these overexpression cell lines respectively.

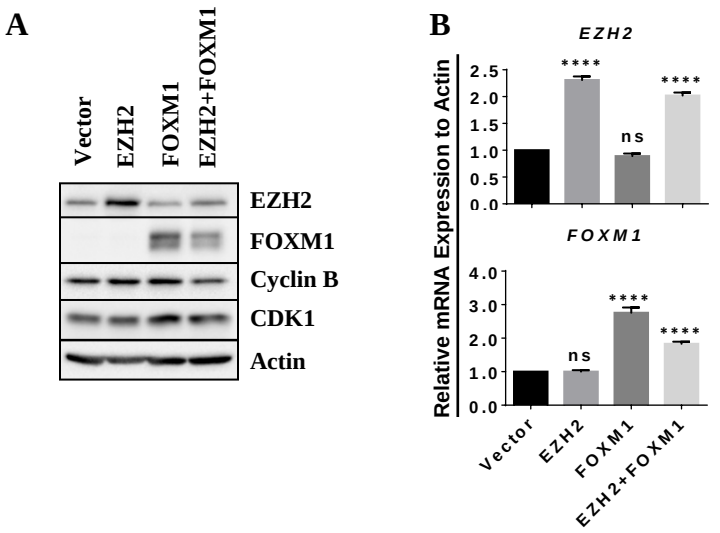

Figure 5.1 Ectopic expression of WT EZH2 and WT FOXM1 in a mammary epithelial cell line.
(*A*) Immunoblots and (*B*) qRT-PCR analysis of MCF10A cell upon ectopic expression of WT EZH2 and WT FOXM1. One way ANOVA was used as statistical analysis and all the data in the graph bars represented ± SEM; ****$P\text{-}value \leq 0.0001$

5.2 Interdependency of EZH2 and FOXM1 in Regulating MMP-mediated Invasion Pathway

Despite the successful transfection, we did not observe any morphological change in these cells at 2D growth (Figure 5.2A) however; we detected a concomitant increased in the invasive capacity with the overexpression status (Figure 5.2B). The increased was even more striking in the double overexpression EZH2-FOXM1 MCF10A cell. Interestingly, the increased in the invasive capacity of double overexpression EZH2-FOXM1 MCF10A cell was not accompanied by the increased in cell proliferation (Figure 5.2C left) compared to single overexpressed WT EZH2 or WT FOXM1 MCF10A cell.

Furthermore, the protein levels for cyclin B and CDK1 were slightly reduced in double overexpression WT EZH2-FOXM1 MCF10A cell (Figure 5.1A) compared to

single overexpressed WT EZH2 or WT FOXM1 MCF10A cell. These observations were consistent with our findings in MDA-MB-231 where the EZH2-FOXM1 axis was more effective in regulating invasion pathway than cell proliferation.

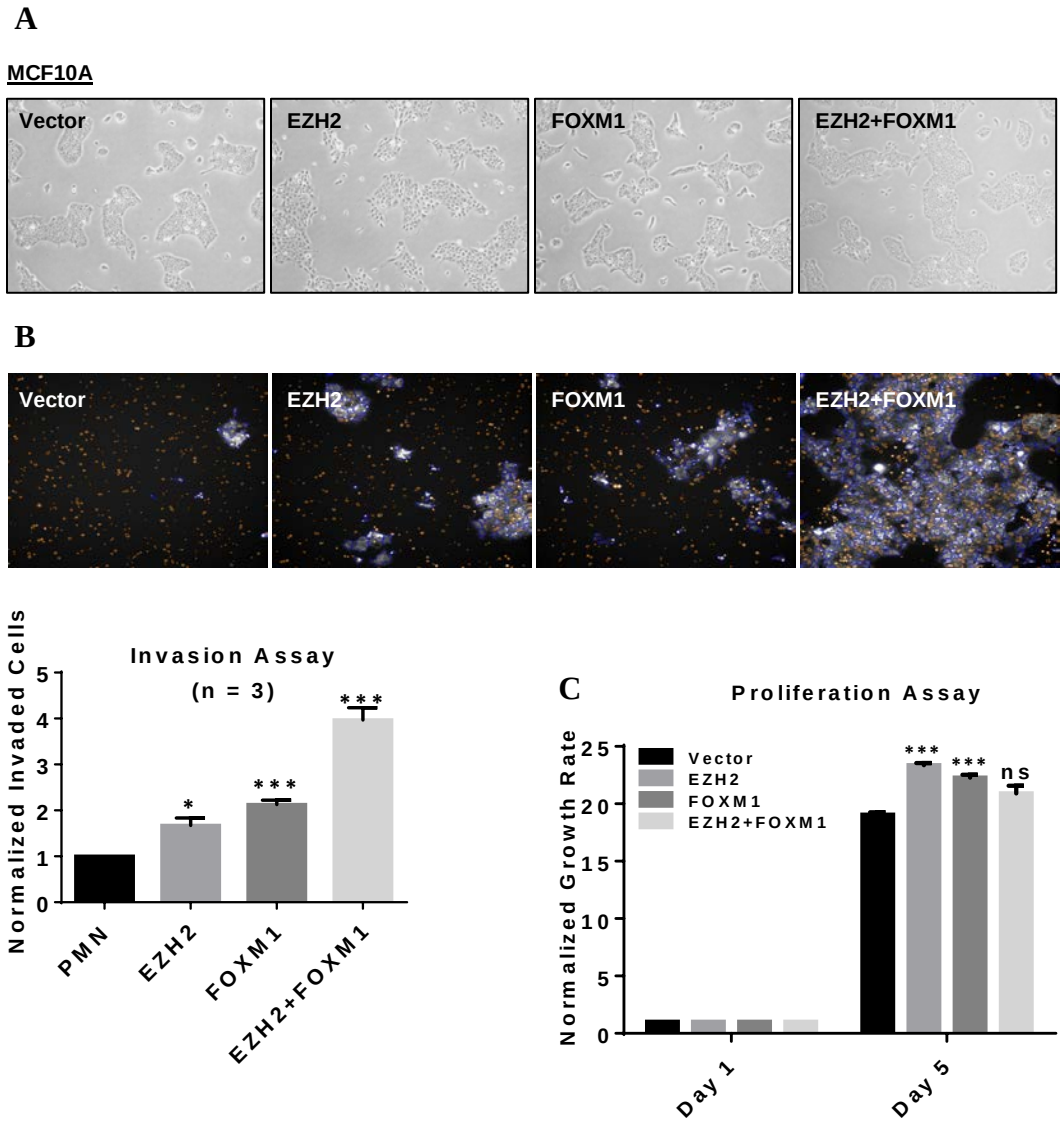

Figure 5.2 Phenotypic analyses in ectopic overexpressed WT EZH2 and WT FOXM1 in MCF10A cell.

(*A*) Micrographs showing ectopic overexpression of WT EZH2, WT FOXM1 and WT EZH2-FOXM1 in MCF10A cells in 2D growth. (*B*) In-vitro matrigel invasion assay images captured using (top) HCS microscopes and (bottom) quantification of invading cells. (*C*) CTG based proliferation assay measured on day 1 and day 5. One way ANOVA was used as statistical analysis and all the data in the graph bars represented ± SEM; **P-value* ≤ 0.05, ****P-value* ≤ 0.001

The changes in the phenotype were also reflected in the mRNA level, where we only observed marked increments of subset of MMP family expressions in double overexpressed WT EZH2-FOXM1 MCF10A cell (Figure 5.3). The increased in the invasive capacity was in part mediated by the role of MMPs with very little contribution from the EMT transcription factors, which was evident from the unchanged mRNA levels for EMT markers in these ectopic overexpression cell lines. This data further supported the finding in MDA-MB-231 cell, where upon EZH2 or FOXM1 depletion the EMT markers were paradoxically increased (Figure 4.3A).

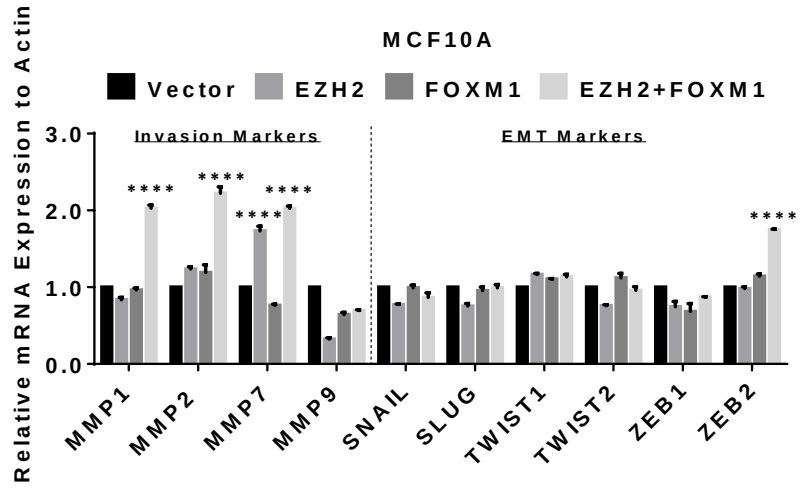

Figure 5.3 mRNA levels for both invasion and EMT markers in ectopic overexpression MCF10A cell lines.
qRT-PCR analysis in MCF10A cell for a subset of MMP families and several EMT-associated transcription factors. Two way ANOVA was used as a statistical analysis and all the data in the graph bars represented ± SEM; ****$P\text{-}value \leq 0.0001$

The double overexpressed WT EZH2-FOXM1-MCF10A cell also displayed enrichment for *MMP2* and *MMP7* promoters (Figure 5.4) in either of its EZH2 or FOXM1 immunoprecipitate. Although, we detected enrichment for *MMP*s promoters in FOXM1-MCF10A cell only in its FOXM1 immunoprecipitate however, we did not

observe concomitant increased in the MMPs mRNA levels (Figure 5.3). This finding indicated that FOXM1 activity was dependent on EZH2 in transactivating its downstream invasion-associated target genes. And consistent with the proliferation status, the enrichment for the proliferation-associated gene promoters; *FOXM1*, *CCNB1* and *AURKB*; was reduced in double overexpressed WT EZH2-FOXM1-MCF10A cell, especially in its FOXM1 immunoprecipitates compared to single overexpressed WT FOXM1-MCF10A cell. On the other hand, the EZH2 immunoprecipitate in double overexpressed WT EZH2-FOXM1 MCF10A cell was not enriched for any of those proliferation-associated gene promoters. The observations in ectopic overexpression MCF10A cell lines not only further validated the findings seen in MDA-MB-231 cell, but also demonstrated a selective active role of EZH2 on FOXM1 and their interdependence in regulating invasion pathway.

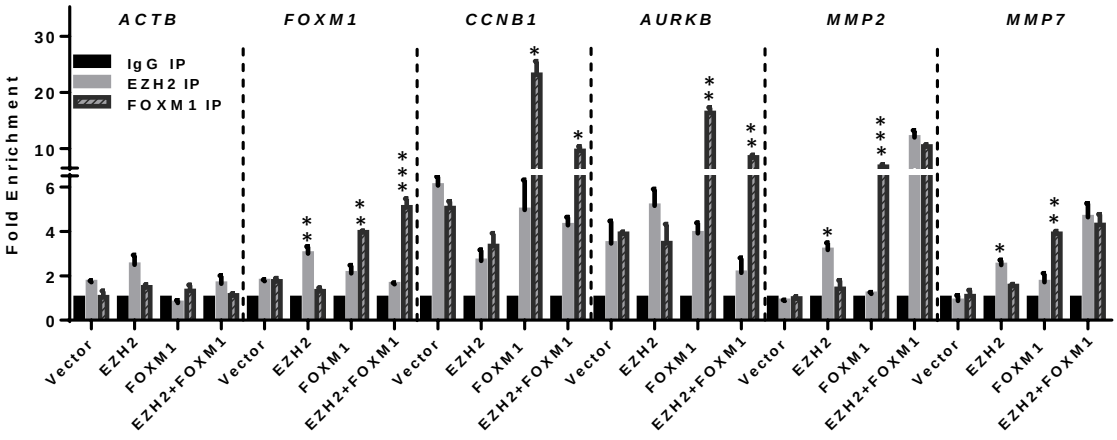

Figure 5.4 Selective EZH2 and FOXM1 co-enrichment on *MMP2* and *MMP7* promoters in double overexpressed WT EZH2-FOXM1 MCF10A cell.
ChIP qPCR of EZH2 and FOXM1 on the promoters of *ACTB, FOXM1*, *CCNB1*, *AURKB*, *MMP2* and *MMP7*. Each ChIP pull down was compared to empty vector MCF10A cell line. Quantification of enrichment was determined as fold enrichment over IgG. Two way ANOVA was used as a statistical analysis and all the data in the graph bars represented ± SEM; **P-value* ≤ 0.05, ***P-value* ≤ 0.01, ****P-value* ≤ 0.001

5.3 Pharmacological Inhibition of Histone Methyltransferase Activity of EZH2

To answer the question of whether histone methyltransferase activity of EZH2 was important for the interaction between EZH2 and FOXM1, we utilized a pharmacological inhibitor, GSK126 small inhibitor compound, which is a selective inhibitor for the enzymatic activity of EZH2 without affecting its protein (McCabe et al. 2012).

To verify for the effect of histone methyltransferase inhibition, we performed immunoblotting on the treated MDA-MB-231 cell and checked for the presence of histone methyltransferase activity. It was evident that the histone methyltransferase activity was completely inhibited after 3-day treatment (Figure 5.5A). As expected, the expression of EZH2, EED and SUZ12 were not affected by the GSK126 treatment, despite a concomitant decrease in the repressive H3K27me3 level. Notably, the expression of FOXM1 and its target in mitotic progression, Cyclin B, were not affected by the epigenetic inhibitor treatment either.

Even at mRNA level, no effect was observed on several proliferation-associated downstream targets of FOXM1 (Figure 5.5B). Strikingly, the expression of MMP2 and MMP7 were induced in a dose dependent manner after the treatment, which recapitulated the earlier observation seen in the EED and SUZ12 depletions (Figure 4.6B).

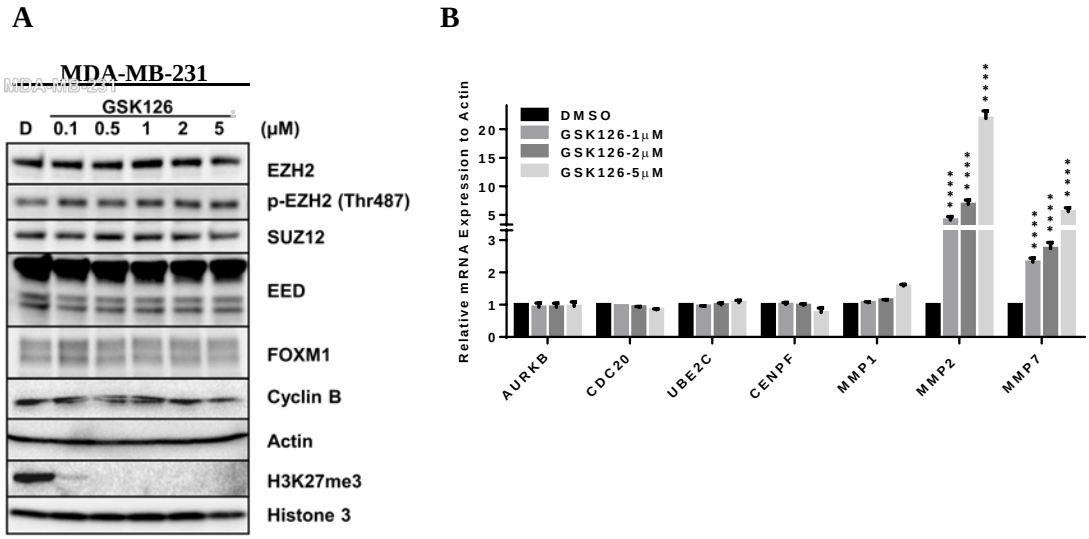

Figure 5.5 GSK126 treatment in MDA-MB-231 cell.
(*A*) Immunoblots and (*B*) qRT-PCR analysis of MDA-MB-231 cell upon GSK126 treatment for 72 hours. Each treatment group was compared to DMSO control and One way ANOVA was used as statistical analysis and all the data in the graph bars represented ± SEM; ****$P\text{-value} \leq 0.0001$

5.4 Histone Methyltransferase Activity of EZH2 Inhibits Invasion Pathway

The subsequent functional assay reiterated the effects seen at both mRNA and protein expressions, where no significant changes were observed in cell proliferation (Figure 5.6A) but a concomitant increased in the invasive capacity (Figure 5.6B) after a dose dependent GSK126 treatment. On the other hand, treatment with 3-Deazaneplanocin A (DZNep) significantly reduced the number of invading cells. DZNep is an inhibitor that efficiently depletes EZH2 and PRC2 proteins and effectively abolish the repressive H3K27me3 activity altogether (Tan et al. 2007).

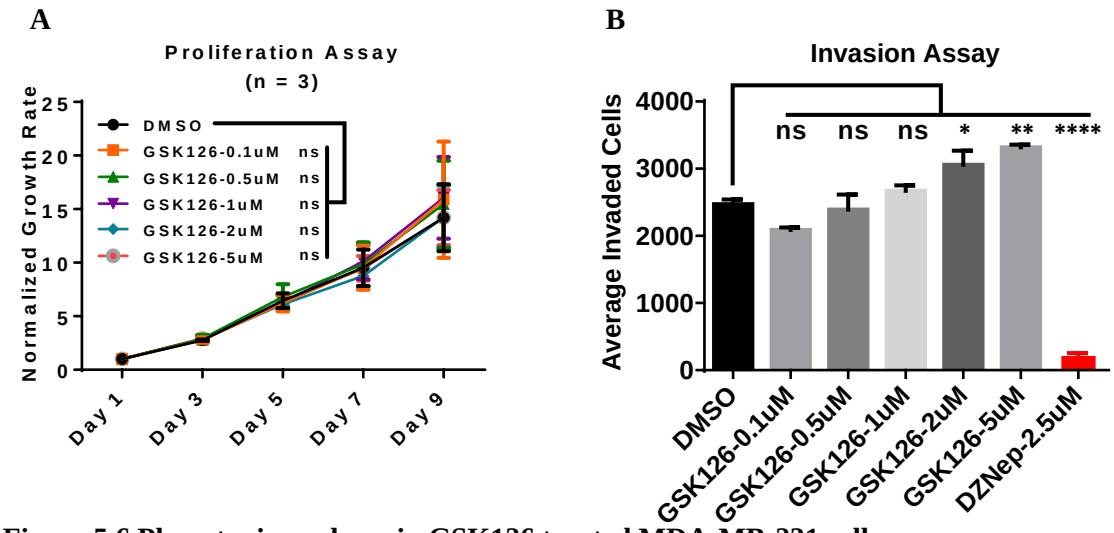

Figure 5.6 Phenotypic analyses in GSK126 treated MDA-MB-231 cell.
(*A*) CTG based proliferation assay measured on every alternate day for 9 days. Statistical analysis comparing treatment group with DMSO treated cell was performed on day 9. (*B*) In-vitro matrigel invasion assay for the quantification of invading cells. One way ANOVA was used as statistical analysis and all the data in the graph bars represented ± SEM; **P-value* ≤ 0.05, ***P-value* ≤ 0.01, *****P-value* ≤ 0.0001

5.5 Inhibition of Histone Methyltransferase Activity of EZH2 Increases EZH2-FOXM1 Interaction

Whether the stability of EZH2/FOXM1 complex remained intact after the selective inhibition of the histone methyltransferase activity of EZH2 was a question raised in the earlier part of this project after the initial detection of EZH2/FOXM1 complex through coIP.

To answer this question, we performed a separate coIP experiment with GSK126 treatment in MDA-MB-231 cell. In each respective immunoprecipitates of FOXM1 (Figure 5.7A), EZH2, phosphorylated-EZH2, and pan-methylated lysine (Figure 5.7B), we were able to detect EZH2/FOXM1 complex in all, but phosphorylated-EZH2 immunoprecipitate (Figure 5.7B). However, after GSK126 treatment, we detected a slight

increased in the binding of EZH2 to FOXM1 and vice versa. Of particular interest was the methylated FOXM1, which was undetected upon GSK126 treatment (Figure 5.7B).

Whether EZH2 had a non-histone methyltransferase activity acting on FOXM1 remained an open discussion however, it was clear that inhibition of the repressive H3K27me3 activity did not affect EZH2/FOXM1 complex.

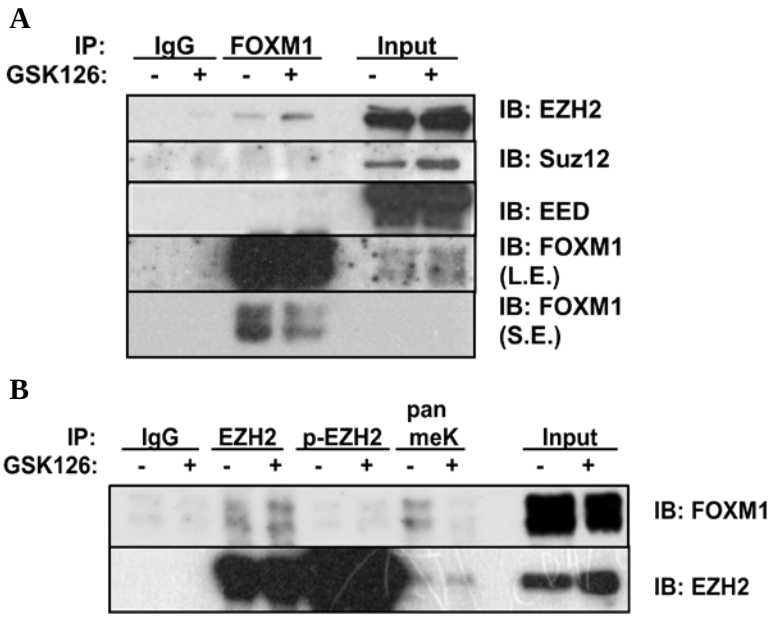

Figure 5.7 coIP in MDA-MB-231 cell treated with GSK126.
Immunoblot analysis showing (*A*) FOXM1 immunoprecipitate and (*B*) EZH2, phospho-EZH2 and pan-methylated lysine immunoprecipitates comparing GSK126 treated and non-treated MDA-MB-231 cells.

5.6 Inhibition of Histone Methyltransferase Activity of EZH2 Increases FOXM1 Enrichment on *MMP*s Promoters

Furthermore, our initial ChIP findings also indicated the histone methyltransferase independent activity of EZH2/FOXM1 complex on *MMP2* and *MMP7* promoters, especially during serum starvation condition (Figure 4.8A). Hence, to validate our

hypothesis, we treated MDA-MB-231 with GSK126 followed by H3K27me3 ChIP. As expected, we observed enrichment for H3K27me3 on both *MMP2* and *MMP7* promoters, possibly due to the EZH2/PRC2 complex acting on the same regions, and the enrichments were gradually decreased with increasing dose of GSK126 (Figure 5.8 bottom).

Although the enrichment of EZH2 on these promoters were not significantly affected after GSK126 treatment (Figure 5.8 top) however, we observed increased in the enrichment of FOXM1 on the same promoters (Figure 5.8 middle). The latter finding further supported the earlier observation in coIP, where we detected increased in the physical interaction between EZH2 and FOXM1 upon GSK126 treatment (Figure 5.7).

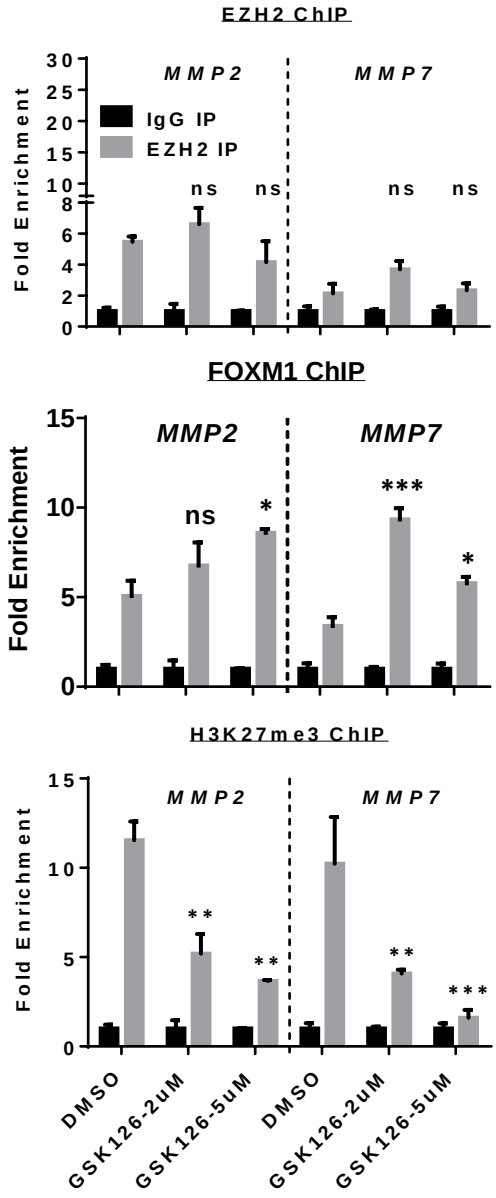

Figure 5.8 ChIP assay in MDA-MB-231 cell treated with GSK126.
ChIP qRT-PCR analysis of EZH2, FOXM1 and H3K27me3 on the promoters of *MMP2* and *MMP7*. Each ChIP pull down was compared to DMSO treated cell. Quantification of enrichment was determined as fold enrichment over IgG. Two way ANOVA was used as a statistical analysis and all the data in the graph bars represented ± SEM; **P-value* ≤ 0.05, ***P-value* ≤ 0.01, ****P-value* ≤ 0.001

Taken together, we concluded that 2 forms of EZH2 complex, canonical EZH2/PRC2 complex and non-canonical EZH2/FOXM1 complex, co-occupied invasion associated promoters i.e. *MMP2* and *MMP7* with each exerting contradictory roles in TNBC progression. EZH2/PRC2 complex exerted its histone methyltransferase activity, which was evident during serum starvation condition and GSK126 treatment by the decrease of EED (Figure 4.8A) and repressive H3K27me3 level (Figure 4.8A and 5.8), while EZH2/FOXM1 complex acted as a transcriptional activator evident by the increased physical interaction at protein level (Figure 5.7) and increased FOXM1 enrichment on *MMP*s promoters (Figure 5.8) that led to increased MMP2 and MMP7 expression (Figure 5.5B) upon GSK126 treatment.

CHAPTER 6: DISCUSSION

6.1 Summary of Results

Our initial screening using both microarray and bioinformatics analyses actually identified role of EZH2 in regulating mitotic pathway. Our data suggested that EZH2 had dual role as a repressor and an activator, as evident from the identification of 2 differentially regulated sets of gene; EZH2 positively-regulated and EZH2 negatively-regulated gene sets (Lee et al. 2011a). Subsequently, we focused our study in the positively-regulated gene sets and found that EZH2 mediated positive regulation on a set of mitotic genes such as CDC20, BUB1, AURKB, CENPF, CCNB2, and UBE2C.

These mitotic genes were also under positive regulation of FOXM1 and when we depleted either EZH2 or FOXM1 in MDA-MB-231, we observed similar reduction in term of cell proliferation. Furthermore, FOXM1 activity had been reported to be the highest during mitotic phase (Laoukili et al. 2008) thus, we speculated a coregulation of EZH2 and FOXM1 in this pathway. Despite our demonstration of a previously unidentified protein-protein interaction between EZH2 and FOXM1 however, our subsequent rescued experiments and ChIP data showed that EZH2 had very little effect in the regulation of mitotic pathway. In fact, the regulation of FOXM1 in the same pathway was more robust than EZH2, further reiterated the commonly known function of FOXM1 as a mitotic regulator (Ye et al. 1999; Wang et al. 2002; Kalinichenko et al. 2004; Krupczak-Hollis et al. 2004; Laoukili et al. 2005; Wonsey and Follettie 2005; Halasi and Gartel 2012).

In the second phase of our study, we recognized the other tumorigenic character of aggressive TNBC aside from its high proliferative activity, which was high invasive capacity and propensity to metastasis. Both EZH2 and FOXM1 have also been

consistently implicated in invasion pathway (Kleer et al. 2003; Ahmad et al. 2010; Ren et al. 2012; TCGA 2012; Xue et al. 2014) hence, we tried to investigate the coregulation of EZH2 and FOXM1 in the invasion pathway. It was at this phase that we were finally able to demonstrate the interdependency of EZH2 and FOXM1 in regulating MMP-dependent breast cancer cell invasion. The finding on the EZH2-FOXM1 interdependency stemmed from both Nocodazole release experiment and ChIP data, where we observed a longer half-life of FOXM1 protein under EZH2 overexpression condition, as well as enrichment of EZH2 on *FOXM1* promoter and vice versa during serum starvation condition respectively.

In accordance with our previous report in TNBC (Lee et al. 2011a), we also detected two separate complexes of EZH2 in MDA-MB-231 cell; the repressive EZH2/PRC2 complex and the activator EZH2/FOXM1 complex. Intriguingly, both complexes contributed to transcriptional regulation of a subset of MMP families in an antagonistic manner, where the EZH2/FOXM1 complex was independent of PRC2 members and their associating repressive H3K27me3 activity. Notably, inhibiting the histone methyltransferase activity of EZH2 promoted further induction in invasive capacity but not proliferation in TNBC.

In the third phase of our study, we further validated the EZH2-FOXM1 axis in invasion pathway by transforming a mammary epithelial cell line, MCF10A. In contrast to reduced cancer cell invasion seen during EZH2 or FOXM1 depletion in MDA-MB-231 cell, ectopic expression of WT EZH2 or WT FOXM1 in MCF10A cell promoted the invasion, and the effect was even more pronounced in double overexpressed WT EZH2-FOXM1-MCF10A cell. Furthermore, single overexpression of WT EZH2 in MCF10A

cell was not able to drive MMPs expressions as effectively as double overexpressed WT EZH2-FOXM1-MCF10A cell. These findings further highlighted the interdependency of EZH2 and FOXM1 seen in TNBC cell line.

6.2 Novelty of the Findings

FOXM1 has been known to play an important role in cancer progression by crosstalking a wide spectrum of cellular processes crucial to tumorigenesis however; the precise underlying mechanism for the broad regulation of FOXM1 in human malignancies is still the subject of speculation. As one of the key cell cycle regulators, FOXM1 hyperactivation in the onset of tumorigenesis could reflect its role as an oncogenic driver. Conversely, cancer cells generally have a higher proliferative capacity compared to normal cells and hyperactivation of FOXM1 could simply be the passenger effect. This is further illustrated by Yau et al where an elevated level of FOXM1 in TNBC does not correlate to proliferation markers (Yau et al. 2011). Furthermore, they also reported that the poor prognostic value of TNBC does not correlate to its proliferative capacity instead; it is a reflection of its metastatic potential, suggesting that FOXM1 possesses an additional tumorigenic role beyond cell cycle regulation.

This observation is further supported by effects of FOXM1 depletion, where certain cancer cells are viable and proliferating but with a severe consequence of reduction in tumorigenicity (Bhat et al. 2011; Wang et al. 2011; Halasi and Gartel 2012; Liu et al. 2012). Herein we revealed the unexpected role of EZH2 in re-directing the role of FOXM1 from a mitotic regulator to an invasion regulator. Consistent with this, ectopic

expression of WT EZH2 was able to stabilize FOXM1 protein past mitotic phase as shown in the Nocodazole release experiment (Figure 3.7A), however the residual FOXM1 expression did not have any effect on cell proliferation (Figure 3.7B). Our results proposed a non-canonical function of EZH2 in activating MMP-mediated invasion pathway in conjunction with FOXM1.

Moreover, this non-canonical role of EZH2 in TNBC was supported by several lines of evidence; 1) EZH2 formed a protein complex with FOXM1 independent of PRC2 subunits (Figure 3.11A-C), 2) EZH2/FOXM1 complex selectively transactivated MMP2 and MMP7 expressions (Figure 4.5A, 4.6A, 4.8A, 4.8C and 5.4), 3) Ectopic overexpression of WT EZH2 and WT FOXM1 in mammary epithelial cell line promoted cancer invasion (Figure 5.2A and 5.3), and 4) Histone methyltransferase activity of EZH2 was dispensable for MMP-mediated invasion pathway (Figure 5.5B, 5.6B and 5.8). In fact, both canonical and non-canonical EZH2 complexes existed in *MMP2* and *MMP7* promoters suggesting 2 layers of regulatory mechanism for these target genes.

Mechanistically, we showed that both EZH2 and FOXM1 were enriched on *MMP2* and *MMP7* promoters with a direct consequence in increased expression of MMP2 and MMP7 as well as increased invasive capacity. Intriguingly, we also detected co-occupancy of EED and enrichment for repressive H3K27me3 on the same regions. This unprecedented observation of co-occupancy of two antagonistic forms of EZH2; canonical repressive EZH2/PRC2 complex and non-canonical activator EZH2/FOXM1 complex, revealed that the two layers of gene regulations; epigenetic and transcriptional activation, were coordinately involved in aggressive breast cancers. In a slightly different study, a promoter co-occupancy of both PRC2 complex and a novel EZH2 partner, Spi-1,

has been linked to antiapoptosis in erythroleukemia (Ridinger-Saison et al. 2013). Here, the transcription factor Spi-1 assumes a repressive role by modulating the activity of PRC2 with a net effect in repression of its pro-apoptotic target.

Our data provided a novel molecular basis that linked two key oncogenic drivers, EZH2 and FOXM1, in promoting MMP-mediated invasion specific to TNBC, offering insights into how EZH2 exerted antagonistic dual role in a more aggressive breast cancer; on one hand as a repressive epigenetic regulator, but on the other as a mediator in redirecting the role of FOXM1 from a mitotic regulator to an invasion regulator. At the same time, we also provided an evidence of the convergence of both genetic and epigenetic regulations by EZH2; EZH2/FOXM1 complex in directing transcriptional activity of MMP2 and MMP7 and EZH2/PRC2 complex in epigenetic repression of *MMP2* and *MMP7* promoters.

6.3 Limitations of the Study

The scope of this project was to investigate the co-regulation of EZH2 and FOXM1 especially in the progression of TNBC hence; only TNBC cell lines were used as our experimental model. The earlier small interfering RNA depletion and coIP experiments were performed in multiple TNBC cell lines to establish the regulation of EZH2 and FOXM1 in these cell lines. However, the subsequent phenotypic and functional experiments were conducted only in MDA-MB-231 cell line, which raised a concern of cell type specific effect. Although our subsequent validation of co-regulation of EZH2 and FOXM1 in a transformed ectopic overexpression mammary epithelial cell line,

MCF10A, was consistent with the observations seen in MDA-MB-231 cell however; we should also expanded our studies in other TNBC cell lines.

Furthermore, the clinical TNBC subtype can be further subclassified into 6 molecular subtypes of TNBC (Lehmann et al. 2011b), and there is a possibility that the co-regulation of EZH2 and FOXM1 might be limited to a particular subtype of TNBC. In contrast to extensive molecular profiling for clinical TNBC subtype that identified 6 subtypes of TNBC, similar work performed in a cell line context was only able to further characterize 3 subtypes of TNBC cell line; basal-like, luminal-like and mesenchymal-like (Charafe-Jauffret et al. 2006). The gap in molecular classification between clinical sample and cell line sample could be the limiting factor in the investigation of context specificity of EZH2-FOXM1 coregulation. Furthermore, there is a growing concern with the use of cancer cell line as a cancer model because long term in-vitro culture could change the pathological behavior of a particular cell line from the actual tumor sample in which they were originally derived from. An alternative to bridge the possible differential gene regulation existing between the clinical sample and the cell line sample would be the use of patient-derived xenograft sample (PDX).

PDX is a form of tumor graft model, where the tumor sample is surgically obtained from a patient, followed by mechanical or chemical digestion into a single cell suspension, before engrafting into a non obese diabetic/severe combined immunodeficient (NOD/SCID) mouse (Siolas and Hannon 2013). Since PDX sample is derived from patient tumor directly and maintained in a 3-dimensional culture condition inside a mouse carrier, which provides a direct contact with microenvironment necessary for tumor growth, it retains pattern of gene expression similar to its parental tumor.

Hence, it offers a better tool for the investigation of molecular regulation and signaling of EZH2-FOXM1 in TNBC progression.

Another limitation of this study was the lack of an in-vivo mouse model as a proof of concept for invasive tumor and metastasis propensity. An in-vitro experiment could not accurately capture advanced tumor progression that involves invasion and ultimately dissemination into distant organs. Although in-vitro matrigel invasion assay is a routinely used experiment to investigate invasive capacity of cancer cell, and it is also able to provide quantitative data on the number of invading cells however, we found that this assay had a low technical replication. Furthermore, in-vitro matrigel invasion assay is not able to recapitulate metastasis event. Hence, the use of in-vivo mouse model or PDX sample would be able to accurately delineate invasion pathway under the regulation of EZH2-FOXM1, and at the same time to provide a molecular mechanism on how the disease progresses past invasion and into metastasis.

6.4 Future Prospects

In this present study, we discovered a novel co-regulation of EZH2 and FOXM1 in MMP-mediated invasion pathway in TNBC and at the same time, we also showed the involvement of repressive EZH2/PRC2 complex in the same pathway. However, there were several unanswered questions pertaining to this dual antagonistic role of EZH2. Firstly, how does EZH2 switch from its role as a canonical repressive PRC2 complex to a non-canonical activator EZH2/FOXM1 complex? Secondly, what causes the significant reduction in H3K27me3 level during starvation condition (Figure 4.6A)? The second

question was particularly intriguing because the reduction in H3K27me3 level was not accompanied by significant reduction in enrichment of EED on *MMP*s promoters. This raised the possibility of involvement of other epigenetic regulator.

Several studies have reported the existence of a non-canonical form of EZH2 however, only a few has identified the upstream regulator that causes the functional switch of EZH2 from an epigenetic repressor to a transcriptional activator (Cha et al. 2005; Wei et al. 2011a; Xu et al. 2012; Kim et al. 2013). The common theme among those studies is the post translational modification on EZH2 causes its functional switch and two regulators have been identified so far; CDK1 and Akt. In the case of CDK1-dependent phosphorylation of EZH2, the event leads to inhibition of histone methyltransferase activity of EZH2 by disrupting its interaction with PRC2 members (Wei et al. 2011a). The resulting net effect is the derepression of EZH2/PRC2 complex target genes and some of them are important for tumor progression.

On the other hand, the study on Akt-dependent phosphorylation of EZH2 by Xu and colleagues have clearly demonstrated the functional switch of EZH2, and it is further accompanied by increment of active histone marks on its target (Xu et al. 2012). Furthermore, they have also identified two forms of EZH2 complex; EZH2/PRC2 complex and EZH2/AR complex, which is consistent with our study where we identified EZH2/PRC2 complex and EZH2/FOXM1 complex. In a slightly different study by Cha and colleagues, phosphorylation of EZH2 by Akt inhibits histone methyltransferase activity of EZH2 however, it does not alter EZH2 interaction with PRC2 members (Cha et al. 2005). Instead, Cha and colleagues hypothesized that the Akt-dependent

phosphorylation of EZH2 switches the histone methyltransferase to a non-histone protein methyltransferase activity.

In our current study, we had demonstrated that the phosphorylation of EZH2 did not interact with FOXM1 (Figure 5.7B). It was possible that our upstream regulator that mediated the functional switch of EZH2/PRC2 complex to EZH2/FOXM1 complex did not involve either CDK1-dependent phosphorylation or Akt-dependent phosphorylation. Furthermore, we also identified two complexes of EZH2 existing together in TNBC, which was consistent with previously reported studies in other cancer models (Lee et al. 2011a; Xu et al. 2012; Jung et al. 2013a), and upon serum deprivation only EED and H3K27me3 levels were downregulated. Hence, we speculated that our upstream regulator was tightly regulated by stress signaling and it had a role in repressing the PRC2 members selectively. Based on these criteria, we had narrowed down our candidate to HIF1 transcription factor. Furthermore, HIF1 transcription factor has been shown to be upregulated during serum deprivation in breast cancer (Shi et al. 2010), and it is also correlated with loss of SUZ12 and H3K27me3 levels in metastatic renal cancer (Vanharanta et al. 2013). In addition, PARADIGM analysis identified activation of HIF1 network together with MYC and FOXM1 specifically in TNBC subtype (2012a), and HIF1 transcription factors has been reported to bind to the promoter of FOXM1 (Xia et al. 2009) and EZH2 (Chang et al. 2011) and directly transactivates their expressions.

Although several studies have highlighted the inverse correlation between EZH2 and repressive H3K27me3 levels particularly in breast cancer progression (Holm et al. 2010; Holm et al. 2012), and our analysis of TCGA database further supported the non-canonical role of EZH2 (Figure 3.3) however, the canonical EZH2/PRC2 complex

activity is not completely loss. As evident from our data that demonstrated dual regulation of EZH2, involving both EZH2/PRC2 complex and EZH2/FOXM1 complex, on *MMP2* and *MMP7* promoters (Figure 4.8 and 5.8). Furthermore, the H3K27me3 levels on these promoters were further downregulated during starvation condition (Figure 4.6A) suggesting that the histone methylation is a reversible process.

Two histone demethylases have been reported that could specifically demethylate H3K27me3 marks; jumonji domain-containing proteins3 (JMJD3) and ubiquitously transcribed X chromosome tetratricopeptide repeat protein (UTX) (Agger et al. 2007; Hong et al. 2007; Xiang et al. 2007). It was possible that these histone demethylases might further downregulate the repressive H3K27me3 marks on *MMP*s promoter during starvation. In accordance to this, HIF1 transcription factor has also been reported to induce the expression of JMJD3 as a stress response during restrictive oxygen growth (Lee et al. 2014).

Taken together, our future works might encompass the investigation into the involvement of HIF transcription factor as the upstream regulator that mediated the switch of EZH2 activity and histone demethylase that further augmented the reduction of repressive H3K27me3 levels in response to nutritional stress. It would also be imperative to extrapolate the study to include tumor-relevant hypoxia condition as HIF1 transcription factor is associated with hypoxia, and both the functional and phenotypic studies could potentially be more robust under this condition. To further demonstrate the specificity of this EZH2/FOXM1 regulation in TNBC invasion, there would be a need to perform similar study in luminal breast cancer subtype as a biological comparison.

6.5 Clinical Implications

In clinical breast cancer TCGA data, high expression of EZH2 and FOXM1 were significantly coexpressed in TNBC compared with other breast cancer subtype, particularly Luminal A breast cancer (Figure 3.3A). Although Luminal B breast cancer also expressed elevated EZH2, FOXM1 and proliferation-associated downstream targets of FOXM1 however; the expression of PRC2 complex downstream targets was reduced, supporting the contention that the activity of histone methyltransferase of EZH2 is more evident in a less aggressive breast cancer but the same activity is reduced or lost in a more aggressive breast cancer.

The elevated expression of proliferation-associated downstream targets of FOXM1 in Luminal B breast cancer reflects the hyperactivation of FOXM1, and not necessarily the coordinate activity of both EZH2 and FOXM1. The high expression of EZH2 and its canonical PRC2 targets seen in TNBC further support the notion of histone methyltransferase independent activity is associated with TNBC as reported previously (Holm et al. 2010; Holm et al. 2012). In addition, high expression of EZH2 but low repressive H3K27me3 level is associated with poor survival outcome in breast cancer, further supporting our finding of depletion of PRC2 members or pharmacological inhibition of H3K27me3 activity increased invasive capacity in TNBC leading to a more aggressive breast cancer phenotype.

The current treatment for localized and advanced TNBC disease is limited to cytotoxic chemotherapy such as antitubulins (eg. Paclitaxel, Docetaxel, etc), anthracyclines (eg. Doxorubicin, Epiribucin, etc), alkylating antineoplastic agents (eg. Cyclophosphamide, etc), antimetabolites (eg. Gemcitabine, Methotrexate, etc) and

platinum-based agents (eg. Carboplatin, Cisplatin, etc). Several studies have shown the effectiveness of these cytotoxic agents in neoadjuvant, adjuvant and metastatic TNBC settings (Sparano et al. 2008; Thomas 2008; Gianni et al. 2009). Standard neoadjuvant and adjuvant regimens typically include combination of both anthracycline agents or an anthracycline with taxane have been shown to improve survival in treatment of early breast cancer and lymph node positive breast cancer (Sparano et al. 2008; Gianni et al. 2009). Some breast cancers eventually develop resistance to either anthracyclines or taxanes, and although a combination of an antitubulin (Ixabepilone) and an antimetabolite (Capecitabine) has been shown to improve progression-free survival however, it fails to improve overall survival in the treatment of metastatic breast cancer (Thomas 2008).

It has been shown previously that elevated expression of FOXM1 in multiple cancers after chemotherapy treatment protects the cancer cells against apoptosis induced by DNA-damaging agent (Halasi and Gartel 2012) This may explain the relapse seen in some of TNBC patients after chemotherapy treatment. Our finding provided the first evidence of involvement of FOXM1 in the progression of TNBC by forming a protein complex with EZH2.

Considering the implication of FOXM1 in multiple human malignancies, it is very attractive to target FOXM1 for a clinical intervention or even as a cancer biomarker. Thiazole antibiotics and proteasome inhibitors have been known to inhibit the expression of FOXM1 (Radhakrishnan et al. 2006; Halasi and Gartel 2012) and some of these are already in use in clinical practice. Hence, incorporating chemotherapeutic agents with FOXM1 inhibitor could potentially contribute to the improvement of therapeutic outcome for TNBC patients.

Our data also showed that targeting the histone methyltransferase activity of EZH2 had no effect in inhibiting the proliferation of breast cancer cells, in fact inhibiting the repressive H3K27me3 activity further promoted cancer cell invasive capacity. Given the importance of EZH2 for cancer progression, therapeutic inhibition of EZH2 protein may prove to be more efficacious in TNBC treatment, as opposed to inhibiting its histone methyltransferase activity.

DZNep is the first EZH2 inhibitor that is widely used for experimental works, however, the inhibitory effect of DZNep is not specific to EZH2 (Glazer et al. 1986). Furthermore, a result in animal models showed that not only DZNep confers non-specific inhibition on global level of H3K27me3, but it also has short half-life and high toxicity issues (Miranda et al. 2009). In order to reduce the toxicity issue and to improve drug specificity, several selective methyltransferase inhibitor for EZH2 have been developed and some are currently in clinical phase 1/2 for the treatment of lymphomas, non-Hodgkin lymphomas and rhabdoid tumors (McCabe et al. 2012; Knutson et al. 2013; Knutson et al. 2014).

However, given that methyltransferase activity of EZH2 could act as a tumor suppressor as shown in our data and reported previously (Ernst et al. 2010; Nikoloski et al. 2010), caution in the development of clinical application of EZH2 inhibitors are warranted. An alternative strategy involving pharmacologic perturbation of the interaction between EZH2 and FOXM1 might be a lucrative avenue. As it could selectively inhibits the tumor promoting property of EZH2/FOXM1 complex while sparing the tumor suppressor property of EZH2/PRC2 complex.

6.6 Conclusions and Proposed Model

In this study, we have identified coregulation of EZH2 and FOXM1 in regulating MMP-mediated cancer cell invasion specifically in TNBC progression. As described in chapter 1.2, the role of EZH2 in cancer progression has been intensively studied and recent findings have also identified the non-canonical role of EZH2 ranging from interaction with non-PRC2 members, non-histone methyltransferase activity and even as a transcription factor. Importantly, we found both canonical and non-canonical roles of EZH2 existing together in an antagonistic manner on the MMP2 and MMP7 promoters in regulating TNBC invasion. EED and SUZ12 as PRC2 members for EZH2 canonical role, while FOXM1 was implicated as the novel partner of EZH2 for its non-canonical role counterpart. Furthermore, in response to stress induced by nutrient deprivation, there was a shift in the equilibrium of EZH2 complexes toward its non-canonical EZH2/FOXM1 complex and accompanied by reduction in the repressive H3K27me3 level on *MMP2* and *MMP7* promoters.

Based on the collective results of Chapter 3, 4 and 5, we proposed a model for EZH2-FOXM1 regulation of MMP target gene expression in TNBC in response to stress induced nutrient deprivation as summarized in Figure 6.1. During normal growth, both canonical EZH2/PRC2 complex and non-canonical EZH2/FOXM1 complex co-occupy *MMP*s promoters. Although the activator EZH2/FOXM1 complex binds to the same promoter, the underlying repressive mechanism via H3K27me3 exerted by the repressive EZH2/PRC2 complex prevents the transactivation of MMP expression. In contrast, during starvation condition the activity of EZH2/PRC2 complex is inhibited by a mechanism that has yet to be elucidated. As a consequent, the activator EZH2/FOXM1

complex is now able to transactivate MMP expression resulting in an enhanced invasive capacity in TNBC and accompanied by a concomitant decrease in the repressive H3K27me3 level on the promoters.

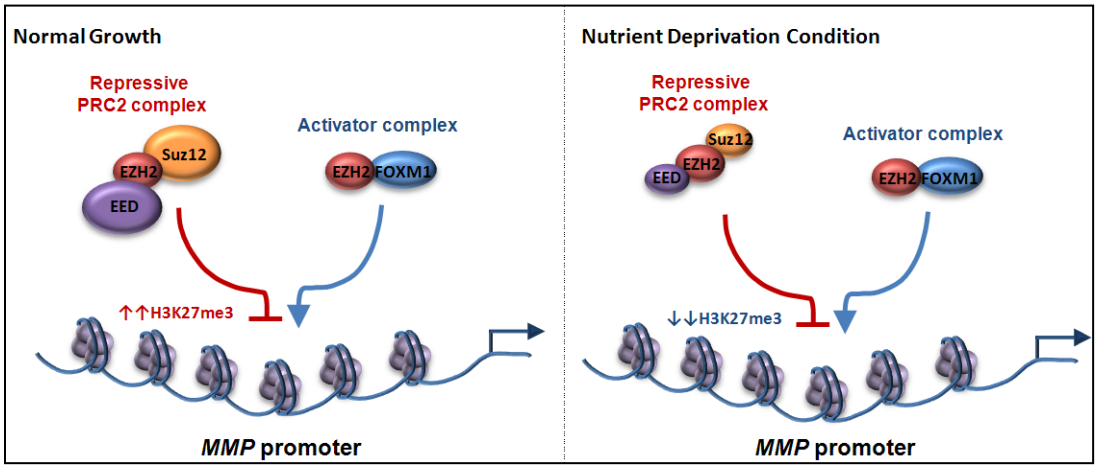

Figure 6.1 A proposed model of dual regulation of EZH2 in regulating MMP-mediated invasion in TNBC.
During normal growth, both canonical and non-canonical complexes of EZH2 were recruited to the promoter of *MMP*s, and both acted in an antagonistic manner preventing the transactivation of MMPs expressions. In contrast, during starvation condition, the EZH2/PRC2 complex activity was repressed, which in turn activated MMPs expressions through EZH2/FOXM1 complex leading to heightened cancer cell invasion.

List of References

2012a. Comprehensive molecular portraits of human breast tumours. *Nature* **490**: 61-70.

2012b. Trends of Female Breast Cancer in Singapore 2006-2010. National Registry of Diseases Office, Singapore.

2013. Singapore Cancer Registry Interim Annual Registry Report Trends in Cancer Incidence in Singapore 2007-2011. National Registry of Diseases Office, Singapore.

Acosta JC, O'Loghlen A, Banito A, Guijarro MV, Augert A, Raguz S, Fumagalli M, Da Costa M, Brown C, Popov N et al. 2008. Chemokine signaling via the CXCR2 receptor reinforces senescence. *Cell* **133**: 1006-1018.

Agger K, Cloos PA, Christensen J, Pasini D, Rose S, Rappsilber J, Issaeva I, Canaani E, Salcini AE, Helin K. 2007. UTX and JMJD3 are histone H3K27 demethylases involved in HOX gene regulation and development. *Nature* **449**: 731-734.

Ahmad A, Wang Z, Kong D, Ali S, Li Y, Banerjee S, Ali R, Sarkar FH. 2010. FoxM1 down-regulation leads to inhibition of proliferation, migration and invasion of breast cancer cells through the modulation of extra-cellular matrix degrading factors. *Breast cancer research and treatment* **122**: 337-346.

Aldinger KA, Lehmann OJ, Hudgins L, Chizhikov VV, Bassuk AG, Ades LC, Krantz ID, Dobyns WB, Millen KJ. 2009. FOXC1 is required for normal cerebellar development and is a major contributor to chromosome 6p25.3 Dandy-Walker malformation. *Nat Genet* **41**: 1037-1042.

Allfrey VG, Faulkner R, Mirsky AE. 1964. Acetylation and Methylation of Histones and Their Possible Role in the Regulation of Rna Synthesis. *Proceedings of the National Academy of Sciences of the United States of America* **51**: 786-794.

Arnoux V, Nassour M, L'Helgoualc'h A, Hipskind RA, Savagner P. 2008. Erk5 controls Slug expression and keratinocyte activation during wound healing. *Molecular biology of the cell* **19**: 4738-4749.

Balli D, Ren X, Chou FS, Cross E, Zhang Y, Kalinichenko VV, Kalin TV. 2012. Foxm1 transcription factor is required for macrophage migration during lung inflammation and tumor formation. *Oncogene* **31**: 3875-3888.

Bao B, Ali S, Banerjee S, Wang Z, Logna F, Azmi AS, Kong D, Ahmad A, Li Y, Padhye S et al. 2012. Curcumin analogue CDF inhibits pancreatic tumor growth by switching on suppressor microRNAs and attenuating EZH2 expression. *Cancer research* **72**: 335-345.

Bao B, Wang Z, Ali S, Kong D, Banerjee S, Ahmad A, Li Y, Azmi AS, Miele L, Sarkar FH. 2011. Over-expression of FoxM1 leads to epithelial-mesenchymal transition

and cancer stem cell phenotype in pancreatic cancer cells. *Journal of cellular biochemistry* **112**: 2296-2306.

Barrios CH, Liu MC, Lee SC, Vanlemmens L, Ferrero JM, Tabei T, Pivot X, Iwata H, Aogi K, Lugo-Quintana R et al. 2010. Phase III randomized trial of sunitinib versus capecitabine in patients with previously treated HER2-negative advanced breast cancer. *Breast cancer research and treatment* **121**: 121-131.

Baselga J, Gomez P, Greil R, Braga S, Climent MA, Wardley AM, Kaufman B, Stemmer SM, Pego A, Chan A et al. 2013. Randomized phase II study of the anti-epidermal growth factor receptor monoclonal antibody cetuximab with cisplatin versus cisplatin alone in patients with metastatic triple-negative breast cancer. *Journal of clinical oncology : official journal of the American Society of Clinical Oncology* **31**: 2586-2592.

Baselga J, Perez EA, Pienkowski T, Bell R. 2006. Adjuvant trastuzumab: a milestone in the treatment of HER-2-positive early breast cancer. *Oncologist* **11 Suppl 1**: 4-12.

Benz CC, Yau C. 2008. Ageing, oxidative stress and cancer: paradigms in parallax. *Nature reviews Cancer* **8**: 875-879.

Bhat UG, Jagadeeswaran R, Halasi M, Gartel AL. 2011. Nucleophosmin interacts with FOXM1 and modulates the level and localization of FOXM1 in human cancer cells. *The Journal of biological chemistry* **286**: 41425-41433.

Bhattacharyya A, Ear US, Koller BH, Weichselbaum RR, Bishop DK. 2000. The breast cancer susceptibility gene BRCA1 is required for subnuclear assembly of Rad51 and survival following treatment with the DNA cross-linking agent cisplatin. *The Journal of biological chemistry* **275**: 23899-23903.

Birve A, Sengupta AK, Beuchle D, Larsson J, Kennison JA, Rasmuson-Lestander A, Muller J. 2001. Su(z)12, a novel Drosophila Polycomb group gene that is conserved in vertebrates and plants. *Development* **128**: 3371-3379.

Boire A, Covic L, Agarwal A, Jacques S, Sherifi S, Kuliopulos A. 2005. PAR1 is a matrix metalloprotease-1 receptor that promotes invasion and tumorigenesis of breast cancer cells. *Cell* **120**: 303-313.

Boyer LA, Plath K, Zeitlinger J, Brambrink T, Medeiros LA, Lee TI, Levine SS, Wernig M, Tajonar A, Ray MK et al. 2006. Polycomb complexes repress developmental regulators in murine embryonic stem cells. *Nature* **441**: 349-353.

Bracken AP, Dietrich N, Pasini D, Hansen KH, Helin K. 2006. Genome-wide mapping of Polycomb target genes unravels their roles in cell fate transitions. *Genes & development* **20**: 1123-1136.

Bracken AP, Pasini D, Capra M, Prosperini E, Colli E, Helin K. 2003. EZH2 is downstream of the pRB-E2F pathway, essential for proliferation and amplified in cancer. *The EMBO journal* **22**: 5323-5335.

Brenner O, Levanon D, Negreanu V, Golubkov O, Fainaru O, Woolf E, Groner Y. 2004. Loss of Runx3 function in leukocytes is associated with spontaneously developed colitis and gastric mucosal hyperplasia. *Proc Natl Acad Sci U S A* **101**: 16016-16021.

Brenton JD, Carey LA, Ahmed AA, Caldas C. 2005. Molecular classification and molecular forecasting of breast cancer: ready for clinical application? *Journal of clinical oncology : official journal of the American Society of Clinical Oncology* **23**: 7350-7360.

Brownell JE, Zhou J, Ranalli T, Kobayashi R, Edmondson DG, Roth SY, Allis CD. 1996. Tetrahymena histone acetyltransferase A: a homolog to yeast Gcn5p linking histone acetylation to gene activation. *Cell* **84**: 843-851.

Burris HA, 3rd. 2000. Docetaxel (Taxotere) in HER-2-positive patients and in combination with trastuzumab (Herceptin). *Seminars in oncology* **27**: 19-23.

Byrski T, Gronwald J, Huzarski T, Grzybowska E, Budryk M, Stawicka M, Mierzwa T, Szwiec M, Wisniowski R, Siolek M et al. 2008. Response to neo-adjuvant chemotherapy in women with BRCA1-positive breast cancers. *Breast cancer research and treatment* **108**: 289-296.

Cameron D, Brown J, Dent R, Jackisch C, Mackey J, Pivot X, Steger GG, Suter TM, Toi M, Parmar M et al. 2013. Adjuvant bevacizumab-containing therapy in triple-negative breast cancer (BEATRICE): primary results of a randomised, phase 3 trial. *The Lancet Oncology* **14**: 933-942.

Cantoni O, Sestili P, Cattabeni F, Geroni C, Grandi M, Giuliani FC. 1989. Cellular and molecular pharmacology of 4'-epidoxorubicin in HeLa cells. Comparison with its parent drug, doxorubicin. *Journal of cancer research and clinical oncology* **115**: 373-378.

Cao Q, Yu J, Dhanasekaran SM, Kim JH, Mani RS, Tomlins SA, Mehra R, Laxman B, Cao X, Kleer CG et al. 2008. Repression of E-cadherin by the polycomb group protein EZH2 in cancer. *Oncogene* **27**: 7274-7284.

Cao R, Tsukada Y, Zhang Y. 2005. Role of Bmi-1 and Ring1A in H2A ubiquitylation and Hox gene silencing. *Molecular cell* **20**: 845-854.

Cao R, Wang L, Wang H, Xia L, Erdjument-Bromage H, Tempst P, Jones RS, Zhang Y. 2002. Role of histone H3 lysine 27 methylation in Polycomb-group silencing. *Science* **298**: 1039-1043.

Cao R, Zhang Y. 2004a. The functions of E(Z)/EZH2-mediated methylation of lysine 27 in histone H3. *Current opinion in genetics & development* **14**: 155-164.

-. 2004b. SUZ12 is required for both the histone methyltransferase activity and the silencing function of the EED-EZH2 complex. *Molecular cell* **15**: 57-67.

Carey LA, Dees EC, Sawyer L, Gatti L, Moore DT, Collichio F, Ollila DW, Sartor CI, Graham ML, Perou CM. 2007. The triple negative paradox: primary tumor chemosensitivity of breast cancer subtypes. *Clinical cancer research : an official journal of the American Association for Cancer Research* **13**: 2329-2334.

Carey LA, Rugo HS, Marcom PK, Mayer EL, Esteva FJ, Ma CX, Liu MC, Storniolo AM, Rimawi MF, Forero-Torres A et al. 2012. TBCRC 001: randomized phase II study of cetuximab in combination with carboplatin in stage IV triple-negative breast cancer. *Journal of clinical oncology : official journal of the American Society of Clinical Oncology* **30**: 2615-2623.

Carr JR, Park HJ, Wang Z, Kiefer MM, Raychaudhuri P. 2010. FoxM1 mediates resistance to herceptin and paclitaxel. *Cancer research* **70**: 5054-5063.

Carroll JS, Liu XS, Brodsky AS, Li W, Meyer CA, Szary AJ, Eeckhoute J, Shao W, Hestermann EV, Geistlinger TR et al. 2005. Chromosome-wide mapping of estrogen receptor binding reveals long-range regulation requiring the forkhead protein FoxA1. *Cell* **122**: 33-43.

Carver EA, Jiang R, Lan Y, Oram KF, Gridley T. 2001. The mouse snail gene encodes a key regulator of the epithelial-mesenchymal transition. *Molecular and cellular biology* **21**: 8184-8188.

Cha TL, Zhou BP, Xia W, Wu Y, Yang CC, Chen CT, Ping B, Otte AP, Hung MC. 2005. Akt-mediated phosphorylation of EZH2 suppresses methylation of lysine 27 in histone H3. *Science* **310**: 306-310.

Chamberlain SJ, Yee D, Magnuson T. 2008. Polycomb repressive complex 2 is dispensable for maintenance of embryonic stem cell pluripotency. *Stem Cells* **26**: 1496-1505.

Chandriani S, Frengen E, Cowling VH, Pendergrass SA, Perou CM, Whitfield ML, Cole MD. 2009. A core MYC gene expression signature is prominent in basal-like breast cancer but only partially overlaps the core serum response. *PloS one* **4**: e6693.

Chang CJ, Yang JY, Xia W, Chen CT, Xie X, Chao CH, Woodward WA, Hsu JM, Hortobagyi GN, Hung MC. 2011. EZH2 promotes expansion of breast tumor initiating cells through activation of RAF1-beta-catenin signaling. *Cancer cell* **19**: 86-100.

Charafe-Jauffret E, Ginestier C, Monville F, Finetti P, Adelaide J, Cervera N, Fekairi S, Xerri L, Jacquemier J, Birnbaum D et al. 2006. Gene expression profiling of breast cell lines identifies potential new basal markers. *Oncogene* **25**: 2273-2284.

Chase A, Cross NC. 2011. Aberrations of EZH2 in cancer. *Clinical cancer research : an official journal of the American Association for Cancer Research* **17**: 2613-2618.

Chaudhary J, Mosher R, Kim G, Skinner MK. 2000. Role of winged helix transcription factor (WIN) in the regulation of Sertoli cell differentiated functions: WIN acts as an early event gene for follicle-stimulating hormone. *Endocrinology* **141**: 2758-2766.

Chen PM, Wu TC, Shieh SH, Wu YH, Li MC, Sheu GT, Cheng YW, Chen CY, Lee H. 2013. MnSOD promotes tumor invasion via upregulation of FoxM1-MMP2 axis and related with poor survival and relapse in lung adenocarcinomas. *Molecular cancer research : MCR* **11**: 261-271.

Chen YJ, Dominguez-Brauer C, Wang Z, Asara JM, Costa RH, Tyner AL, Lau LF, Raychaudhuri P. 2009. A conserved phosphorylation site within the forkhead domain of FoxM1B is required for its activation by cyclin-CDK1. *The Journal of biological chemistry* **284**: 30695-30707.

Coppe JP, Patil CK, Rodier F, Sun Y, Munoz DP, Goldstein J, Nelson PS, Desprez PY, Campisi J. 2008. Senescence-associated secretory phenotypes reveal cell-nonautonomous functions of oncogenic RAS and the p53 tumor suppressor. *PLoS biology* **6**: 2853-2868.

Curtis C, Shah SP, Chin SF, Turashvili G, Rueda OM, Dunning MJ, Speed D, Lynch AG, Samarajiwa S, Yuan Y et al. 2012. The genomic and transcriptomic architecture of 2,000 breast tumours reveals novel subgroups. *Nature* **486**: 346-352.

Czermin B, Melfi R, McCabe D, Seitz V, Imhof A, Pirrotta V. 2002. Drosophila enhancer of Zeste/ESC complexes have a histone H3 methyltransferase activity that marks chromosomal Polycomb sites. *Cell* **111**: 185-196.

Dai B, Kang SH, Gong W, Liu M, Aldape KD, Sawaya R, Huang S. 2007. Aberrant FoxM1B expression increases matrix metalloproteinase-2 transcription and enhances the invasion of glioma cells. *Oncogene* **26**: 6212-6219.

Dang CV. 1999. c-Myc target genes involved in cell growth, apoptosis, and metabolism. *Molecular and cellular biology* **19**: 1-11.

de Napoles M, Mermoud JE, Wakao R, Tang YA, Endoh M, Appanah R, Nesterova TB, Silva J, Otte AP, Vidal M et al. 2004. Polycomb group proteins Ring1A/B link ubiquitylation of histone H2A to heritable gene silencing and X inactivation. *Developmental cell* **7**: 663-676.

Dehay C, Kennedy H. 2007. Cell-cycle control and cortical development. *Nature reviews Neuroscience* **8**: 438-450.

Derfoul A, Juan AH, Difilippantonio MJ, Palanisamy N, Ried T, Sartorelli V. 2011. Decreased microRNA-214 levels in breast cancer cells coincides with increased cell proliferation, invasion and accumulation of the Polycomb Ezh2 methyltransferase. *Carcinogenesis* **32**: 1607-1614.

Du J, Li L, Ou Z, Kong C, Zhang Y, Dong Z, Zhu S, Jiang H, Shao Z, Huang B et al. 2012. FOXC1, a target of polycomb, inhibits metastasis of breast cancer cells. *Breast Cancer Res Treat* **131**: 65-73.

Eeckhoute J, Carroll JS, Geistlinger TR, Torres-Arzayus MI, Brown M. 2006. A cell-type-specific transcriptional network required for estrogen regulation of cyclin D1 and cell cycle progression in breast cancer. *Genes Dev* **20**: 2513-2526.

Elsheikh SE, Green AR, Rakha EA, Powe DG, Ahmed RA, Collins HM, Soria D, Garibaldi JM, Paish CE, Ammar AA et al. 2009. Global histone modifications in breast cancer correlate with tumor phenotypes, prognostic factors, and patient outcome. *Cancer research* **69**: 3802-3809.

Ernst T, Chase AJ, Score J, Hidalgo-Curtis CE, Bryant C, Jones AV, Waghorn K, Zoi K, Ross FM, Reiter A et al. 2010. Inactivating mutations of the histone methyltransferase gene EZH2 in myeloid disorders. *Nature genetics* **42**: 722-726.

Farmer H, McCabe N, Lord CJ, Tutt AN, Johnson DA, Richardson TB, Santarosa M, Dillon KJ, Hickson I, Knights C et al. 2005. Targeting the DNA repair defect in BRCA mutant cells as a therapeutic strategy. *Nature* **434**: 917-921.

Feng Q, Wang H, Ng HH, Erdjument-Bromage H, Tempst P, Struhl K, Zhang Y. 2002. Methylation of H3-lysine 79 is mediated by a new family of HMTases without a SET domain. *Current biology : CB* **12**: 1052-1058.

Ferlay J, Soerjomataram I, Dikshit R, Eser S, Mathers C, Rebelo M, Parkin DM, Forman D, Bray F. 2015. Cancer incidence and mortality worldwide: sources, methods and major patterns in GLOBOCAN 2012. *International journal of cancer Journal international du cancer* **136**: E359-386.

Fischle W, Wang Y, Jacobs SA, Kim Y, Allis CD, Khorasanizadeh S. 2003. Molecular basis for the discrimination of repressive methyl-lysine marks in histone H3 by Polycomb and HP1 chromodomains. *Genes & development* **17**: 1870-1881.

Fong PC, Boss DS, Yap TA, Tutt A, Wu P, Mergui-Roelvink M, Mortimer P, Swaisland H, Lau A, O'Connor MJ et al. 2009. Inhibition of poly(ADP-ribose) polymerase in tumors from BRCA mutation carriers. *N Engl J Med* **361**: 123-134.

Forero-Torres A, Varley KE, Abramson V, Li Y, Vaklavas C, Lin NU, Liu MC, Rugo HS, Nanda R, Stroniolo AM et al. 2015. TBCRC 019: phase II trial of nab-PAC

with/without the anti-death receptor 5 monoclonal antibody tigatuzumab in patients with triple negative breast cancer. *Clinical cancer research : an official journal of the American Association for Cancer Research*.

Foulkes WD, Stefansson IM, Chappuis PO, Begin LR, Goffin JR, Wong N, Trudel M, Akslen LA. 2003. Germline BRCA1 mutations and a basal epithelial phenotype in breast cancer. *Journal of the National Cancer Institute* **95**: 1482-1485.

Francis NJ, Kingston RE, Woodcock CL. 2004. Chromatin compaction by a polycomb group protein complex. *Science* **306**: 1574-1577.

Fujii S, Ito K, Ito Y, Ochiai A. 2008. Enhancer of zeste homologue 2 (EZH2) down-regulates RUNX3 by increasing histone H3 methylation. *J Biol Chem* **283**: 17324-17332.

Fujii S, Tokita K, Wada N, Ito K, Yamauchi C, Ito Y, Ochiai A. 2011. MEK-ERK pathway regulates EZH2 overexpression in association with aggressive breast cancer subtypes. *Oncogene* **30**: 4118-4128.

Garrick D, De Gobbi M, Samara V, Rugless M, Holland M, Ayyub H, Lower K, Sloane-Stanley J, Gray N, Koch C et al. 2008. The role of the polycomb complex in silencing alpha-globin gene expression in nonerythroid cells. *Blood* **112**: 3889-3899.

Gianni L, Norton L, Wolmark N, Suter TM, Bonadonna G, Hortobagyi GN. 2009. Role of anthracyclines in the treatment of early breast cancer. *Journal of clinical oncology : official journal of the American Society of Clinical Oncology* **27**: 4798-4808.

Gilkes DM, Semenza GL. 2013. Role of hypoxia-inducible factors in breast cancer metastasis. *Future Oncol* **9**: 1623-1636.

Glazer RI, Hartman KD, Knode MC, Richard MM, Chiang PK, Tseng CK, Marquez VE. 1986. 3-Deazaneplanocin: a new and potent inhibitor of S-adenosylhomocysteine hydrolase and its effects on human promyelocytic leukemia cell line HL-60. *Biochemical and biophysical research communications* **135**: 688-694.

Gong A, Huang S. 2012. FoxM1 and Wnt/beta-catenin signaling in glioma stem cells. *Cancer research* **72**: 5658-5662.

Gonzalez ME, DuPrie ML, Krueger H, Merajver SD, Ventura AC, Toy KA, Kleer CG. 2011. Histone methyltransferase EZH2 induces Akt-dependent genomic instability and BRCA1 inhibition in breast cancer. *Cancer Res* **71**: 2360-2370.

Gonzalez ME, Li X, Toy K, DuPrie M, Ventura AC, Banerjee M, Ljungman M, Merajver SD, Kleer CG. 2009. Downregulation of EZH2 decreases growth of estrogen receptor-negative invasive breast carcinoma and requires BRCA1. *Oncogene* **28**: 843-853.

Gonzalez ME, Moore HM, Li X, Toy KA, Huang W, Sabel MS, Kidwell KM, Kleer CG. 2014a. EZH2 expands breast stem cells through activation of NOTCH1 signaling. *Proc Natl Acad Sci U S A* **111**: 3098-3103.

-. 2014b. EZH2 expands breast stem cells through activation of NOTCH1 signaling. *Proceedings of the National Academy of Sciences of the United States of America* **111**: 3098-3103.

Guenther MG, Levine SS, Boyer LA, Jaenisch R, Young RA. 2007. A chromatin landmark and transcription initiation at most promoters in human cells. *Cell* **130**: 77-88.

Haase VH. 2010. Hypoxic regulation of erythropoiesis and iron metabolism. *Am J Physiol Renal Physiol* **299**: F1-13.

Halasi M, Gartel AL. 2009. A novel mode of FoxM1 regulation: positive auto-regulatory loop. *Cell Cycle* **8**: 1966-1967.

-. 2012. Suppression of FOXM1 sensitizes human cancer cells to cell death induced by DNA-damage. *PLoS One* **7**: e31761.

Halasi M, Pandit B, Wang M, Nogueira V, Hay N, Gartel AL. 2013. Combination of oxidative stress and FOXM1 inhibitors induces apoptosis in cancer cells and inhibits xenograft tumor growth. *The American journal of pathology* **183**: 257-265.

Hanahan D, Weinberg RA. 2011. Hallmarks of cancer: the next generation. *Cell* **144**: 646-674.

He A, Shen X, Ma Q, Cao J, von Gise A, Zhou P, Wang G, Marquez VE, Orkin SH, Pu WT. 2012. PRC2 directly methylates GATA4 and represses its transcriptional activity. *Genes Dev* **26**: 37-42.

Herschkowitz JI, He X, Fan C, Perou CM. 2008. The functional loss of the retinoblastoma tumour suppressor is a common event in basal-like and luminal B breast carcinomas. *Breast cancer research : BCR* **10**: R75.

Holm K, Grabau D, Lovgren K, Aradottir S, Gruvberger-Saal S, Howlin J, Saal LH, Ethier SP, Bendahl PO, Stal O et al. 2012. Global H3K27 trimethylation and EZH2 abundance in breast tumor subtypes. *Molecular oncology* **6**: 494-506.

Holm K, Hegardt C, Staaf J, Vallon-Christersson J, Jonsson G, Olsson H, Borg A, Ringner M. 2010. Molecular subtypes of breast cancer are associated with characteristic DNA methylation patterns. *Breast cancer research : BCR* **12**: R36.

Hong S, Cho YW, Yu LR, Yu H, Veenstra TD, Ge K. 2007. Identification of JmjC domain-containing UTX and JMJD3 as histone H3 lysine 27 demethylases.

Proceedings of the National Academy of Sciences of the United States of America **104**: 18439-18444.

Huang C, Qiu Z, Wang L, Peng Z, Jia Z, Logsdon CD, Le X, Wei D, Huang S, Xie K. 2012. A novel FoxM1-caveolin signaling pathway promotes pancreatic cancer invasion and metastasis. *Cancer research* **72**: 655-665.

Isakoff SJ, Mayer EL, He L, Traina TA, Carey LA, Krag KJ, Rugo HS, Liu MC, Stearns V, Come SE et al. 2015. TBCRC009: A Multicenter Phase II Clinical Trial of Platinum Monotherapy With Biomarker Assessment in Metastatic Triple-Negative Breast Cancer. *Journal of clinical oncology : official journal of the American Society of Clinical Oncology*.

Jack JW, Judd BH. 1979. Allelic pairing and gene regulation: A model for the zeste-white interaction in Drosophila melanogaster. *Proceedings of the National Academy of Sciences of the United States of America* **76**: 1368-1372.

Jacobs JJ, Kieboom K, Marino S, DePinho RA, van Lohuizen M. 1999. The oncogene and Polycomb-group gene bmi-1 regulates cell proliferation and senescence through the ink4a locus. *Nature* **397**: 164-168.

Jenuwein T, Laible G, Dorn R, Reuter G. 1998. SET domain proteins modulate chromatin domains in eu- and heterochromatin. *Cellular and molecular life sciences : CMLS* **54**: 80-93.

Jesinger RA. 2014. Breast anatomy for the interventionalist. *Techniques in vascular and interventional radiology* **17**: 3-9.

Jones CA, Ng J, Peterson AJ, Morgan K, Simon J, Jones RS. 1998. The Drosophila esc and E(z) proteins are direct partners in polycomb group-mediated repression. *Molecular and cellular biology* **18**: 2825-2834.

Jung HY, Jun S, Lee M, Kim HC, Wang X, Ji H, McCrea PD, Park JI. 2013a. PAF and EZH2 induce Wnt/beta-catenin signaling hyperactivation. *Molecular cell* **52**: 193-205.

-. 2013b. PAF and EZH2 induce Wnt/beta-catenin signaling hyperactivation. *Mol Cell* **52**: 193-205.

Kaestner KH, Knochel W, Martinez DE. 2000. Unified nomenclature for the winged helix/forkhead transcription factors. *Genes & development* **14**: 142-146.

Kalinichenko VV, Major ML, Wang X, Petrovic V, Kuechle J, Yoder HM, Dennewitz MB, Shin B, Datta A, Raychaudhuri P et al. 2004. Foxm1b transcription factor is essential for development of hepatocellular carcinomas and is negatively regulated by the p19ARF tumor suppressor. *Genes & development* **18**: 830-850.

Karadedou CT, Gomes AR, Chen J, Petkovic M, Ho KK, Zwolinska AK, Feltes A, Wong SY, Chan KY, Cheung YN et al. 2012. FOXO3a represses VEGF expression through FOXM1-dependent and -independent mechanisms in breast cancer. *Oncogene* **31**: 1845-1858.

Ketel CS, Andersen EF, Vargas ML, Suh J, Strome S, Simon JA. 2005. Subunit contributions to histone methyltransferase activities of fly and worm polycomb group complexes. *Molecular and cellular biology* **25**: 6857-6868.

Kim E, Kim M, Woo DH, Shin Y, Shin J, Chang N, Oh YT, Kim H, Rheey J, Nakano I et al. 2013. Phosphorylation of EZH2 activates STAT3 signaling via STAT3 methylation and promotes tumorigenicity of glioblastoma stem-like cells. *Cancer cell* **23**: 839-852.

Kirmizis A, Bartley SM, Farnham PJ. 2003. Identification of the polycomb group protein SU(Z)12 as a potential molecular target for human cancer therapy. *Molecular cancer therapeutics* **2**: 113-121.

Kirmizis A, Bartley SM, Kuzmichev A, Margueron R, Reinberg D, Green R, Farnham PJ. 2004. Silencing of human polycomb target genes is associated with methylation of histone H3 Lys 27. *Genes & development* **18**: 1592-1605.

Kleer CG, Cao Q, Varambally S, Shen R, Ota I, Tomlins SA, Ghosh D, Sewalt RG, Otte AP, Hayes DF et al. 2003. EZH2 is a marker of aggressive breast cancer and promotes neoplastic transformation of breast epithelial cells. *Proceedings of the National Academy of Sciences of the United States of America* **100**: 11606-11611.

Kleff S, Andrulis ED, Anderson CW, Sternglanz R. 1995. Identification of a gene encoding a yeast histone H4 acetyltransferase. *The Journal of biological chemistry* **270**: 24674-24677.

Knutson SK, Kawano S, Minoshima Y, Warholic NM, Huang KC, Xiao Y, Kadowaki T, Uesugi M, Kuznetsov G, Kumar N et al. 2014. Selective inhibition of EZH2 by EPZ-6438 leads to potent antitumor activity in EZH2-mutant non-Hodgkin lymphoma. *Molecular cancer therapeutics* **13**: 842-854.

Knutson SK, Warholic NM, Wigle TJ, Klaus CR, Allain CJ, Raimondi A, Porter Scott M, Chesworth R, Moyer MP, Copeland RA et al. 2013. Durable tumor regression in genetically altered malignant rhabdoid tumors by inhibition of methyltransferase EZH2. *Proceedings of the National Academy of Sciences of the United States of America* **110**: 7922-7927.

Koontz JI, Soreng AL, Nucci M, Kuo FC, Pauwels P, van Den Berghe H, Dal Cin P, Fletcher JA, Sklar J. 2001. Frequent fusion of the JAZF1 and JJAZ1 genes in endometrial stromal tumors. *Proceedings of the National Academy of Sciences of the United States of America* **98**: 6348-6353.

Kops GJ, Medema RH, Glassford J, Essers MA, Dijkers PF, Coffer PJ, Lam EW, Burgering BM. 2002. Control of cell cycle exit and entry by protein kinase B-regulated forkhead transcription factors. *Mol Cell Biol* **22**: 2025-2036.

Korver W, Roose J, Clevers H. 1997. The winged-helix transcription factor Trident is expressed in cycling cells. *Nucleic acids research* **25**: 1715-1719.

Kousidou OC, Roussidis AE, Theocharis AD, Karamanos NK. 2004. Expression of MMPs and TIMPs genes in human breast cancer epithelial cells depends on cell culture conditions and is associated with their invasive potential. *Anticancer research* **24**: 4025-4030.

Krupczak-Hollis K, Wang X, Kalinichenko VV, Gusarova GA, Wang IC, Dennewitz MB, Yoder HM, Kiyokawa H, Kaestner KH, Costa RH. 2004. The mouse Forkhead Box m1 transcription factor is essential for hepatoblast mitosis and development of intrahepatic bile ducts and vessels during liver morphogenesis. *Developmental biology* **276**: 74-88.

Kuilman T, Michaloglou C, Vredeveld LC, Douma S, van Doorn R, Desmet CJ, Aarden LA, Mooi WJ, Peeper DS. 2008. Oncogene-induced senescence relayed by an interleukin-dependent inflammatory network. *Cell* **133**: 1019-1031.

Kuzmichev A, Margueron R, Vaquero A, Preissner TS, Scher M, Kirmizis A, Ouyang X, Brockdorff N, Abate-Shen C, Farnham P et al. 2005. Composition and histone substrates of polycomb repressive group complexes change during cellular differentiation. *Proceedings of the National Academy of Sciences of the United States of America* **102**: 1859-1864.

Kuzmichev A, Nishioka K, Erdjument-Bromage H, Tempst P, Reinberg D. 2002. Histone methyltransferase activity associated with a human multiprotein complex containing the Enhancer of Zeste protein. *Genes & development* **16**: 2893-2905.

Kwok JM, Peck B, Monteiro LJ, Schwenen HD, Millour J, Coombes RC, Myatt SS, Lam EW. 2010. FOXM1 confers acquired cisplatin resistance in breast cancer cells. *Molecular cancer research : MCR* **8**: 24-34.

Lai E, Prezioso VR, Smith E, Litvin O, Costa RH, Darnell JE, Jr. 1990. HNF-3A, a hepatocyte-enriched transcription factor of novel structure is regulated transcriptionally. *Genes & development* **4**: 1427-1436.

Lam AK, Ngan AW, Leung MH, Kwok DC, Liu VW, Chan DW, Leung WY, Yao KM. 2013. FOXM1b, which is present at elevated levels in cancer cells, has a greater transforming potential than FOXM1c. *Frontiers in oncology* **3**: 11.

Laoukili J, Alvarez M, Meijer LA, Stahl M, Mohammed S, Kleij L, Heck AJ, Medema RH. 2008. Activation of FoxM1 during G2 requires cyclin A/Cdk-dependent relief of autorepression by the FoxM1 N-terminal domain. *Molecular and cellular biology* **28**: 3076-3087.

Laoukili J, Kooistra MR, Bras A, Kauw J, Kerkhoven RM, Morrison A, Clevers H, Medema RH. 2005. FoxM1 is required for execution of the mitotic programme and chromosome stability. *Nature cell biology* **7**: 126-136.

Laoukili J, Stahl M, Medema RH. 2007. FoxM1: at the crossroads of ageing and cancer. *Biochimica et biophysica acta* **1775**: 92-102.

Lee HY, Choi K, Oh H, Park YK, Park H. 2014. HIF-1-dependent induction of Jumonji domain-containing protein (JMJD) 3 under hypoxic conditions. *Molecules and cells* **37**: 43-50.

Lee JM, Lee JS, Kim H, Kim K, Park H, Kim JY, Lee SH, Kim IS, Kim J, Lee M et al. 2012. EZH2 generates a methyl degron that is recognized by the DCAF1/DDB1/CUL4 E3 ubiquitin ligase complex. *Mol Cell* **48**: 572-586.

Lee MH, Reynisdottir I, Massague J. 1995. Cloning of p57KIP2, a cyclin-dependent kinase inhibitor with unique domain structure and tissue distribution. *Genes Dev* **9**: 639-649.

Lee ST, Li Z, Wu Z, Aau M, Guan P, Karuturi RK, Liou YC, Yu Q. 2011a. Context-specific regulation of NF-kappaB target gene expression by EZH2 in breast cancers. *Molecular cell* **43**: 798-810.

-. 2011b. Context-specific regulation of NF-kappaB target gene expression by EZH2 in breast cancers. *Mol Cell* **43**: 798-810.

Lehmann BD, Bauer JA, Chen X, Sanders ME, Chakravarthy AB, Shyr Y, Pietenpol JA. 2011a. Identification of human triple-negative breast cancer subtypes and preclinical models for selection of targeted therapies. *The Journal of clinical investigation* **121**: 2750-2767.

-. 2011b. Identification of human triple-negative breast cancer subtypes and preclinical models for selection of targeted therapies. *J Clin Invest* **121**: 2750-2767.

Lepilina A, Coon AN, Kikuchi K, Holdway JE, Roberts RW, Burns CG, Poss KD. 2006. A dynamic epicardial injury response supports progenitor cell activity during zebrafish heart regeneration. *Cell* **127**: 607-619.

Lessard J, Schumacher A, Thorsteinsdottir U, van Lohuizen M, Magnuson T, Sauvageau G. 1999. Functional antagonism of the Polycomb-Group genes eed and Bmi1 in hemopoietic cell proliferation. *Genes & development* **13**: 2691-2703.

Levine SS, Weiss A, Erdjument-Bromage H, Shao Z, Tempst P, Kingston RE. 2002. The core of the polycomb repressive complex is compositionally and functionally conserved in flies and humans. *Molecular and cellular biology* **22**: 6070-6078.

Li D, Wei P, Peng Z, Huang C, Tang H, Jia Z, Cui J, Le X, Huang S, Xie K. 2013. The critical role of dysregulated FOXM1-PLAUR signaling in human colon cancer

progression and metastasis. *Clinical cancer research : an official journal of the American Association for Cancer Research* **19**: 62-72.

Li H, Ma X, Wang J, Koontz J, Nucci M, Sklar J. 2007. Effects of rearrangement and allelic exclusion of JJAZ1/SUZ12 on cell proliferation and survival. *Proceedings of the National Academy of Sciences of the United States of America* **104**: 20001-20006.

Li Q, Zhang N, Jia Z, Le X, Dai B, Wei D, Huang S, Tan D, Xie K. 2009. Critical role and regulation of transcription factor FoxM1 in human gastric cancer angiogenesis and progression. *Cancer research* **69**: 3501-3509.

Li Z, Jia Z, Gao Y, Xie D, Wei D, Cui J, Mishra L, Huang S, Zhang Y, Xie K. 2015. Activation of vitamin D receptor signaling downregulates the expression of nuclear FOXM1 protein and suppresses pancreatic cancer cell stemness. *Clinical cancer research : an official journal of the American Association for Cancer Research* **21**: 844-853.

Liu S, Guo W, Shi J, Li N, Yu X, Xue J, Fu X, Chu K, Lu C, Zhao J et al. 2012. MicroRNA-135a contributes to the development of portal vein tumor thrombus by promoting metastasis in hepatocellular carcinoma. *Journal of hepatology* **56**: 389-396.

Liu VC, Wong LY, Jang T, Shah AH, Park I, Yang X, Zhang Q, Lonning S, Teicher BA, Lee C. 2007. Tumor evasion of the immune system by converting CD4+CD25- T cells into CD4+CD25+ T regulatory cells: role of tumor-derived TGF-beta. *J Immunol* **178**: 2883-2892.

Lok GT, Chan DW, Liu VW, Hui WW, Leung TH, Yao KM, Ngan HY. 2011. Aberrant activation of ERK/FOXM1 signaling cascade triggers the cell migration/invasion in ovarian cancer cells. *PloS one* **6**: e23790.

Lord CJ, Garrett MD, Ashworth A. 2006. Targeting the double-strand DNA break repair pathway as a therapeutic strategy. *Clinical cancer research : an official journal of the American Association for Cancer Research* **12**: 4463-4468.

Luger K, Mader AW, Richmond RK, Sargent DF, Richmond TJ. 1997. Crystal structure of the nucleosome core particle at 2.8 A resolution. *Nature* **389**: 251-260.

Ma RY, Tong TH, Cheung AM, Tsang AC, Leung WY, Yao KM. 2005. Raf/MEK/MAPK signaling stimulates the nuclear translocation and transactivating activity of FOXM1c. *Journal of cell science* **118**: 795-806.

Maertens GN, El Messaoudi-Aubert S, Racek T, Stock JK, Nicholls J, Rodriguez-Niedenführ M, Gil J, Peters G. 2009. Several Distinct Polycomb Complexes Regulate and Co-Localize on the <italic>INK4a</italic> Tumor Suppressor Locus. *PloS one* **4**: e6380.

Majewski IJ, Ritchie ME, Phipson B, Corbin J, Pakusch M, Ebert A, Busslinger M, Koseki H, Hu Y, Smyth GK et al. 2010. Opposing roles of polycomb repressive complexes in hematopoietic stem and progenitor cells. *Blood* **116**: 731-739.

Major ML, Lepe R, Costa RH. 2004. Forkhead box M1B transcriptional activity requires binding of Cdk-cyclin complexes for phosphorylation-dependent recruitment of p300/CBP coactivators. *Molecular and cellular biology* **24**: 2649-2661.

Makretsov NA, Huntsman DG, Nielsen TO, Yorida E, Peacock M, Cheang MC, Dunn SE, Hayes M, van de Rijn M, Bajdik C et al. 2004. Hierarchical clustering analysis of tissue microarray immunostaining data identifies prognostically significant groups of breast carcinoma. *Clinical cancer research : an official journal of the American Association for Cancer Research* **10**: 6143-6151.

Mani SA, Guo W, Liao MJ, Eaton EN, Ayyanan A, Zhou AY, Brooks M, Reinhard F, Zhang CC, Shipitsin M et al. 2008. The epithelial-mesenchymal transition generates cells with properties of stem cells. *Cell* **133**: 704-715.

Mani SA, Yang J, Brooks M, Schwaninger G, Zhou A, Miura N, Kutok JL, Hartwell K, Richardson AL, Weinberg RA. 2007. Mesenchyme Forkhead 1 (FOXC2) plays a key role in metastasis and is associated with aggressive basal-like breast cancers. *Proc Natl Acad Sci U S A* **104**: 10069-10074.

Margueron R, Justin N, Ohno K, Sharpe ML, Son J, Drury WJ, 3rd, Voigt P, Martin SR, Taylor WR, De Marco V et al. 2009. Role of the polycomb protein EED in the propagation of repressive histone marks. *Nature* **461**: 762-767.

Mariani-Costantini R, Escot C, Theillet C, Gentile A, Merlo G, Lidereau R, Callahan R. 1988. In situ c-myc expression and genomic status of the c-myc locus in infiltrating ductal carcinomas of the breast. *Cancer research* **48**: 199-205.

Martin C, Zhang Y. 2005. The diverse functions of histone lysine methylation. *Nature reviews Molecular cell biology* **6**: 838-849.

Matsuoka S, Edwards MC, Bai C, Parker S, Zhang P, Baldini A, Harper JW, Elledge SJ. 1995. p57KIP2, a structurally distinct member of the p21CIP1 Cdk inhibitor family, is a candidate tumor suppressor gene. *Genes Dev* **9**: 650-662.

McCabe MT, Ott HM, Ganji G, Korenchuk S, Thompson C, Van Aller GS, Liu Y, Graves AP, Della Pietra A, 3rd, Diaz E et al. 2012. EZH2 inhibition as a therapeutic strategy for lymphoma with EZH2-activating mutations. *Nature* **492**: 108-112.

McCabe N, Turner NC, Lord CJ, Kluzek K, Bialkowska A, Swift S, Giavara S, O'Connor MJ, Tutt AN, Zdzienicka MZ et al. 2006. Deficiency in the repair of DNA damage by homologous recombination and sensitivity to poly(ADP-ribose) polymerase inhibition. *Cancer research* **66**: 8109-8115.

Miller K, Wang M, Gralow J, Dickler M, Cobleigh M, Perez EA, Shenkier T, Cella D, Davidson NE. 2007. Paclitaxel plus bevacizumab versus paclitaxel alone for metastatic breast cancer. *N Engl J Med* **357**: 2666-2676.

Millour J, Constantinidou D, Stavropoulou AV, Wilson MS, Myatt SS, Kwok JM, Sivanandan K, Coombes RC, Medema RH, Hartman J et al. 2010. FOXM1 is a transcriptional target of ERalpha and has a critical role in breast cancer endocrine sensitivity and resistance. *Oncogene* **29**: 2983-2995.

Millour J, de Olano N, Horimoto Y, Monteiro LJ, Langer JK, Aligue R, Hajji N, Lam EW. 2011. ATM and p53 regulate FOXM1 expression via E2F in breast cancer epirubicin treatment and resistance. *Molecular cancer therapeutics* **10**: 1046-1058.

Miranda TB, Cortez CC, Yoo CB, Liang G, Abe M, Kelly TK, Marquez VE, Jones PA. 2009. DZNep is a global histone methylation inhibitor that reactivates developmental genes not silenced by DNA methylation. *Molecular cancer therapeutics* **8**: 1579-1588.

Montgomery ND, Yee D, Chen A, Kalantry S, Chamberlain SJ, Otte AP, Magnuson T. 2005. The murine polycomb group protein Eed is required for global histone H3 lysine-27 methylation. *Current biology : CB* **15**: 942-947.

Mortemousque B, Amati-Bonneau P, Couture F, Graffan R, Dubois S, Colin J, Bonneau D, Morissette J, Lacombe D, Raymond V. 2004. Axenfeld-Rieger anomaly: a novel mutation in the forkhead box C1 (FOXC1) gene in a 4-generation family. *Arch Ophthalmol* **122**: 1527-1533.

Moynahan ME, Chiu JW, Koller BH, Jasin M. 1999. Brca1 controls homology-directed DNA repair. *Molecular cell* **4**: 511-518.

Muller J, Hart CM, Francis NJ, Vargas ML, Sengupta A, Wild B, Miller EL, O'Connor MB, Kingston RE, Simon JA. 2002. Histone methyltransferase activity of a Drosophila Polycomb group repressor complex. *Cell* **111**: 197-208.

Munzel P, Marx D, Kochel H, Schauer A, Bock KW. 1991. Genomic alterations of the c-myc protooncogene in relation to the overexpression of c-erbB2 and Ki-67 in human breast and cervix carcinomas. *Journal of cancer research and clinical oncology* **117**: 603-607.

Nagase T, Seki N, Tanaka A, Ishikawa K, Nomura N. 1995. Prediction of the coding sequences of unidentified human genes. IV. The coding sequences of 40 new genes (KIAA0121-KIAA0160) deduced by analysis of cDNA clones from human cell line KG-1. *DNA research : an international journal for rapid publication of reports on genes and genomes* **2**: 167-174, 199-210.

Negri A, Oliveri C, Sforzini S, Mignione F, Viarengo A, Banni M. 2013. Transcriptional response of the mussel Mytilus galloprovincialis (Lam.) following exposure to heat stress and copper. *PloS one* **8**: e66802.

Nekrasov M, Wild B, Muller J. 2005. Nucleosome binding and histone methyltransferase activity of Drosophila PRC2. *EMBO reports* **6**: 348-353.

Nieto MA, Sargent MG, Wilkinson DG, Cooke J. 1994. Control of cell behavior during vertebrate development by Slug, a zinc finger gene. *Science* **264**: 835-839.

Nikoloski G, Langemeijer SM, Kuiper RP, Knops R, Massop M, Tonnissen ER, van der Heijden A, Scheele TN, Vandenberghe P, de Witte T et al. 2010. Somatic mutations of the histone methyltransferase gene EZH2 in myelodysplastic syndromes. *Nature genetics* **42**: 665-667.

Oguro H, Iwama A, Morita Y, Kamijo T, van Lohuizen M, Nakauchi H. 2006. Differential impact of Ink4a and Arf on hematopoietic stem cells and their bone marrow microenvironment in Bmi1-deficient mice. *The Journal of experimental medicine* **203**: 2247-2253.

Ohm JE, McGarvey KM, Yu X, Cheng L, Schuebel KE, Cope L, Mohammad HP, Chen W, Daniel VC, Yu W et al. 2007. A stem cell-like chromatin pattern may predispose tumor suppressor genes to DNA hypermethylation and heritable silencing. *Nature genetics* **39**: 237-242.

Okabe H, Satoh S, Kato T, Kitahara O, Yanagawa R, Yamaoka Y, Tsunoda T, Furukawa Y, Nakamura Y. 2001. Genome-wide analysis of gene expression in human hepatocellular carcinomas using cDNA microarray: identification of genes involved in viral carcinogenesis and tumor progression. *Cancer research* **61**: 2129-2137.

Oktyabri D, Tange S, Terashima M, Ishimura A, Suzuki T. 2014. EED regulates epithelial-mesenchymal transition of cancer cells induced by TGF-beta. *Biochemical and biophysical research communications* **453**: 124-130.

Paik JH, Kollipara R, Chu G, Ji H, Xiao Y, Ding Z, Miao L, Tothova Z, Horner JW, Carrasco DR et al. 2007. FoxOs are lineage-restricted redundant tumor suppressors and regulate endothelial cell homeostasis. *Cell* **128**: 309-323.

Park HJ, Carr JR, Wang Z, Nogueira V, Hay N, Tyner AL, Lau LF, Costa RH, Raychaudhuri P. 2009. FoxM1, a critical regulator of oxidative stress during oncogenesis. *The EMBO journal* **28**: 2908-2918.

Park HJ, Gusarova G, Wang Z, Carr JR, Li J, Kim KH, Qiu J, Park YD, Williamson PR, Hay N et al. 2011. Deregulation of FoxM1b leads to tumour metastasis. *EMBO molecular medicine* **3**: 21-34.

Pasini D, Bracken AP, Jensen MR, Lazzerini Denchi E, Helin K. 2004. Suz12 is essential for mouse development and for EZH2 histone methyltransferase activity. *The EMBO journal* **23**: 4061-4071.

Perou CM, Sorlie T, Eisen MB, van de Rijn M, Jeffrey SS, Rees CA, Pollack JR, Ross DT, Johnsen H, Akslen LA et al. 2000. Molecular portraits of human breast tumours. *Nature* **406**: 747-752.

Pilarsky C, Wenzig M, Specht T, Saeger HD, Grutzmann R. 2004. Identification and validation of commonly overexpressed genes in solid tumors by comparison of microarray data. *Neoplasia* **6**: 744-750.

Radhakrishnan SK, Bhat UG, Hughes DE, Wang IC, Costa RH, Gartel AL. 2006. Identification of a chemical inhibitor of the oncogenic transcription factor forkhead box M1. *Cancer research* **66**: 9731-9735.

Ren B, Cam H, Takahashi Y, Volkert T, Terragni J, Young RA, Dynlacht BD. 2002. E2F integrates cell cycle progression with DNA repair, replication, and G(2)/M checkpoints. *Genes Dev* **16**: 245-256.

Ren G, Baritaki S, Marathe H, Feng J, Park S, Beach S, Bazeley PS, Beshir AB, Fenteany G, Mehra R et al. 2012. Polycomb protein EZH2 regulates tumor invasion via the transcriptional repression of the metastasis suppressor RKIP in breast and prostate cancer. *Cancer research* **72**: 3091-3104.

Ridinger-Saison M, Evanno E, Gallais I, Rimmele P, Selimoglu-Buet D, Sapharikas E, Moreau-Gachelin F, Guillouf C. 2013. Epigenetic silencing of Bim transcription by Spi-1/PU.1 promotes apoptosis resistance in leukaemia. *Cell death and differentiation* **20**: 1268-1278.

Rietzler M, Bittner M, Kolanus W, Schuster A, Holzmann B. 1998. The human WD repeat protein WAIT-1 specifically interacts with the cytoplasmic tails of beta7-integrins. *The Journal of biological chemistry* **273**: 27459-27466.

Rouleau M, McDonald D, Gagne P, Ouellet ME, Droit A, Hunter JM, Dutertre S, Prigent C, Hendzel MJ, Poirier GG. 2007. PARP-3 associates with polycomb group bodies and with components of the DNA damage repair machinery. *Journal of cellular biochemistry* **100**: 385-401.

Sanders DA, Ross-Innes CS, Beraldi D, Carroll JS, Balasubramanian S. 2013. Genome-wide mapping of FOXM1 binding reveals co-binding with estrogen receptor alpha in breast cancer cells. *Genome biology* **14**: R6.

Sandhu R, Parker JS, Jones WD, Livasy CA, Coleman WB. 2010. Microarray-Based Gene Expression Profiling for Molecular Classification of Breast Cancer and Identification of New Targets for Therapy. *Lab Medicine* **41**: 364-372.

Schlesinger Y, Straussman R, Keshet I, Farkash S, Hecht M, Zimmerman J, Eden E, Yakhini Z, Ben-Shushan E, Reubinoff BE et al. 2007. Polycomb-mediated methylation on Lys27 of histone H3 pre-marks genes for de novo methylation in cancer. *Nature genetics* **39**: 232-236.

Schumacher A, Lichtarge O, Schwartz S, Magnuson T. 1998. The murine Polycomb-group gene eed and its human orthologue: functional implications of evolutionary conservation. *Genomics* **54**: 79-88.

Semenza GL. 2012. Hypoxia-inducible factors in physiology and medicine. *Cell* **148**: 399-408.

Sewalt RG, van der Vlag J, Gunster MJ, Hamer KM, den Blaauwen JL, Satijn DP, Hendrix T, van Driel R, Otte AP. 1998. Characterization of interactions between the mammalian polycomb-group proteins Enx1/EZH2 and EED suggests the existence of different mammalian polycomb-group protein complexes. *Molecular and cellular biology* **18**: 3586-3595.

Shi B, Liang J, Yang X, Wang Y, Zhao Y, Wu H, Sun L, Zhang Y, Chen Y, Li R et al. 2007a. Integration of estrogen and Wnt signaling circuits by the polycomb group protein EZH2 in breast cancer cells. *Mol Cell Biol* **27**: 5105-5119.

-. 2007b. Integration of estrogen and Wnt signaling circuits by the polycomb group protein EZH2 in breast cancer cells. *Molecular and cellular biology* **27**: 5105-5119.

Shi Y, Chang M, Wang F, Ouyang X, Jia Y, Du H. 2010. Role and mechanism of hypoxia-inducible factor-1 in cell growth and apoptosis of breast cancer cell line MDA-MB-231. *Oncology letters* **1**: 657-662.

Shin YJ, Kim JH. 2012. The role of EZH2 in the regulation of the activity of matrix metalloproteinases in prostate cancer cells. *PloS one* **7**: e30393.

Shogren-Knaak M, Ishii H, Sun JM, Pazin MJ, Davie JR, Peterson CL. 2006. Histone H4-K16 acetylation controls chromatin structure and protein interactions. *Science* **311**: 844-847.

Shook D, Keller R. 2003. Mechanisms, mechanics and function of epithelial-mesenchymal transitions in early development. *Mechanisms of development* **120**: 1351-1383.

Silver DP, Richardson AL, Eklund AC, Wang ZC, Szallasi Z, Li Q, Juul N, Leong CO, Calogrias D, Buraimoh A et al. 2010. Efficacy of neoadjuvant Cisplatin in triple-negative breast cancer. *Journal of clinical oncology : official journal of the American Society of Clinical Oncology* **28**: 1145-1153.

Simon JA, Lange CA. 2008. Roles of the EZH2 histone methyltransferase in cancer epigenetics. *Mutation research* **647**: 21-29.

Siolas D, Hannon GJ. 2013. Patient-derived tumor xenografts: transforming clinical samples into mouse models. *Cancer research* **73**: 5315-5319.

Sirohi B, Arnedos M, Popat S, Ashley S, Nerurkar A, Walsh G, Johnston S, Smith IE. 2008. Platinum-based chemotherapy in triple-negative breast cancer. *Annals of oncology : official journal of the European Society for Medical Oncology / ESMO* **19**: 1847-1852.

Sorlie T, Perou CM, Tibshirani R, Aas T, Geisler S, Johnsen H, Hastie T, Eisen MB, van de Rijn M, Jeffrey SS et al. 2001. Gene expression patterns of breast carcinomas distinguish tumor subclasses with clinical implications. *Proc Natl Acad Sci U S A* **98**: 10869-10874.

Sorlie T, Tibshirani R, Parker J, Hastie T, Marron JS, Nobel A, Deng S, Johnsen H, Pesich R, Geisler S et al. 2003. Repeated observation of breast tumor subtypes in independent gene expression data sets. *Proceedings of the National Academy of Sciences of the United States of America* **100**: 8418-8423.

Sparano JA, Wang M, Martino S, Jones V, Perez EA, Saphner T, Wolff AC, Sledge GW, Jr., Wood WC, Davidson NE. 2008. Weekly paclitaxel in the adjuvant treatment of breast cancer. *N Engl J Med* **358**: 1663-1671.

Stock JK, Giadrossi S, Casanova M, Brookes E, Vidal M, Koseki H, Brockdorff N, Fisher AG, Pombo A. 2007. Ring1-mediated ubiquitination of H2A restrains poised RNA polymerase II at bivalent genes in mouse ES cells. *Nature cell biology* **9**: 1428-1435.

Storz P, Doppler H, Copland JA, Simpson KJ, Toker A. 2009. FOXO3a promotes tumor cell invasion through the induction of matrix metalloproteinases. *Molecular and cellular biology* **29**: 4906-4917.

Suzuki A, Lu J, Kusakai G, Kishimoto A, Ogura T, Esumi H. 2004. ARK5 is a tumor invasion-associated factor downstream of Akt signaling. *Molecular and cellular biology* **24**: 3526-3535.

Suzuki J, Chen YY, Scott GK, Devries S, Chin K, Benz CC, Waldman FM, Hwang ES. 2009. Protein acetylation and histone deacetylase expression associated with malignant breast cancer progression. *Clinical cancer research : an official journal of the American Association for Cancer Research* **15**: 3163-3171.

Tan J, Yang X, Zhuang L, Jiang X, Chen W, Lee PL, Karuturi RK, Tan PB, Liu ET, Yu Q. 2007. Pharmacologic disruption of Polycomb-repressive complex 2-mediated gene repression selectively induces apoptosis in cancer cells. *Genes & development* **21**: 1050-1063.

Tapia C, Kutzner H, Mentzel T, Savic S, Baumhoer D, Glatz K. 2006. Two mitosis-specific antibodies, MPM-2 and phospho-histone H3 (Ser28), allow rapid and

precise determination of mitotic activity. *The American journal of surgical pathology* **30**: 83-89.

Taunton J, Hassig CA, Schreiber SL. 1996. A mammalian histone deacetylase related to the yeast transcriptional regulator Rpd3p. *Science* **272**: 408-411.

TCGA. 2012. Comprehensive molecular portraits of human breast tumours. *Nature* **490**: 61-70.

Teh MT, Wong ST, Neill GW, Ghali LR, Philpott MP, Quinn AG. 2002. FOXM1 is a downstream target of Gli1 in basal cell carcinomas. *Cancer research* **62**: 4773-4780.

Telli ML, Jensen KC, Vinayak S, Kurian AW, Lipson JA, Flaherty PJ, Timms K, Abkevich V, Schackmann EA, Wapnir IL et al. 2015. Phase II Study of Gemcitabine, Carboplatin, and Iniparib As Neoadjuvant Therapy for Triple-Negative and BRCA1/2 Mutation-Associated Breast Cancer With Assessment of a Tumor-Based Measure of Genomic Instability: PrECOG 0105. *Journal of clinical oncology : official journal of the American Society of Clinical Oncology*.

Thomas ES. 2008. Ixabepilone plus capecitabine for metastatic breast cancer progressing after anthracycline and taxane treatment. *Journal of clinical oncology : official journal of the American Society of Clinical Oncology* **26**: 2223.

Tonini T, Bagella L, D'Andrilli G, Claudio PP, Giordano A. 2004. Ezh2 reduces the ability of HDAC1-dependent pRb2/p130 transcriptional repression of cyclin A. *Oncogene* **23**: 4930-4937.

Tsuda H, Takarabe T, Hasegawa F, Fukutomi T, Hirohashi S. 2000. Large, central acellular zones indicating myoepithelial tumor differentiation in high-grade invasive ductal carcinomas as markers of predisposition to lung and brain metastases. *The American journal of surgical pathology* **24**: 197-202.

Tutt A, Robson M, Garber JE, Domchek SM, Audeh MW, Weitzel JN, Friedlander M, Arun B, Loman N, Schmutzler RK et al. 2010. Oral poly(ADP-ribose) polymerase inhibitor olaparib in patients with BRCA1 or BRCA2 mutations and advanced breast cancer: a proof-of-concept trial. *Lancet* **376**: 235-244.

Uddin S, Hussain AR, Ahmed M, Siddiqui K, Al-Dayel F, Bavi P, Al-Kuraya KS. 2012. Overexpression of FoxM1 offers a promising therapeutic target in diffuse large B-cell lymphoma. *Haematologica* **97**: 1092-1100.

van der Vlag J, Otte AP. 1999. Transcriptional repression mediated by the human polycomb-group protein EED involves histone deacetylation. *Nature genetics* **23**: 474-478.

Vanharanta S, Shu W, Brenet F, Hakimi AA, Heguy A, Viale A, Reuter VE, Hsieh JJ, Scandura JM, Massague J. 2013. Epigenetic expansion of VHL-HIF signal output drives multiorgan metastasis in renal cancer. *Nature medicine* **19**: 50-56.

Varambally S, Dhanasekaran SM, Zhou M, Barrette TR, Kumar-Sinha C, Sanda MG, Ghosh D, Pienta KJ, Sewalt RG, Otte AP et al. 2002. The polycomb group protein EZH2 is involved in progression of prostate cancer. *Nature* **419**: 624-629.

Vaske CJ, Benz SC, Sanborn JZ, Earl D, Szeto C, Zhu J, Haussler D, Stuart JM. 2010. Inference of patient-specific pathway activities from multi-dimensional cancer genomics data using PARADIGM. *Bioinformatics* **26**: i237-245.

Villa R, Pasini D, Gutierrez A, Morey L, Occhionorelli M, Vire E, Nomdedeu JF, Jenuwein T, Pelicci PG, Minucci S et al. 2007. Role of the polycomb repressive complex 2 in acute promyelocytic leukemia. *Cancer cell* **11**: 513-525.

Vire E, Brenner C, Deplus R, Blanchon L, Fraga M, Didelot C, Morey L, Van Eynde A, Bernard D, Vanderwinden JM et al. 2006. The Polycomb group protein EZH2 directly controls DNA methylation. *Nature* **439**: 871-874.

Visse R, Nagase H. 2003. Matrix metalloproteinases and tissue inhibitors of metalloproteinases: structure, function, and biochemistry. *Circ Res* **92**: 827-839.

Visvader JE, Lindeman GJ. 2008. Cancer stem cells in solid tumours: accumulating evidence and unresolved questions. *Nature reviews Cancer* **8**: 755-768.

Wagener N, Macher-Goeppinger S, Pritsch M, Husing J, Hoppe-Seyler K, Schirmacher P, Pfitzenmaier J, Haferkamp A, Hoppe-Seyler F, Hohenfellner M. 2010. Enhancer of zeste homolog 2 (EZH2) expression is an independent prognostic factor in renal cell carcinoma. *BMC cancer* **10**: 524.

Wan H, Dingle S, Xu Y, Besnard V, Kaestner KH, Ang SL, Wert S, Stahlman MT, Whitsett JA. 2005. Compensatory roles of Foxa1 and Foxa2 during lung morphogenesis. *J Biol Chem* **280**: 13809-13816.

Wang GL, Jiang BH, Rue EA, Semenza GL. 1995. Hypoxia-inducible factor 1 is a basic-helix-loop-helix-PAS heterodimer regulated by cellular O2 tension. *Proceedings of the National Academy of Sciences of the United States of America* **92**: 5510-5514.

Wang H, Wang L, Erdjument-Bromage H, Vidal M, Tempst P, Jones RS, Zhang Y. 2004. Role of histone H2A ubiquitination in Polycomb silencing. *Nature* **431**: 873-878.

Wang IC, Meliton L, Tretiakova M, Costa RH, Kalinichenko VV, Kalin TV. 2008. Transgenic expression of the forkhead box M1 transcription factor induces formation of lung tumors. *Oncogene* **27**: 4137-4149.

Wang X, Kiyokawa H, Dennewitz MB, Costa RH. 2002. The Forkhead Box m1b transcription factor is essential for hepatocyte DNA replication and mitosis during mouse liver regeneration. *Proceedings of the National Academy of Sciences of the United States of America* **99**: 16881-16886.

Wang Z, Banerjee S, Kong D, Li Y, Sarkar FH. 2007. Down-regulation of Forkhead Box M1 transcription factor leads to the inhibition of invasion and angiogenesis of pancreatic cancer cells. *Cancer research* **67**: 8293-8300.

Wang Z, Park HJ, Carr JR, Chen YJ, Zheng Y, Li J, Tyner AL, Costa RH, Bagchi S, Raychaudhuri P. 2011. FoxM1 in tumorigenicity of the neuroblastoma cells and renewal of the neural progenitors. *Cancer research* **71**: 4292-4302.

Wei Y, Chen YH, Li LY, Lang J, Yeh SP, Shi B, Yang CC, Yang JY, Lin CY, Lai CC et al. 2011a. CDK1-dependent phosphorylation of EZH2 suppresses methylation of H3K27 and promotes osteogenic differentiation of human mesenchymal stem cells. *Nature cell biology* **13**: 87-94.

-. 2011b. CDK1-dependent phosphorylation of EZH2 suppresses methylation of H3K27 and promotes osteogenic differentiation of human mesenchymal stem cells. *Nat Cell Biol* **13**: 87-94.

Weigel D, Jurgens G, Kuttner F, Seifert E, Jackle H. 1989. The homeotic gene fork head encodes a nuclear protein and is expressed in the terminal regions of the Drosophila embryo. *Cell* **57**: 645-658.

Weinberg RA. 1995. The retinoblastoma protein and cell cycle control. *Cell* **81**: 323-330.

Wicha MS, Liu S, Dontu G. 2006. Cancer stem cells: an old idea--a paradigm shift. *Cancer research* **66**: 1883-1890; discussion 1895-1886.

Widschwendter M, Fiegl H, Egle D, Mueller-Holzner E, Spizzo G, Marth C, Weisenberger DJ, Campan M, Young J, Jacobs I et al. 2007. Epigenetic stem cell signature in cancer. *Nature genetics* **39**: 157-158.

Wieczorek E, Reszka E, Gromadzinska J, Wasowicz W. 2012. Genetic polymorphism of matrix metalloproteinases in breast cancer. *Neoplasma* **59**: 237-247.

Wierstra I. 2011. The transcription factor FOXM1c binds to and transactivates the promoter of the tumor suppressor gene E-cadherin. *Cell Cycle* **10**: 760-766.

Wierstra I, Alves J. 2006a. Despite its strong transactivation domain, transcription factor FOXM1c is kept almost inactive by two different inhibitory domains. *Biological chemistry* **387**: 963-976.

-. 2006b. Transcription factor FOXM1c is repressed by RB and activated by cyclin D1/Cdk4. *Biological chemistry* **387**: 949-962.

Wonsey DR, Follettie MT. 2005. Loss of the forkhead transcription factor FoxM1 causes centrosome amplification and mitotic catastrophe. *Cancer research* **65**: 5181-5189.

Wu SC, Zhang Y. 2011. Cyclin-dependent kinase 1 (CDK1)-mediated phosphorylation of enhancer of zeste 2 (Ezh2) regulates its stability. *J Biol Chem* **286**: 28511-28519.

Xia L, Huang W, Tian D, Zhu H, Zhang Y, Hu H, Fan D, Nie Y, Wu K. 2012. Upregulated FoxM1 expression induced by hepatitis B virus X protein promotes tumor metastasis and indicates poor prognosis in hepatitis B virus-related hepatocellular carcinoma. *Journal of hepatology* **57**: 600-612.

Xia LM, Huang WJ, Wang B, Liu M, Zhang Q, Yan W, Zhu Q, Luo M, Zhou ZZ, Tian DA. 2009. Transcriptional up-regulation of FoxM1 in response to hypoxia is mediated by HIF-1. *Journal of cellular biochemistry* **106**: 247-256.

Xiang Y, Zhu Z, Han G, Lin H, Xu L, Chen CD. 2007. JMJD3 is a histone H3K27 demethylase. *Cell research* **17**: 850-857.

Xiao H, Verdier-Pinard P, Fernandez-Fuentes N, Burd B, Angeletti R, Fiser A, Horwitz SB, Orr GA. 2006. Insights into the mechanism of microtubule stabilization by Taxol. *Proceedings of the National Academy of Sciences of the United States of America* **103**: 10166-10173.

Xu K, Wu ZJ, Groner AC, He HH, Cai C, Lis RT, Wu X, Stack EC, Loda M, Liu T et al. 2012. EZH2 oncogenic activity in castration-resistant prostate cancer cells is Polycomb-independent. *Science* **338**: 1465-1469.

Xue J, Lin X, Chiu WT, Chen YH, Yu G, Liu M, Feng XH, Sawaya R, Medema RH, Hung MC et al. 2014. Sustained activation of SMAD3/SMAD4 by FOXM1 promotes TGF-beta-dependent cancer metastasis. *The Journal of clinical investigation* **124**: 564-579.

Yan J, Ng SB, Tay JL, Lin B, Koh TL, Tan J, Selvarajan V, Liu SC, Bi C, Wang S et al. 2013. EZH2 overexpression in natural killer/T-cell lymphoma confers growth advantage independently of histone methyltransferase activity. *Blood* **121**: 4512-4520.

Yang WM, Inouye C, Zeng Y, Bearss D, Seto E. 1996. Transcriptional repression by YY1 is mediated by interaction with a mammalian homolog of the yeast global regulator RPD3. *Proceedings of the National Academy of Sciences of the United States of America* **93**: 12845-12850.

Yang X, Karuturi RKM, Sun F, Aau M, Yu K, Shao R, Miller LD, Tan PBO, Yu Q. 2009. <italic>CDKN1C</italic> (p57^{KIP2}) Is a Direct Target of EZH2 and Suppressed by Multiple Epigenetic Mechanisms in Breast Cancer Cells. *PLoS One* **4**: e5011.

Yao KM, Sha M, Lu Z, Wong GG. 1997. Molecular analysis of a novel winged helix protein, WIN. Expression pattern, DNA binding property, and alternative splicing within the DNA binding domain. *The Journal of biological chemistry* **272**: 19827-19836.

Yau C, Wang Y, Zhang Y, Foekens JA, Benz CC. 2011. Young age, increased tumor proliferation and FOXM1 expression predict early metastatic relapse only for endocrine-dependent breast cancers. *Breast cancer research and treatment* **126**: 803-810.

Ye H, Holterman AX, Yoo KW, Franks RR, Costa RH. 1999. Premature expression of the winged helix transcription factor HFH-11B in regenerating mouse liver accelerates hepatocyte entry into S phase. *Molecular and cellular biology* **19**: 8570-8580.

Ye H, Kelly TF, Samadani U, Lim L, Rubio S, Overdier DG, Roebuck KA, Costa RH. 1997. Hepatocyte nuclear factor 3/fork head homolog 11 is expressed in proliferating epithelial and mesenchymal cells of embryonic and adult tissues. *Molecular and cellular biology* **17**: 1626-1641.

Yin Y, Stephen CW, Luciani MG, Fahraeus R. 2002. p53 Stability and activity is regulated by Mdm2-mediated induction of alternative p53 translation products. *Nature cell biology* **4**: 462-467.

Yoshida K, Miki Y. 2004. Role of BRCA1 and BRCA2 as regulators of DNA repair, transcription, and cell cycle in response to DNA damage. *Cancer Sci* **95**: 866-871.

Yuan ZM, Huang Y, Ishiko T, Nakada S, Utsugisawa T, Kharbanda S, Wang R, Sung P, Shinohara A, Weichselbaum R et al. 1998. Regulation of Rad51 function by c-Abl in response to DNA damage. *J Biol Chem* **273**: 3799-3802.

Zeidler M, Varambally S, Cao Q, Chinnaiyan AM, Ferguson DO, Merajver SD, Kleer CG. 2005. The Polycomb group protein EZH2 impairs DNA repair in breast epithelial cells. *Neoplasia* **7**: 1011-1019.

Zeitlinger J, Stark A, Kellis M, Hong JW, Nechaev S, Adelman K, Levine M, Young RA. 2007. RNA polymerase stalling at developmental control genes in the Drosophila melanogaster embryo. *Nature genetics* **39**: 1512-1516.

Zhang Y, Zhang N, Dai B, Liu M, Sawaya R, Xie K, Huang S. 2008. FoxM1B transcriptionally regulates vascular endothelial growth factor expression and promotes the angiogenesis and growth of glioma cells. *Cancer research* **68**: 8733-8742.